50272-101

REPORT DOCUMENTATION PAGE	1. REPORT NO. NSF/RA-790094	2.	3. Recipient's Accession No. PB298123

4. Title and Subtitle

Simple Shear Behavior of Fine Grained Soils Subjected to Earthquake and Other Repeated Loading, Final Report

5. Report Date: March 1979

6.

7. Author(s)

T.F. Zimmie, C.H.L. Floess

8. Performing Organization Rept. No.

9. Performing Organization Name and Address

Rensselaer Polytechnic Institute
Department of Civil Engineering
Troy, New York 12181

10. Project/Task/Work Unit No.

11. Contract(C) or Grant(G) No.

(C) PFR7614220
(G) (formerly ENV7614220)

12. Sponsoring Organization Name and Address

Engineering and Applied Science (EAS)
National Science Foundation
1800 G Street, N.W.
Washington, D.C. 20550

13. Type of Report & Period Covered: Final

14.

15. Supplementary Notes

16. Abstract (Limit: 200 words)

This report contains the results of a laboratory investigation on the behavior of fine grained soils subjected to repeated loads. Emphasis was placed on high strain level repetitive loading such as that caused by earthquakes and storm waves. Consolidated constant volume (CCV) tests were performed using a Norwegian Geotechnical Institute (NGI) direct simple shear device. The NGI device has been modified for cyclic loading capabilities. Because the in situ structure of cohesive soils is an important parameter in determining their behavior, only natural undisturbed soil samples were tested. These included a Gulf of Alaska marine clay from the Copper River prodelta and Concord Blue clay. Test data on the Gulf of Alaska clay include lateral stress measurements. These were made by using calibrated reinforced rubber membranes. The additional information provided by the lateral stress measurements considerably adds to the knowledge of the stress conditions existing in the sample. This aids in the interpretation of test results. Included in this report is a literature review, a discussion of the stress conditions existing in direct simple shear samples, a description of equipment and testing procedures, and the presentation of test results.

17. Document Analysis a. Descriptors

Soils
Soil properties
Earthquakes
Loads (forces)
Cyclic loads

b. Identifiers/Open-Ended Terms

Fine grained soils
Storm waves
Concord Blue clay
Consolidated constant volume (CCV)
Norwegian Geotechnical Institute (NGI)
Gulf of Alaska marine clay

c. COSATI Field/Group

18. Availability Statement	19. Security Class (This Report)	21. No. of Pages
NTIS	20. Security Class (This Page)	22. Price PCA07/MF A01

(See ANSI-Z39.18) See Instructions on Reverse

OPTIONAL FORM 272 (4-77)
(Formerly NTIS-35)
Department of Commerce

SIMPLE SHEAR BEHAVIOR OF FINE GRAINED SOILS SUBJECTED TO EARTHQUAKE AND OTHER REPEATED LOADING

by

Thomas F. Zimmie
and
Carsten H.L. Floess

SIMPLE SHEAR BEHAVIOR OF FINE GRAINED SOILS SUBJECTED TO EARTHQUAKE AND OTHER REPEATED LOADING

by

Thomas F. Zimmie

and

Carsten H.L. Floess

Sponsored by the National Science Foundation
Directorate for Applied Science and
Research Applications (ASRA)

GRANT No. PFR76-14220
(FORMERLY ENV76-14220)

FINAL REPORT

MARCH 1979

Department of Civil Engineering
Rensselaer Polytechnic Institute
Troy, New York 12181

TABLE OF CONTENTS

TABLE OF CONTENTS (continued)

ACKNOWLEDGEMENT

The authors would like to express their thanks to Professor Dwight Sangrey, Cornell University, for his valuable cooperation in this project, providing us with soil samples, guidance, and many helpful comments.

We would like to express our appreciation to the United States Geological Survey for providing us with the undisturbed offshore marine samples. We could have never obtained these samples otherwise.

We would like to thank Mrs. Betty Alix for typing this report.

Funds for this project were provided by a grant from the National Science Foundation, Grant No. PFR76-14220 (formerly ENV76-14220), sponsored by the Earthquake Engineering Program for the Directorate for Applied Science and Research Applications (ASRA) (formerly RANN).

The principal investigator for this project was Thomas F. Zimmie, Associate Professor, Civil Engineering.

Dr. S.C.Liu was the initial Program Manager for the research project whereas Dr. W. Hakala was the Program Manager for the latter portion of the project.

Please note that although the project is sponsored by the National Science Foundation, any opinions, findings, conclusions and/or recommendations expressed by this publication are those of the authors and do not necessarily reflect the view of NSF.

ABSTRACT

This report contains the results of a laboratory investigation on the behavior of fine grained soils subjected to repeated loads. Emphasis was placed on high strain level repetitive loading such as that caused by earthquakes and storm waves.

Consolidated constant volume (CCV) tests were performed using a Norwegian Geotechnical Institute (NGI) direct simple shear device. The NGI device has been modified for cyclic loading capabilities.

Because the in situ structure of cohesive soils is an important parameter in determining their behavior, only natural undisturbed soil samples were tested. These included a Gulf of Alaska marine clay from the Copper River prodelta and Concord Blue clay.

Test data on the Gulf of Alaska clay include lateral stress measurements. These were made by using calibrated reinforced rubber membranes. The additional information provided by the lateral stress measurements considerably adds to the knowledge of the stress conditions existing in the sample. This aids in the interpretation of test results.

Included in this report is a literature review, a discussion of the stress conditions existing in direct simple shear samples, a description of equipment and testing procedures, and the presentation of test results.

PART 1

INTRODUCTION

The behavior of fine grained soils subjected to transient or cyclic loading is becoming increasingly more important for the modern geotechnical engineer. Typical examples of transient or repetitive loading include earthquake loads, wind and wave loads, traffic loads, blasting, pile driving, fluctuating live loads, and machine vibrations.

The failure of soils subjected to repetitive loading can often be catastrophic. Unsatisfactory performance of soils during earthquakes is a major contributor to property damage and loss of life. The Niigata and Alaska earthquakes of 1964 are classic examples of this fact. Failures of slopes and embankments, collapse or settlement of buildings, failures of retaining walls and waterfront structures, and disruption of lifeline support systems are typical examples of earthquake induced damage.

Failure during earthquakes can occur in earth gravity structures (embankments, dams, retaining walls) and also in foundations. There is clear evidence that the failures can be attributed to increased stress due to the earthquake accelerations and also to a deterioration of soil strength or shearing resistance. The term "liquefaction" is generally applied to this phenomenon and for most researchers and experienced practitioners this problem is associated with loose sands and other coarse grained soils. As a result, research and publications have been concerned for the most part with the dynamic response of these soils rather than fine grained silts

and clays.

The behavior of fine grained soils subjected to earthquake or other repeated loading is not as clear as for the case of cohesionless soils. In documented cases where clay slopes have failed during earthquakes, the failures have been attributed to the liquefaction of sand layers or lenses in the slope (118). However, there are other cases which show that clay soils do lose strength and fail under dynamic or cyclic loading conditions. For example, pile driving in clay causes strength deterioration (37,84). The best example is probably the marine landsliding and slumping in soft clays which result from the cycled pressures caused by storm waves. This phenomenon has been well documented (86,142), with slopes as gentle as a half degree having failed (45).

Numerous specific topics could be the focus of a research effort concerning the response of fine grained soils subjected to repetitive loads. Compared with work on sands, little has been done. The major objective of the laboratory investigation reported herein is the study of the fundamental behavior of clay soils on an effective stress basis. Emphasis was placed on high strain level repetitive loading such as occurs during earthquakes and storm wave loads.

All laboratory testing was performed using the Norwegian Geotechnical Institute (NGI) direct simple shear device. This device has been modified for cyclic loading capabilities. The NGI direct simple shear device has been used by a number of researchers for cyclic loading studies (149), and it is an excellent device in spite of some limitations (98,149). Quite uniform strains and stresses can be obtained with this device (23,82).

As noted previously, the NGI direct simple shear device is not perfect, and it has limitations from a theoretical viewpoint. However, no geotechnical testing apparatus is perfect; all have their advantages and disadvantages.

With consideration for known limitations, the NGI direct simple shear device will provide excellent results within practical reality.

To obtain an understanding of clay soil behavior in the field, the soil's structure should be preserved as found in situ. Therefore, only undisturbed samples of cohesive soils were tested. The soils tested in this investigation include Concord Blue clay (24,40) and Gulf of Alaska clay from the Copper River delta (12,45). The Copper River delta region has experienced extensive sliding and slumping, with a large slide having been associated with the 1964 Alaska earthquake. Petroleum related activities in the outer continental shelf of the Gulf of Alaska require the identification and evaluation of geologic and geotechnical problems associated with this region.

Consolidated constant volume (CCV) static and cyclic tests were performed. Samples were tested after application of various stress histories resulting in normally consolidated and slightly overconsolidated specimens. Cyclic tests were conducted using loading frequencies applicable to earthquake and storm wave loading situations, typically 0.5 or 0.1 Hz. Static tests were performed following cyclic tests in which failure did not occur.

This report contains a summary and interpretation of test results. Also included are a comparison of results with published literature, some theoretical considerations, a literature review and a description of laboratory testing equipment and procedures.

PART 2

LITERATURE REVIEW, BACKGROUND

A. Research Results

Some early research efforts investigating cyclic soil behavior have been published, e.g., Casagrande (13,14). However, most of the work has been done in the past 10-15 years, and at present there is a large amount of research and interest in soil dynamics (103).

Early studies indicated that cohesive soils were less subject to strength loss from cyclic loading than sands (78). Consequently, most cyclic loading studies have dealt with noncohesive soils, i.e., sands (119) and even gravels (148). Much of the published literature deals with the "liquefaction" of these noncohesive soils (15,16,17,43,120,127,143,154). A variety of specific research topics dealing with noncohesive soils have also been investigated, for example, time and rate effects (49,104,119), influence of testing technique and sample preparation (71,89,132,133), determination of moduli and damping characteristics (20,125,130), effect of stress and seismic history (128), determination of settlements following cyclic loading (77,153), effect of relative density (16,119), and the effect of multidirectional loading (101). Investigations of specific applied problems have also been undertaken (21,66,79,81,123,124,126).

Recent planning and construction have frequently encountered clay soils which may be subjected to cyclic loading. Especially notable is the area of offshore construction. A number of specific large scale construction

projects such as the Alaskan pipeline have also encountered numerous clay soil deposits. These activities have provided a stimulus for renewed interest in the cyclic behavior of clay soils. Emphasis in this section is placed on the behavior of clay soils subjected to large strain cyclic loading, such as caused by earthquake and storm wave loadings.

Early studies of the cyclic loading behavior of clay soils were connected with pavement design (74). Much of this research dealt with partially saturated, compacted soils. Cyclic loads were typically applied by repeated compressive loadings on triaxial samples. This type of loading resulted in both a permanent or residual strain and a cyclic strain during each loading cycle. It was generally found that below a certain cyclic stress level, equilibrium conditions resulted and failure did not occur in the sample. Lashine (75) found that cyclic load application less than 0.75 to 0.80 of the static undrained strength did not cause failure on normally consolidated, reconstituted samples of silty clay. Other researchers have found similar results (11,115). These results for one-directional cyclic loading of clay soils indicated that the cyclic strength was not much less than the static undrained strength. This type of strength reduction could easily be handled in design.

Early earthquake related research investigated the behavior of clay soils subjected to reversing stresses or strains. The effect of reversing, two-directional loading on clays was found to be much more severe than for one-directional loading. Seed and Chan (122) found that the ratio of one-directional undrained cyclic strength to two-directional undrained cyclic strength ranged from 1.2 to 3.5 for the soils tested.

These results provided a stimulus for investigating the two directional cyclic behavior of clay soils.

Specific research projects have studied the areas of cyclic loading strength (2,80,85,112,121,146,152), stress strain behavior, i.e., moduli and damping characteristics (4,5,20,47,48,49,50,70,138,139), shear strength and stress strain behavior following cyclic loading (80,90,140), rate effects (80,90,116), soil characteristics, e.g., void ratio and confining pressure (49,104), stress and seismic history (54), anisotropy (95,110), and long term effects such as changes in strength and volume (10,40,90). Specific applications have also been investigated. These include ground response to earthquake loading (56,57,104), earthquake and wave loadings on offshore structures (3,8,25,26,38,39,52,53,88,111,131), pile driving (27,37,60,113), traffic loading (11,75), slope stability (6,63,86), soil structure interaction (104), and frozen soils (135,136,145).

The cyclic behavior of soils has been investigated on an effective stress basis and on a total stress basis. Pore pressure changes have been used as an explanation for the liquefaction phenomenon in sands, although the pore pressure changes and the resulting effective stresses have not often been used as a basic parameter in predicting soil behavior. Finn, Martin and others (32,33,34,83) have recently proposed a procedure, applicable to saturated sands, for predicting the magnitude of pore pressure changes due to cyclic loading. The method is based on a set of constitutive equations which take into account the initial in situ shear modulus,

the variation of shear modulus with shear strain, the simultaneous generation and dissipation of pore pressures, damping characteristics, and strain hardening effects. The resulting pore pressures have been incorporated into soil response analyses to predict the behavior of horizontal soil layers subjected to earthquake loadings (30,35).

Sangrey (112,115), working with fine grained soils, has used an effective stress approach to study cyclic loading behavior. This approach may be briefly summarized as follows. When undrained saturated soil is subjected to a load-unload cycle there will be a residual pore pressure and distortional strain after the cycle. Depending on the stress history, this can be either a positive or a negative pore pressure. With additional load cycles these residual pore pressures and strains accumulate until either the soil fails or it attains a stable equilibrium condition with no subsequent deterioration even after many cycles of loading. For a particular soil there is a "critical level of repeated stress" (115) separating these two types of behavior.

These alternative consequences can be explained if the effective stresses are considered. The accumulation of positive residual pore pressure decreases the effective stress in the soil, and if the pore pressure accumulates to sufficient levels the effective stresses decrease to the failure condition for the soil. If the pore pressures do not accumulate to this critical level, the soil maintains a nonfailure equilibrium con-

dition. Pore pressure build-up is a function of the level of repeated stress. Consequently, the critical level of repeated stress is just low enough so that pore pressures do not build up to the failure condition.

Recently, Sangrey et al (114) presented a behavioral model based on critical void ratio and critical state concepts (107,117) to describe the response of soils to cyclic loading. Egan and Sangrey (24) have also developed a critical state model to predict the magnitude of excess pore pressures generated by cyclic loading. The critical state concepts employ the use of void ratio and effective stresses as key parameters to define the state of the soil.

Other theoretical models and analytical procedures have also been used to describe the cyclic behavior of soils. A general analytical model describing the anisotropic, elasto-plastic, path dependent, stress-strain-strength properties of saturated clays under undrained loading conditions has been developed by Prevost (95,96,97,99). This model uses the concepts of isotropic and kinematic hardening from plasticity theory. The stress strain behavior of clays can then be determined for complex loading paths, and subsequently used in finite element analyses. Pender (93) also describes a model for small strain cyclic loading of soil based on the critical state theory and plasticity theory. Descriptions of cyclic soil behavior have also been based on elastic and visoelastic models (44), rheologic models (64), fatigue (144), and endochronic theory (65).

Empirical models of the behavior of clay soils subjected to cyclic loading have also been proposed. A nonlinear response analysis model has been developed by Idriss et al (56). This model is based on the degradation of the initial stress-strain backbone curve as cyclic loading progresses. The numerical value of the degradation is found by means of strain controlled laboratory tests. The model has also been incorporated into nonlinear response analyses of horizontal soil layers subjected to earthquake accelerations.

Probability theory and reliability analysis have also been used to describe cyclic loading of soils. From a historical viewpoint, probability theory has been used in fatigue testing. In fatigue testing of metals for example, a log-normal distribution is often used as a model for the number of cycles to failure (100). Ferritto and Forrest (28) recently developed a Monte Carlo simulation technique to predict the probability of liquefaction of sand layers; stochastic models for predicting the seismic failure of soil deposits have also been developed (22). Due to the many uncertainties in soil dynamics, especially in determining the loading conditions and the soil parameters for use in analyses, it appears that probability theory and reliability analysis have many potential applications (1,51).

B. Testing Techniques and Equipment

Many problems concerning the cyclic loading behavior of soils require a knowledge of moduli and damping parameters, soil strength, or other empirical data. Some of this data is best measured in the laboratory

under controlled conditions. An attempt is usually made to simulate field conditions in laboratory testing devices. Conceptually, it may appear relatively simple to build such an apparatus, but in practice it is extremely difficult to do so. It may be impossible to construct a completely satisfactory laboratory apparatus (76). The laboratory testing equipment most commonly used in soil load-deformation studies are triaxial devices and direct shear or simple shear type devices (72). This is true whether the tests are static or cyclic.

Kjellman (62) described the Swedish Geotechnical Institute (SGI) direct simple shear device which was first built in 1936. In this device, a cylindrical sample is confined by a rubber membrane and a series of sliding metal rings. The Norwegian Geotechnical Institute (NGI) direct simple shear apparatus was developed by Bjerrum and Bishop around 1961 (9). It is basically an adaptation of the SGI device. The NGI apparatus also tests cylindrical samples but they are confined by a wire reinforced rubber membrane. The device is described by Bjerrum and Landva (9). The Cambridge simple shear apparatus is described by Roscoe (106). The Cambridge device has hinged rigid walls surrounding a rectangular sample. Later models of the Cambridge apparatus employ special load cells in the rigid walls which measure normal and shear stresses (107). These direct simple shear devices have frequently been used for cyclic loading studies of soil (2,83,90,92).

A number of practical problems exist with the direct simple shear apparatus. The most serious problem is the lack of complimentary shear stresses on the vertical sides of the sample. The sample is also fairly

small and therefore no soil element is far away from the displacement boundary conditions. Also, during shear, the sides of the sample must stretch (98). These difficulties make the interpretation of direct simple shear tests rather difficult.

Numerous investigators have theoretically and experimentally analyzed the stress conditions existing in direct simple shear device samples (23,82,98,129,150). The findings of these studies are further discussed in Part 5 of this report. The qualitative conclusions obtained from these investigations should be recognized, especially when interpreting test results. The direct simple shear device is not perfect, however the device has been useful for studying the cyclic loading behavior of soils. Direct simple shear test results have been found to be consistant with the results of triaxial tests and shake table tests (19,36,92,119). Thus, while uncertainties exist as to the stress distributions produced in direct simple shear devices, they clearly produce reasonable test results.

Direct simple shear devices simulate earthquake loading conditions better than triaxial devices (83,119). However, triaxial devices are probably the most versatile laboratory soil testing equipment available today from the standpoint of pore pressure measurements, stress path variability, and back pressure application. Triaxial equipment has also frequently been used for cyclic loading studies of soil (11,76,91,115). It is the most widely used testing apparatus for determining the liquefaction characteristics of cohesionless soil (149).

In a typical cyclic loading triaxial test, the cylindrical sample is first consolidated under an isotropic state of stress. The axial load is then cycled between two limits under undrained conditions. It is also possible to impose an anisotropic consolidation stress or to perform con-

trolled strain tests. If care is taken in the preparation and performence of cyclic triaxial tests, the test results have been found to be quite repeatable, even when using different testing devices (132).

As with any laboratory testing device, the triaxial apparatus has some limitations. Stress concentrations occur near the ends of the sample, although this effect can be lessened by using lubricated end plates (61). The stress and deformation conditions are nonuniform in most cases (94). Experimental details such as piston friction, membrane leakage, and air diffusion must also be recognized (7,16). For cyclic testing, the extension and compression phases of the test may produce different results. For example, hysteresis loops may be asymmetric in strain controlled tests and necking tends to occur in stress controlled tests. The major principle stress also changes directions by 90° during cyclic tests. In spite of these difficulties, cyclic loading triaxial tests can produce valid results (76,119).

Cyclic torsional simple shear devices have been developed to overcome some of the difficulties encountered with the direct simple shear device (149). These devices also permit control of K_o conditions in the sample. When the cylindrical sample is subjected to a torque, the shear stress varies linearly with distance along the radius of the sample. In an effort to overcome this difficulty, the hollow cylinder torsional shear apparatus was developed (58,151). Some of these devices use samples with tapered ends to ensure uniform shearing strains throughout the sample.

Hollow cylinder torsional simple shear devices also have their limitations (149,150). Wright et al (150) developed criteria for selecting sample size and configuration for which the central zone of the sample is free of end effects. Although stress distributions in torsional hollow cylinder samples may be more uniform than in direct simple shear samples, difficulties exist in sample preparation for undisturbed soils. For some soils it may not be possible to make hollow cylinder samples.

Shake table tests have also been used to determine the cyclic loading behavior of soils (19,31,101). The large sample size used in these tests decreases the potential effects of stress concentrations which are important in the small samples used in direct simple shear tests. Data from shake table tests correlates well with data from direct simple shear and torsional shear tests (19). The main difficulties with this test are the large sample size and the effects of membrane compliance (119).

Resonant column tests and ultrasonic pulse tests have been used to determine modulus and damping data (4,5,134,149). These devices are based on the theory of wave propagation in prismatic rods. These devices are primarily used for small cyclic strain applications. The resonant column test is described by Richart et al (105). The ultrasonic pulse test is not commonly used in soil dynamics.

A number of non routine testing devices also exist for cyclic loading testing of soils (46,147). However, these devices have mainly been used as research tools to date, and not on a routine basis.

Model tests have also been employed in soil dynamics studies. Kovacs et al (63) used this approach in their study of the seismic behavior of clay banks. Rowe (109) used centrifuge model tests to study the behavior of offshore gravity platforms. Richart (104) describes some soil structure interaction tests for footings using photoelastic methods. These model tests clearly have their merits and many potential applications in soil dynamics and earthquake engineering.

PART 3

EQUIPMENT

The Norwegian Geotechnical Institute (NGI) direct simple shear apparatus, model number 4, was used for this investigation. This device was developed by NGI and it is manufactured commercially by Geonor. It is similar to the machine described by Bjerrum and Landva (9).

The direct simple shear apparatus was designed to produce uniform shear strains throughout the soil sample. The cylindrical sample is confined in a wire reinforced rubber membrane that constrains the sample in the radial direction. The wire reinforcement keeps the horizontal cross sectional area constant during consolidation and shear. The sample assembly also keeps the upper and the lower ends of the sample parallel at all times.

Sands, silts, stiff clays, soft clays, and quick clays can be tested under drained or under constant volume conditions. Either stress controlled or strained controlled testing modes can be performed.

A. Shear Apparatus

The NGI direct simple shear device consists of the sample assembly, the vertical loading unit, and the horizontal loading unit. The sample assembly is shown in Figure 1; the complete apparatus is shown in Figure 2. Photographs of the device are shown in Figure 3.

The sample assembly consists of the pedestal, upper cap,* lower cap,* wire reinforced rubber membrane, and O-rings. The upper and lower caps

*Geonor refers to the upper and lower caps as the upper and lower filter holders.

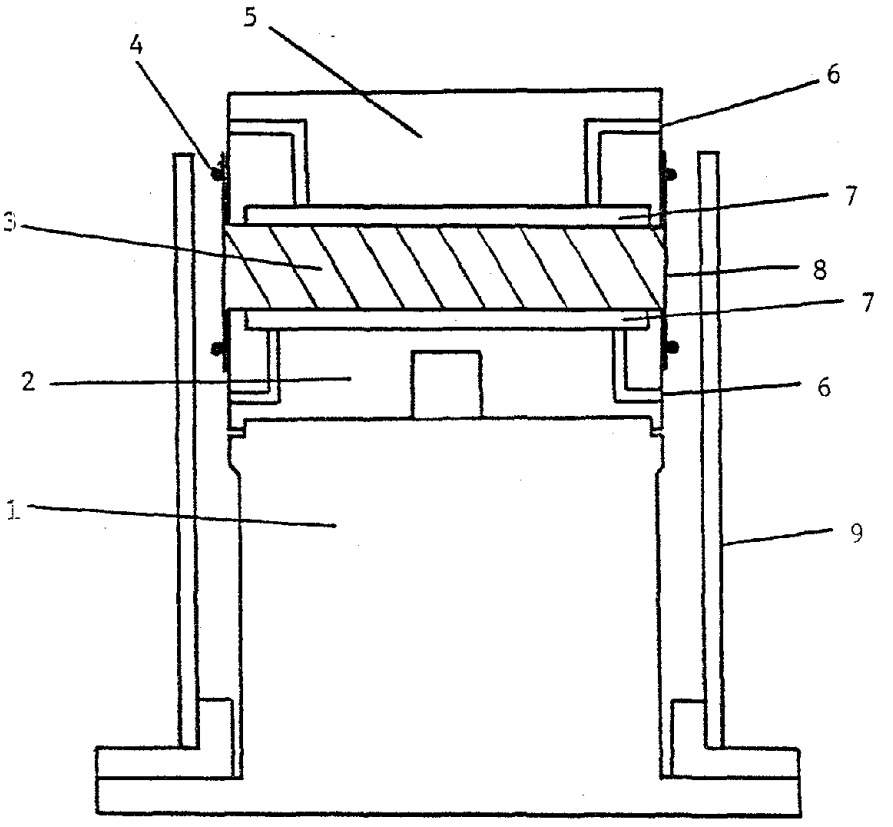

1. Pedestal
2. Lower Cap
3. Sample
4. O-Ring
5. Upper Cap
6. Drainage Tube
7. Porous Stone
8. Reinforced Rubber Membrane
9. Plastic Cylinder

FIGURE 1. THE NGI DIRECT SIMPLE SHEAR DEVICE
SAMPLE ASSEMBLY

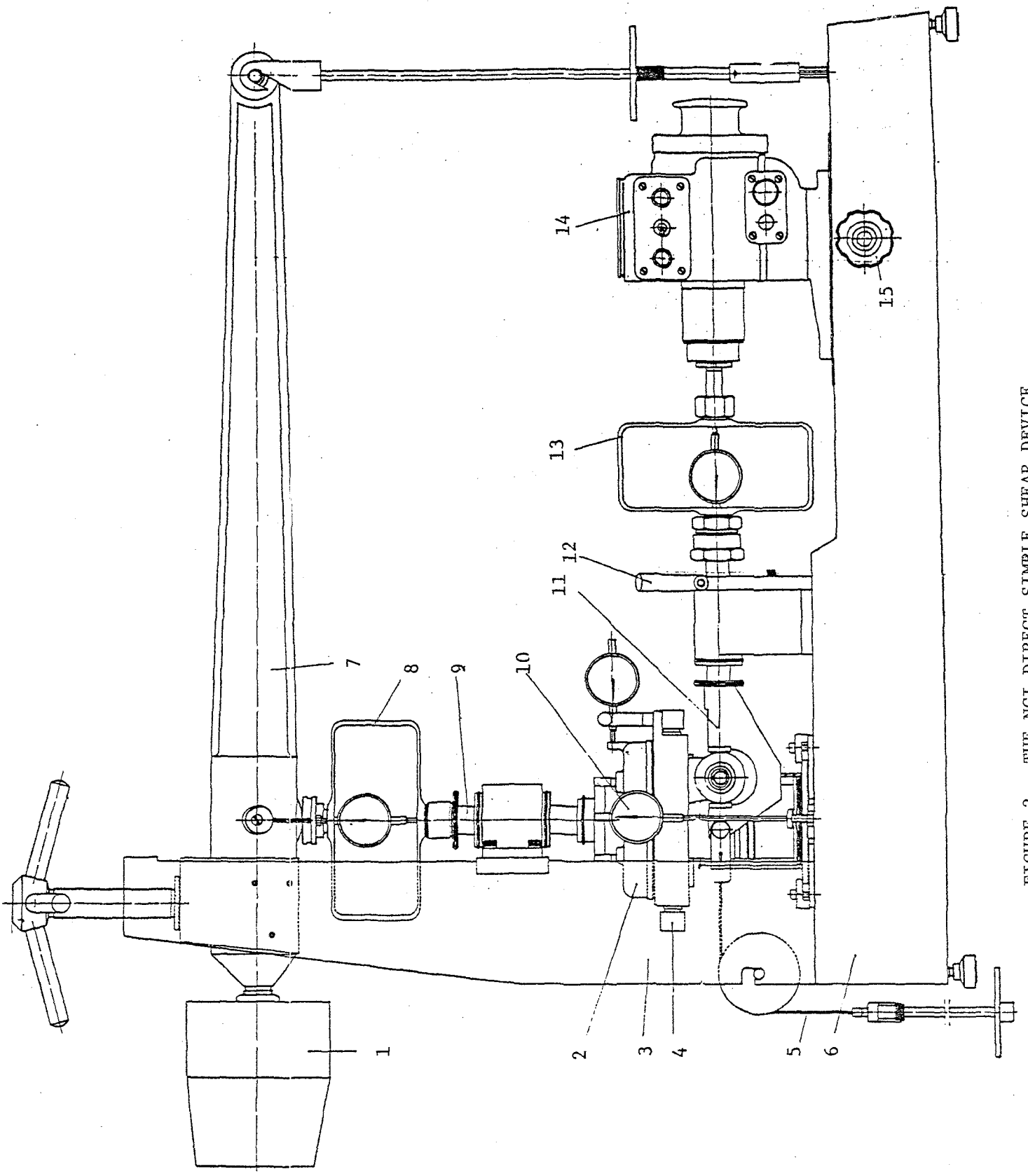

FIGURE 2. THE NGI DIRECT SIMPLE SHEAR DEVICE

1. Counter Weight
2. Sliding Shear Box
3. Tower
4. Lugs
5. Hanger
6. Base
7. Lever Arm
8. Proving Ring Load Gauge
9. Piston
10. Vertical Dial Gauge
11. Connection Fork
12. Locking Clamp
13. Proving Ring Load Gauge
14. Electric Motor and Gear Box
15. Adjusting Mechanism

FIGURE 2. (CONTINUED)

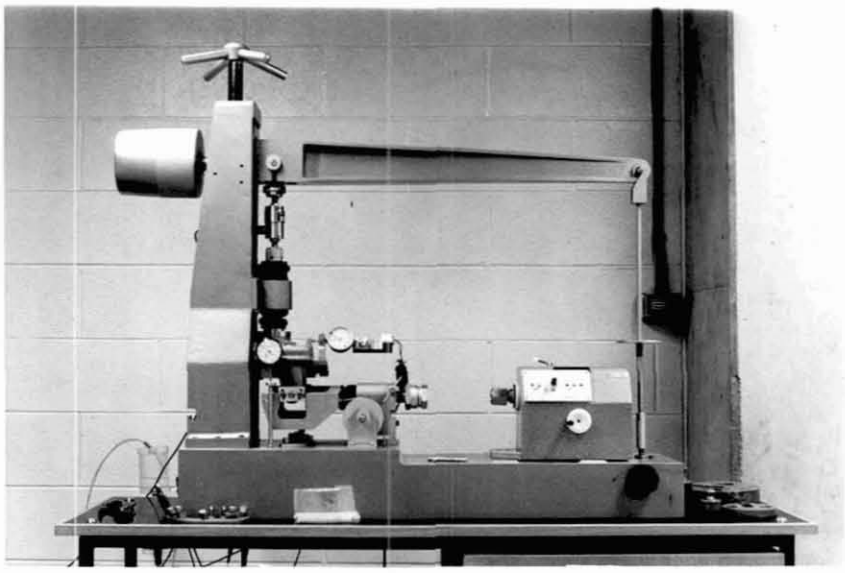

(a)

(b)

FIGURE 3. (a) THE NGI DIRECT SIMPLE SHEAR DEVICE
(b) GENERAL VIEW OF TESTING AREA

have recesses for porous stones*. Either smooth porous stones or porous stones with 1 mm long needles can be used. The needles help to prevent slippage between the sample and the stones. The caps are equipped with drainage tubes that can be connected to an external water source. Alternatively, a plastic cylinder can be placed around the sample; the cylinder is filled with water to keep the sample submerged. The O-rings provide a water tight seal between the wire reinforced rubber membrane and the caps.

The sample assembly unit is available for either the standard 50 cm^2 sample size or a smaller 1.875 in. (4.76 cm) diameter sample size. The 1.875 in. diameter sample size is used to accomodate the smaller undisturbed sample cores commonly obtained in the U.S.A.

The vertical loading unit consists of the base, the tower, the 10:1 lever arm, the proving ring load gauge, the piston, the sliding shear box, the vertical dial gauge, and the adjusting mechanism. A counterweight balances the weight of the lever arm, the proving ring load gauge, the piston, the sliding shear box, and the top cap.

The horizontal loading unit for strain controlled testing includes the electric motor and gear box, the proving ring load gauge, the horizontal piston, the locking clamp, the connection fork, the sliding shear box, and the horizontal dial gauge.

The gear box has a stepless speed adjustment with a range of 10 minutes per mm to 300 minutes per mm of travel. The total available travel is 45 mm. The direction of movement is controlled by a switch, and the power will shut off automatically when either end position is reached.

*Geonor refers to the porous stones as filter plates.

The horizontal loading unit for the stress controlled testing mode consists of the horizontal piston, the locking clamp, the connection fork, the sliding shear box, the dial gauge, the axle with two mounted pulleys, and the hanger. The hanger is attached to the connection fork by two wires that are taken through holes in the table on which the shear apparatus is placed. Stress increments are applied to the sample by placing suitable weights on the hanger. For stress controlled testing, the horizontal proving ring load gauge is not needed and is disconnected.

The connection between the top cap of the sample assembly and the lower part of the sliding shear box is made by two adjustable lugs. The lugs are brought into contact with the cap by means of two allenhead screws. The sample is sheared by moving the top cap while holding the bottom cap and the pedestal stationary. For strain controlled tests, a constant rate of shear strain is applied to the sample by the gear box and electric motor. For stress controlled tests, the horizontal shear stress is applied by adding dead load increments to the hanger.

By using the horizontal loading unit for stress controlled tests, a constant static shear stress can also be applied. This can be used to simulate shear stresses on horizontal planes that occur in field situations such as slopes.

To measure the applied vertical and horizontal loads, rectangular proving ring load cells are used. Interchangable proving rings with ranges of 50, 100, 200, 400, and 800 kg are available. Vertical and horizontal displacements are measured by dial gauges.

During shear, undrained conditions are simulated by keeping the volume of the sample constant. Assuming that the horizontal cross sectional area does not change, constant volume is maintained by adjusting the vertical stress on the sample while keeping the sample height constant. The change in vertical stress is equated to the change in pore water pressure that would occur during an undrained test.

The fine adjustments in the vertical load, needed to maintain constant volume conditions, are made by the adjusting mechanism. After consolidation, the lever arm is pinned to the adjusting mechanism, providing the desired consolidation stress. Once pinned into position, the vertical load can be changed by controlled movements of the lever arm upwards and downwards. This is accomplished by rotating a worm gear connected to the adjusting knob.

B. Trimming Apparatus

The trimming apparatus and methods are in principle similar to those described by Landva (73). The trimming apparatus was designed for use with the soft sensitive clays that are common in Norway. The basic design principles are that the sample should be completely and rigidly supported at all times, and never touched by hand.

The trimming apparatus consists of a base, and a set of three yokes. The base has two vertical columns on which the yokes can slide. The yokes can be positioned at any point on the columns by locking thumb screws. The base also has two pins by which it can be attached to the direct simple shear apparatus.

One yoke acts as the guide for the reinforced rubber membrane expander. The membrane expander consists of a cylindrical porous stone that is pressed into the yoke. The wire reinforced section of the membrane is placed inside the cylindrical porous stone, and the unreinforced parts are folded over the ends. The yoke contains a fitting to which a rubber hose connected to a vacuum source can be attached. When vacuum is applied, the diameter of the reinforced rubber membrane is increased. The membrane can then be mounted on the sample with a minimum of disturbance.

The second yoke guides the stainless steel cutting cylinder. It contains provisions for attaching the lower cap to the bottom of the sample. The third yoke acts as a guide for attaching the upper cap to the sample.

Proper use of the trimming apparatus ensures that the sample stands vertical, and that the ends are horizontal and parallel. A photograph of the trimming apparatus is shown in Figure 4.

C. Reinforced Rubber Membranes

The reinforced rubber membranes used in this investigation were manufactured by Geonor. The reinforcement consists of constantan wire with a diameter of .15 mm, a Young's Modulus E of 1.55×10^6 kg/cm^2, and a tensile strength of 5,800 kg/cm^2. The wire is wound at 20 turns per centimeter of height. The rubber material is natural latex. The membranes are manufactured in two sizes, the standard 50 cm^2 size and the 1.875 in. (4.76 cm) diameter size. A photograph of the membranes is also shown in Figure 4.

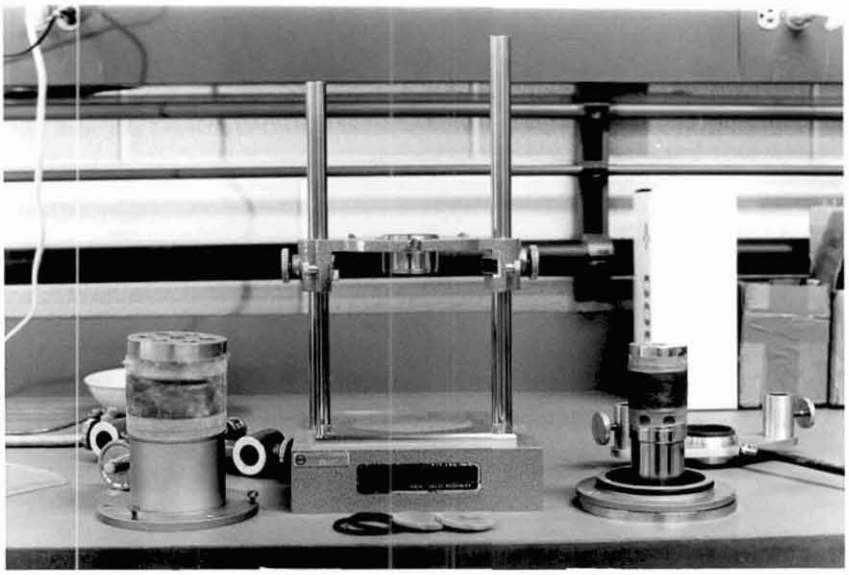

FIGURE 4. NGI TRIMMING APPARATUS AND REINFORCED RUBBER MEMBRANES

Geonor recommends a maximum lateral stress of 1.8 kg/cm^2 for these membranes. Membranes are also manufactured using stainless steel suture thread as reinforcement. The maximum recommended lateral stress for these membranes is 5.0 kg/cm^2. Only the constantan wire reinforced rubber membranes were used for this study.

The membranes must provide adequate lateral strength to maintain a constant cross sectional area during consolidation and shear. The wire reinforcement will deform as the lateral stress increases, but this gives only a small error (41). For the consolidation stresses used in this testing program, the membranes were found to have adequate strength; the reinforcement wires did not break and the membranes did not appear to be stretched after the completion of tests.

The membranes must also allow for vertical strains in the sample during consolidation and for drained testing. Vertical strains are allowed by the spaces between the reinforcement wire windings. If the consolidation strains are very large, the wire windings tend to overlap. This occurred for a test on a Gulf of Alaska sample consolidated to 1.0 kg/cm^2. Consequently, all other Gulf of Alaska samples were consolidated under smaller stresses.

Calibrated reinforced rubber membranes for measurement of lateral stress are also manufactured by Geonor. These membranes operate on a strain gauge principle; the change in resistance of the wire windings is measured. The entire height of the reinforcement wire windings is 3 cm; the middle centimeter acts as the strain gauge. These membranes were calibrated by applying known hydrostatic stresses and by measuring the resulting change in resistance. The resistance changes were measured by a strain gauge indicator

calibrated directly in microinches per inch.

The active reinforcement wire is made from constantan and it has the same physical properties as given previously for the ordinary membranes. The electrical resistance of the entire length of active wire is 138 ohms and the gauge factor is 2.18 for the 50 cm^2 membranes.

These membranes perform the same function as the ordinary ones do. They must maintain the sample at a constant cross sectional area, and they must allow for vertical strains during consolidation and drained shear. The recommended maximum lateral stress for these membranes is 1.4 kg/cm^2.

Some difficulties were encountered in the use of these calibrated membranes. With two of the membranes used in this investigation, water came into contact with the active wire resulting in partial short circuits. This resulted in a decreased resistance, and erroneous microstrain readings. It is essential that the rubber material (butyl latex or neoprene) used for these membranes form a watertight seal around the active wire.

The resistance of the active reinforcement wire is also very sensitive to temperature changes. Temperature variations result in resistance changes that can be mistaken for changes in lateral stress. To compensate for temperature changes, a matching "dummy" membrane and the active membrane are connected in a bridge arrangement. If the temperature coefficient of resistivity and the gauge factor for the active and the "dummy" membranes are equal, resistance changes caused by temperature fluctuations will balance. Under these conditions, microstrain readings are not affected by small temperature changes. The active and dummy membranes must be placed as close to each other as physically possible.

The resistance of one calibrated membrane used in this study was approximately 18 ohms less than the resistance of the other membranes. Because of this large difference in resistance, a balanced bridge circuit could not be obtained unless an 18 ohm resistor was connected in series with this membrane.

Since the material characteristics of the 18 ohm resistor are different than those of the wire reinforcement in the membranes, resistance changes caused by temperature fluctuations were not completely balanced. This caused observed variations in microstrain readings when this particular membrane was used.

Difficulties were also encountered in mounting both calibrated and uncalibrated membranes around the clay samples during the trimming process. Wrapping the membranes on the cylindrical porous stone expander proved to be difficult and time consuming, especially for unused membranes. After a few uses, the membranes were easier to work with. Applying too much vacuum to the membrane expander often resulted with the reinforcement wires forming chords instead of circular arcs. Although the wires did not break free from the rubber membrane, it was impossible to mount membranes around the sample in this condition. Too little vacuum, however, did not stretch the membranes enough for disturbance free mounting around the sample. With some practice, the proper amount of vacuum could be obtained.

The average life of membranes which did not have any problems on their first use ranged from 5 to 10 tests.

D. Modification for Cyclic Loading Capabilities

The direct simple shear apparatus was modified by Geonor for cyclic loading capabilities. With the existing modifications, stress controlled tests with a square wave loading can be performed.

The cyclic loading mechanism is illustrated in Fig. 5. The hydraulic piston travels up and down at controlled frequencies. The weights shown are attached by wires to the connection fork. When the piston is in the down position, the left weights hang free; when the piston is up, it supports these weights. Providing that exactly twice as much weight (including the weight of the hanger) hangs from the left side as from the right side, equal shear forces will alternately be transmitted in opposite directions to the sample. The mechanism shown therefore induces a stress controlled square wave loading on the sample.

The control unit consists of a counter and a timer. The counter can be preset for a given number of cycles, and cycling will terminate after the desired number of cycles has been reached. The timer has a digital control for the cycling frequency. Half period frequencies from 1 to 99 seconds are possible. The timer controls a 4-way solenoid operated air value that actuates the piston motion.

Some difficulities were encountered with the cyclic loading mechanism as supplied by Geonor. Initially, the timer operated erratically. Investigation showed that a power relay in the control unit caused large voltage spikes which interfered with the operation of the timer. Some rewiring in the control unit has alleviated this problem, and the control

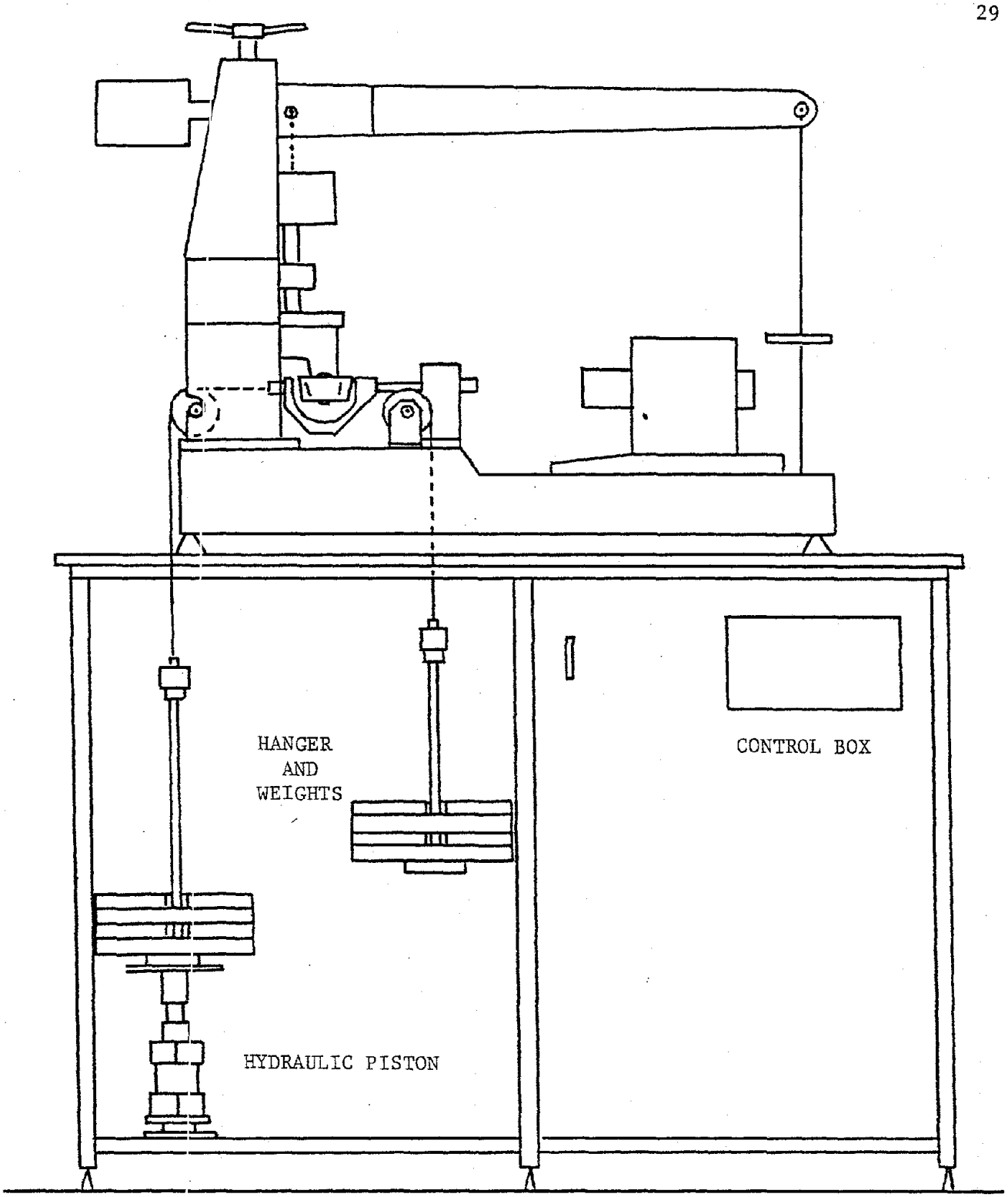

FIGURE 5. NGI DIRECT SIMPLE SHEAR DEVICE WITH MODIFICATIONS FOR CYCLIC LOADING CAPABILITIES

unit has worked properly since then.

Another problem involves the loading system itself. During cyclic loading it was observed that the shear strains were generally larger on the left (piston) side than on the right. It was found that this was caused by the impact loading of the left weight as it dropped free from its support on the piston. To compensate for this, some weight can be removed from the left hanger; this results in approximately symmetric shear strains.

E. Data Acquisition

To facilitate data acquisition, some modifications were made to the direct simple shear apparatus.

The vertical load proving ring was replaced by a Schaevitz FTD-1U-200 load cell. This load cell has a capacity of 200 lb (90.5 kg) in tension or compression. The linearity and resolution are better than .2% and .1%, respectively.

A Hewlett Packard 7DCDT-050 Linear Variable Differential Transformer (LVDT) was used for measurement of horizontal displacements. The range of this LVDT is $\pm$ .050 in. (1.27 mm). This range was found to provide excellent resolution at small strains. The LVDT was connected in series with the original dial gauge by a special aluminum mounting block. Horizontal displacements could therefore be measured by either the LVDT or by the dial gauge. Typically, the LVDT and the dial gauge were used together, providing a convenient crosscheck at all times.

Both the LVDT and the load cell have integral signal conditioning for DC operation; both were powered by constant DC voltage power supplies. The voltage outputs of the LVDT and the load cell, plus the square wave loading pattern were recorded on a Gould Brush 2400 four channel recorder. Microstrain readings from the calibrated reinforced rubber membranes were measured by a BLH 120C strain gauge indicator.

The data for each individual test was put into computer files. The data was processed and reduced at RPI's Interactive Computer Graphics Center. Appropriate plots could then be produced and viewed on computer terminals; hard copies could be made if desired.

F. Equipment Calibration

Proving Ring Load Cells

Proving ring load cells with ranges of 50, 100, 200, 400 and 800 kg were supplied and calibrated by Geonor. All were linear throughout their ranges.

Load Cell

The Schaevitz load cell used for measurement of vertical load was calibrated directly on the direct simple shear apparatus. While supporting the bottom of the sliding shear box, loads were applied to the load cell through the lever arm, and the corresponding voltages measured. The voltage output was linear throughout its range.

LVDT

The Hewlett Packard LVDT used for measurement of horizontal displacements was also calibrated on the direct simple shear apparatus. Voltage

outputs were recorded for displacements measured by the dial gauge. The voltage output was linear for $\pm$ 3.0 mm displacement.

Friction

Friction in the vertical load unit and the horizontal load unit originates primarily in the ball bearing bushings. This friction can be measured by the 50 kg proving ring load cell or by the Schaevitz load cell. It was found to be negligible.

Membrane Resistance

The resistance of the reinforced rubber membranes to shear can be determined by shearing them when they are filled with water. Ladd and Edgers (68) found that the resistance to shear increases with increasing shear strain and with decreasing normal loads. It was also found that the resistance was less than .01 kg/cm^2 for a normal stress of .3 kg/cm^2. Normal loads greater than .3 kg/cm^2 caused the O-rings that seal the membrane to the caps to slip. Data was therefore not available for normal stresses greater than .3 kg/cm^2. Similar results were also found by Geonor (41).

Results such as these are valid only for the particular membrane tested. It seems reasonable however, that results for other membranes would be similar. Since the samples tested for this study were consolidated to stresses greater than .3 kg/cm^2, it was felt that the membrane resistance could be considered negligible.

Vertical Deformation

Vertical deformations of the soil sample are measured between two reference points, the top half of the sliding shear box and the base. Since the parts of the direct simple shear apparatus between these two points deform under the action of a vertical stress, it is important to distinguish this deformation from the deformation of the sample itself. This is especially important for constant volume tests, where the vertical stress is changed to keep the sample height (volume) constant. As the vertical stress is changed, the equipment deformation also changes, and this must be taken into account.

The parts of the direct simple shear apparatus of interest for deformation studies include the sliding shear box assembly, the caps, the porous stones, and the pedestal. The deformation of all these parts can be measured by inserting between the caps a steel dummy sample in place of a soil sample. Vertical loads are applied through the lever arm, and the vertical deflection is measured by the vertical dial gauge. The steel dummy sample also deforms under stress application, but the deformation of this steel cylinder can be determined from theoretical considerations; it was found to be negligible.

Most of the vertical deformation is due to the seating and compression of the porous stones. To insure consistent results, the same porous stones were placed in the upper and lower caps for all tests. These stones were marked so that they could always be placed with the same orientation in the caps.

An effort was made to determine equipment deformation such as would occur during the actual testing situation. Using the steel dummy sample, the sample assembly was prepared just as it would be during test conditions; the consolidation loading sequence was also identical to that in actual tests. After the final consolidation load was applied, the vertical load was decreased in small increments. This vertical load decrease is necessary to maintain constant volume conditions for the normally consolidated and slightly overconsolidated soils tested in this program.

Equipment deformation measured during these tests showed some variation. The variation occurred mainly during the loading sequence; the slope of the deformation-load curve for unloading was virtually identical for each trial. Average deformation curves for loading and unloading were obtained for each consolidation history used. An example is shown in Figure 6 for 50 cm^2 diameter samples normally consolidated to .510 kg/cm^2.

During constant volume testing, the equipment deformation curve is entered at the appropriate consolidation stress. As the load is changed, the vertical dial gauge reading is changed according to this curve. Thus, the equipment deformation is accounted for, and the volume of the sample remains constant.

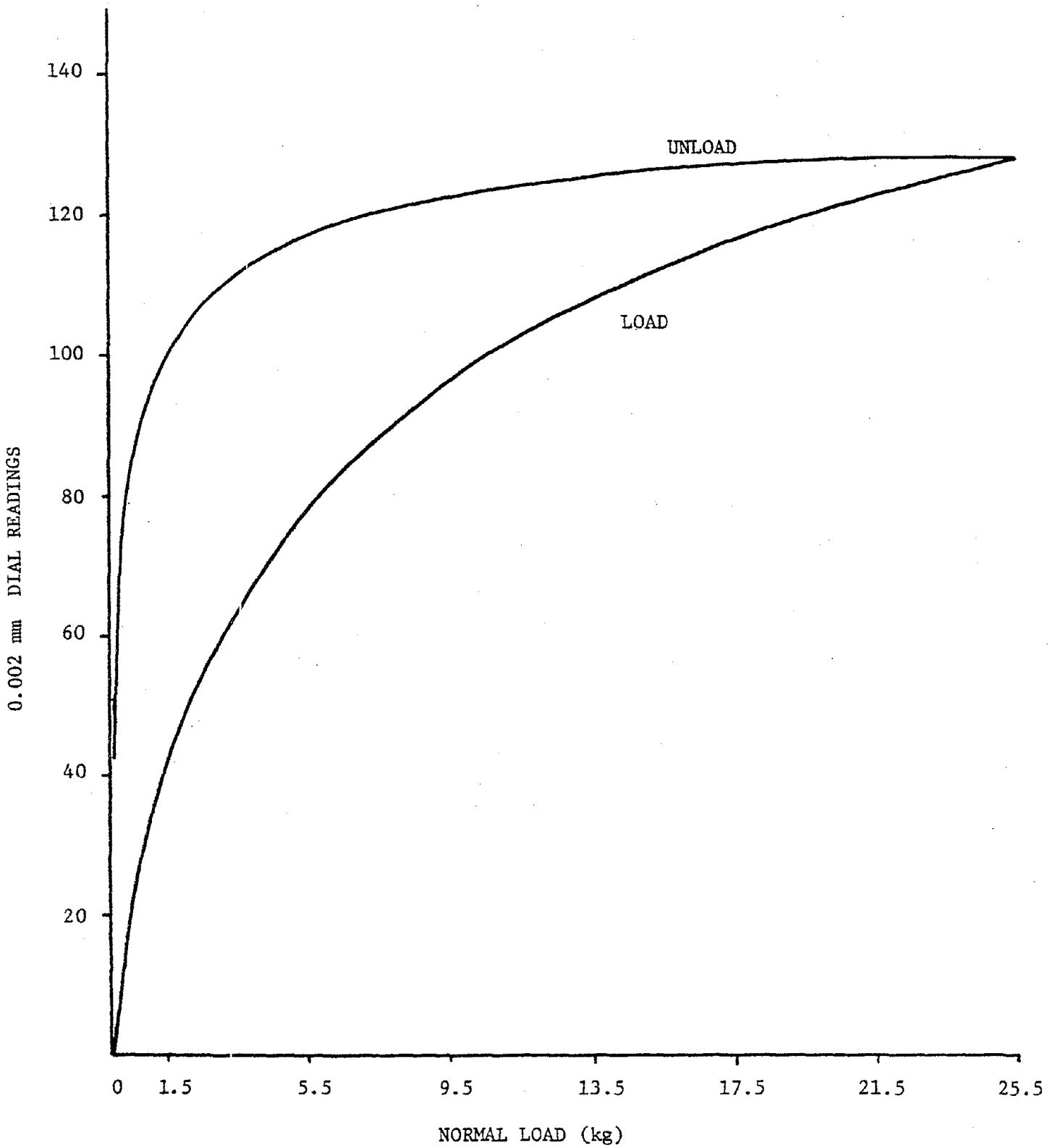

FIGURE 6. EXAMPLE OF EQUIPMENT DEFORMATION CURVES FOR THE 50 cm^2 SAMPLE SIZE WITH CONSOLIDATION TO .510 kg/cm^2.

PART 4

TESTING PROCEDURES

The soils investigated in this study were stored in an environmentally controlled storage room under high humidity conditions. The storage temperature was kept at approximately 3°C to simulate in situ conditions and to prevent the generation of gases in the samples. The soils used, Concord Blue Clay and Gulf of Alaska Clay are described in PART 6. The Concord Blue Clay samples were sealed in wax and plastic; the Gulf of Alaska Clay was sealed in its core tube.

When a sample was needed for testing, it was removed from the storage room and placed in an adjacent environmentally controlled room for sample trimming. This room was also maintained under high humidity conditions to prevent sample drying during the trimming operation. However, room temperature (approximately 20°C) was maintained in this chamber. For the Gulf of Alaska Clay, only the soil needed for the test was extruded from the tube. The core tube was then immediately resealed following the extrusion.

The trimming apparatus supplied with the NGI direct simple shear device was used for all tests. The NGI direct simple shear device and the trimming apparatus are described in PART 3. Except for minor details, the trimming method used was identical to that described by Geonor (41). Because of the rather lengthy procedure, and the close mechanical tolerances of the trimming apparatus, some practice was needed to obtain consistent results. The average trimming time was approximately 45 minutes.

From the leftover trimmings, 4 water content samples were taken. If possible, undrained shear strength and sensitivity were measured by using the Swedish fall cone method, a pocket penetrometer and a torvane device. The initial sample height was also measured during the trimming operation.

After sample trimming was completed, the sample was carefully moved from the environmentally controlled room to the NGI direct simple shear apparatus. Since the sample was now sealed in its membrane, sample drying was not a problem. Drainage hoses leading to water supplies were connected to the upper and lower caps of the sample. For the Gulf of Alaska Clay, a sea water solution (obtained from a local aquarium supply store) was used as the water supply. A quantity of water was circulated through the caps and the inclosed porous stones to flush out any air which may have been trapped during the trimming process.

The sample was next clamped to the direct simple shear device. The sliding shear box was brought into contact with the top of the sample, and the normal load lever arm was leveled. A small weight (10 grams) was placed at the end of the lever arm to insure contact between the sample and the shear box. For tests in which lateral stress measurements were taken, the calibrated membrane was connected to a strain gauge indicator. Because the calibrated membranes are very sensitive to temperature changes which may be caused by handling the sample, the sample was allowed to sit for 1 hour before taking an initial reading on the strain gauge indicator and beginning consolidation.

After taking an initial reading on the vertical deformation dial gauge, sample consolidation was begun. Consolidation loads were applied in increments similar to the standard laboratory consolidation test. The time between each load increment was approximately twice the time for 100%

primary consolidation. The final consolidation load was applied for a minimum of 24 hours, and the sample was then ready for testing.

All tests were run under "undrained" conditions by maintaining the sample at a constant volume. Since the sample has a constant cross-sectional area, constant volume tests are conducted by adjusting the normal load to keep the sample height constant. During shear, drainage is allowed, and a rate of strain is selected such that no excess pore water pressures develop in the sample during the test. The change in vertical stress in the sample is equated to the change in excess pore pressures which would have been measured had drainage been prevented (98).

Static tests were run at a sufficiently slow rate to prevent a build-up of pore pressure while keeping a reasonable testing time. Typically, static tests were performed in 7 hours. Square wave form, controlled stress cyclic tests were performed at frequencies of .5 or .1 Hz. These frequencies were selected to simulate earthquake or storm wave loading applications. It may be argued that the use of such high frequencies can impede accurate pore pressure measurements. However, previous research has shown that the permanent accumulation of pore pressures can be measured under these conditions (90). However, the measurement of pore pressure changes within a given cycle of loading may not be possible at high loading frequencies. For cyclic tests that did not fail, a static test was performed immediately afterwards.

Following the completion of testing, the sample assembly was removed from the shear apparatus. A final water content of the sample was taken at this time.

The data obtained from each individual test was compiled from the strip chart recordings. The data was reduced and processed by computer to obtain the desired results. Using a computer graphics system, the data was plotted for quick visual observation. The test results are presented and discussed in PARTS 7 and 8.

PART 5

STRESS CONDITIONS IN THE NGI SAMPLE

A. Background

Cyclic shear stresses induced on an in situ soil element by either wave or earthquake loadings can often be closely approximated by cyclic shear stresses applied on the horizontal planes of the soil element. If an initial shear stress exists on the horizontal planes prior to cyclic loading, the cyclic shear stresses can be superimposed on this static shear stress.

The cyclic direct simple shear apparatus was developed to reproduce these field conditions in the laboratory. The stress conditions imposed on a soil element in the field and on the boundaries of the NGI direct simple shear sample are shown in Figure 7. The lack of complementary shear stresses on the vertical boundaries of the sample imply that the boundary stress conditions are not ideal, making the interpretation of direct simple shear tests rather difficult.

With regard to the SGI direct simple shear device, Kjellman (62) noted that for equilibrium requirements, the normal stresses on the upper and lower surfaces of the sample must be unevenly distributed. The shearing stresses on these surfaces must also be unevenly distributed, since they must be zero close to the front and rear of the sample. It was concluded that the distribution of stresses in the sample is not perfect, but certainly better than in conventional direct shear devices.

Hvorslev and Kaufman (55) also noted that with the SGI direct simple shear device neither the vertical normal stresses nor the horizontal shear stresses acting on the sample are distributed uniformly. The nonuniformity tends to increase with increasing deformation.

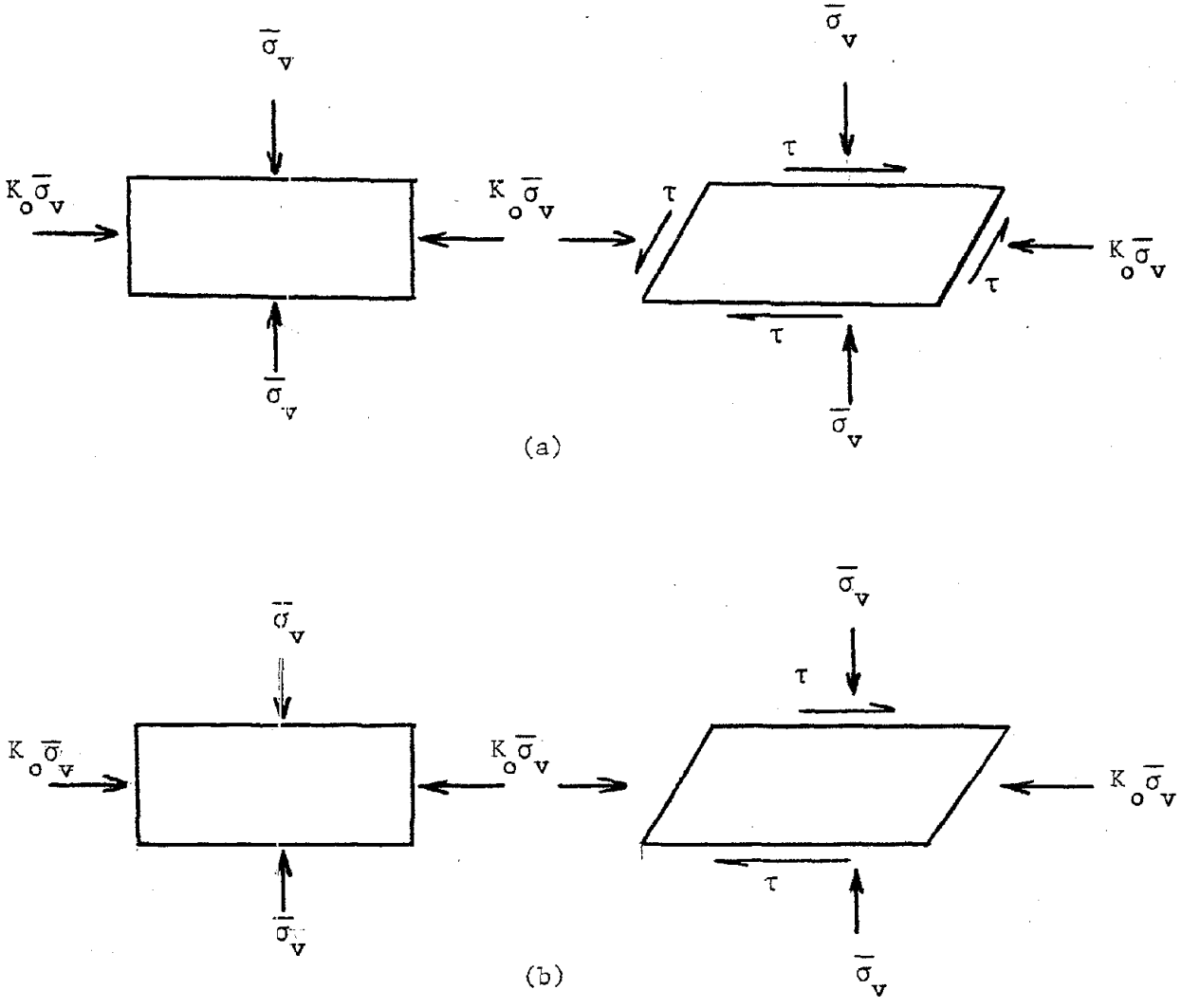

FIGURE 7. (a) APPLIED STRESS CONDITIONS ON AN IN-SITU SOIL ELEMENT

(b) APPLIED STRESS CONDITIONS ON A NGI DIRECT SIMPLE SHEAR SOIL SAMPLE

Roscoe (106) analyzed the stresses acting on a sample in the Cambridge simple shear device using the theory of elasticity and assuming a linear elastic, isotropic material. He concluded that the moment produced by the shear stresses acting on the upper and lower sample boundaries is exactly balanced by the moments produced by the nonuniform horizontal and vertical stress distributions acting on the sample boundaries. The distribution of shear stresses acting on the upper and lower boundaries of the sample is also nonuniform. The magnitude of the shear stress is zero at the outer edges since there are no complimentary shear stresses on the end faces of the sample. However, the shear stress increases rapidly with distance from the ends of the sample, and it is quite uniform in the middle third of the upper and lower boundaries of the sample. The sample was also found to be approximately subjected to simple shear strain. Roscoe points out that these results are strictly valid only for elastic materials, but that the solutions should apply to soils for small strains, and that they can be considered as a guide for the behavior of soils at larger strains.

Duncan and Dunlop (23) also investigated the stress distributions within a sample tested in a Cambridge simple shear apparatus. The stress conditions were analyzed using the finite element method, and employing nonlinear and anisotropic stress strain characteristics for the material. Stress conditions were found to be nonuniform. For equilibrium, the horizontal shear stresses increase in magnitude from the top and bottom of the sample, reaching a maximum at midheight. These stress non-

uniformities result from the lack of complimentary shear stresses on the ends of the sample. It was also determined that progressive failure occurred within the sample, with failure beginning near the ends of the specimen. The size of the failure zones gradually increase and they eventually merge with increasing shear strain. It is evident that the stress conditions are sufficiently nonuniform to result in early failure of some zones within the sample.

Duncan and Dunlop (23) pointed out however, that their analysis shows that the stress nonuniformities are most severe near the ends of the sample. They concluded that the stresses in the center of the sample correspond closely to pure shear conditions. Assuming a uniform stress condition provides a simple and useful means of comparing strength values measured in simple shear with those measured in other tests.

Lucks et al (82) analyzed the stress conditions existing in a NGI direct simple shear sample. A three-dimensional finite element model was employed assuming linear elastic, isotropic material parameters. It was found that stress concentrations can be expected at the edges of the sample, but that these concentrations are quite local. Approximately 70% of the sample was found to have fairly uniform stress conditions, especially at low strains. The authors also concluded that progressive yielding is of minor importance.

Prevost and Hoeg (98) recently investigated the stress conditions occurring in simple shear test samples. The effects of partial boundary slippage at or immediately inside the interface between the soil specimen and the top and bottom caps of the Cambridge simple shear apparatus were determined using an isotropic elastic analysis. Such slippage was found to increase the nonuniformity of stress distributions in the sample. It

is therefore important to provide the best possible seating between the sample and the caps. It was also noted that a substantial change in lateral stress can occur on soil samples being tested in simple shear devices.

A finite element study of the NGI direct simple shear test sample for cyclic loading conditions was conducted by Shen et al (129). It was found that the shear strain distribution in the soil sample is nonuniform and asymmetric. For the soils studied, the NGI direct simple shear device may introduce an error of 5 to 15% in shear modulus determination. It was concluded however, that this magnitude of error may be viewed as acceptable for most geotechnical engineering work.

Wright et al (150) also studied the stress distributions in samples tested by the Cambridge simple shear device and the NGI direct simple shear device. Results were based on elasticity theory using the Saint Venant solution (141) for a fixed end beam of square or circular cross-section subjected to an end load. It was concluded on the basis of this study and an experimental photoelastic study that the stress distributions within the sample are totally nonuniform. The authors noted however, that their conclusions were based on elasticity theory and that the boundary conditions in the Saint Venant problem are not exactly the same as in simple shear samples. It was argued however, that it is important to determine the character of the stress distributions, and to compute their order of magnitude in order to interpret simple shear test results.

In a recent state of the art publication on the measurement of soil properties, Woods (149) noted that the results of analytical studies are dependent on the assumptions made in the analysis. Quantitative interpretation of the results may be limited by the assumptions made, but the general trends observed should not be ignored. It was concluded that despite the internal complexities and uncertainties associated with the cyclic simple shear test, the test has been a useful tool in studying cyclic shear phenomena. For practical purposes, the potential effects of nonuniformities in stress distribution may be minimal.

It should be noted that all laboratory soil testing devices have their advantages and disadvantages. Most devices test relatively small samples and thereby make boundary effects and end conditions, with their resulting stress concentrations, a major concern. Just as theoretical studies are dependent on the assumptions made, the same can be said for experimental results.

Even though quantitative results based on assumed stress conditions may not be strictly valid, the general conclusions and trends cannot be ignored, and these have sucessfully been used in geotechnical engineering practice.

B. Assumed Stress Conditions Used For the Interpretation of Test Results

Because of difficulties in maintaining undrained conditions in direct shear devices, undrained tests have often been carried out as constant volume tests. Taylor (137) first used this approach in 1952 for a box shear test. He demonstrated that simply running a fast test did not prevent drainage for typical clays.

Undrained conditions are simulated on the NGI direct simple shear device by maintaining a constant volume (9). Since the reinforced rubber mem-

branes maintain the sample at a constant cross-sectional area, constant volume tests are conducted by adjusting the normal vertical load to keep the sample height constant. During shear, the sample is drained and a rate of strain is selected so that excess pore pressures in the sample are zero during the test. The change in vertical stress on the sample is equated to the change in excess pore pressures which would have been measured had drainage been prevented (98).

Prevost and Hoeg (98) note that it will not be possible in general to conduct a constant volume test which is truly identical to an undrained test. In a constant volume test, incompressibility is satisfied only in an average sense for the entire sample, while in a truly undrained test, incompressibility is satisfied everywhere within the sample. However, in a truly undrained test, there is also a redistribution of pore pressures within the sample, and the measured excess pore pressure is valid only as an average value.

Although some arguments may exist, it will be assumed for this investigation that the measured change in vertical normal stress is equal to the pore pressures which would be generated in an undrained test. Because the excess pore pressures are zero throughout the sample during shear, all measured normal stresses are effective stresses.

For tests in which lateral stresses were measured, the vertical and horizontal normal stresses along with the shear stress acting on the upper and lower horizontal boundaries of the sample are known. The measured stresses acting on a NGI direct simple shear sample are shown in Figure 8. The stresses assumed to be acting on an infinitesmal element at the center of the sample are also shown in this figure.

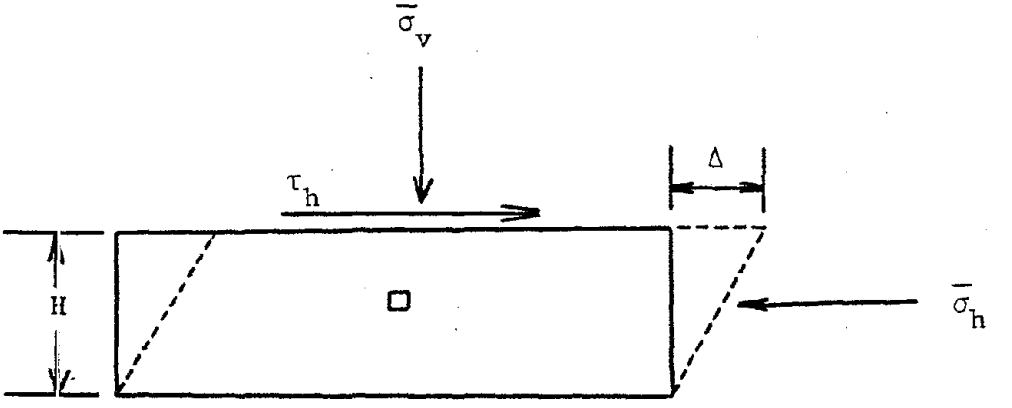

(a)

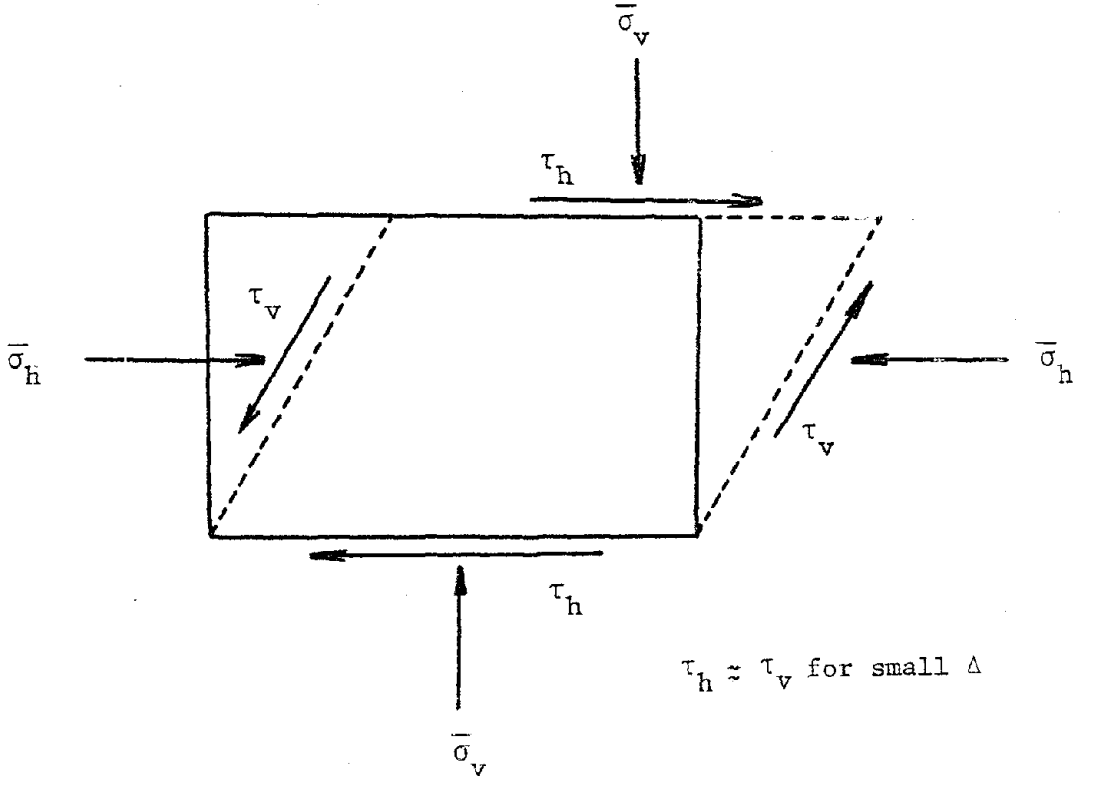

(b)

FIGURE 8. (a) MEASURED BOUNDARY STRESSES ACTING ON THE NGI DIRECT SIMPLE SHEAR SAMPLE

(b) ASSUMED STRESS CONDITIONS ACTING ON AN ELEMENT FROM THE CENTER OF THE SAMPLE

The shear stress acting on the sides of this element are assumed to be equal to the horizontal shear stress.

From the three measured stresses, a Mohr's circle of stress can be drawn for the soil element at any stage during the test as shown in Figure 9. The variables indicated in the figure can be determined from the geometry of the Mohr's circle along with the known values of the vertical effective normal stress $\bar{\sigma}_v$, the horizontal effective normal stress $\bar{\sigma}_h$, and the horizontal shear stress τ_h as follows:

$$\bar{p} = \frac{\bar{\sigma}_v + \bar{\sigma}_h}{2} = \frac{\bar{\sigma}_1 + \bar{\sigma}_3}{2}$$

$$q = \left[\frac{(\bar{\sigma}_v - \bar{\sigma}_h)^2}{4} + \tau_h^2 \right]^{1/2} = \frac{\bar{\sigma}_1 - \bar{\sigma}_3}{2}$$

where $\bar{p}$ and q define the uppermost point of the Mohr's circle or the effective stress point (72). The major and minor effective principle stresses are $\bar{\sigma}_1$ and $\bar{\sigma}_3$.

$$\phi_m = \sin^{-1}\left(\frac{q}{\bar{p}}\right)$$

where ϕ_m is the mobilized friction angle of the soil,

$$\theta_p = \tan^{-1}\left[\frac{\tau_h}{\frac{(\bar{\sigma}_v - \bar{\sigma}_h)}{2} + q}\right]$$

where θ_p is the angle between the horizontal plane and the plane on which the major principle stress acts,

$$\theta_q = 45 - \theta_p$$

where θ_q is the angle between the horizontal plane and the plane on which the maximum shear stress acts.

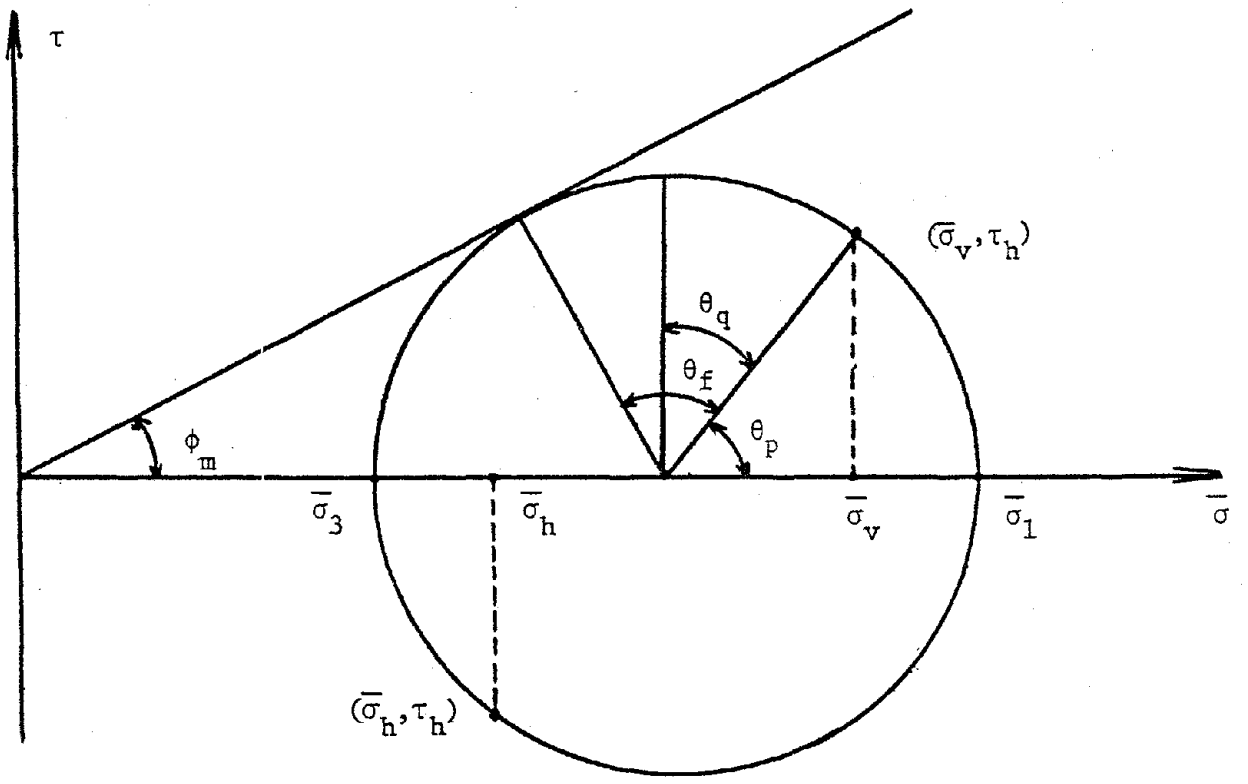

$$\bar{p} = \frac{\bar{\sigma}_v + \bar{\sigma}_h}{2} = \frac{\bar{\sigma}_1 + \bar{\sigma}_3}{2}$$

$$q = \left[\frac{(\bar{\sigma}_v - \bar{\sigma}_h)^2}{4} + \tau_h^2\right]^{1/2} = \frac{\bar{\sigma}_1 - \bar{\sigma}_3}{2}$$

$$\phi_m = \sin^{-1}\left(\frac{q}{\bar{p}}\right)$$

$$\theta_p = \tan^{-1}\left[\frac{\tau_h}{\frac{(\bar{\sigma}_v - \bar{\sigma}_h)}{2} + q}\right]$$

$$\theta_q = 45 - \theta_p$$

$$\theta_f = 45 + \frac{\phi_m}{2} - \theta_p$$

$$\bar{\sigma}_1 = \bar{p} + q$$

$$\bar{\sigma}_3 = \bar{p} - q$$

FIGURE 9. MOHR'S CIRCLE OF STRESS FOR A SOIL ELEMENT AT THE CENTER OF THE NGI DIRECT SIMPLE SHEAR SAMPLE

$$\theta_f = 45 + \frac{\phi_m}{2} - \theta_p$$

where θ_f is the angle between the horizontal plane and the plane of maximum obliquity, and

$$\overline{\sigma}_1 = \overline{p} + q$$

$$\overline{\sigma}_3 = \overline{p} - q$$

Note that the above equations are valid for no cohesion, i.e., c = 0.

All tests that were performed during this study were analyzed on the basis of the assumptions and equations presented here. Actual test results are presented in Part 7.

PART 6

SOILS

To obtain an understanding of clay soil behavior in the field, the soil's structure should be preserved as found in situ. Therefore, only undisturbed samples of cohesive soils were tested in the laboratory. Two different fine grained soils were used in this investigation; these soils are described in this section. The problems associated with these soils are also noted, along with reasons for obtaining laboratory test data.

A. Gulf of Alaska Clay

Petroleum related activities in the outer continental shelf region in the Gulf of Alaska may stimulate major marine construction in this area. Therefore, it is important to identify and evaluate geologic and geotechnical problems associated with this region.

Marine geologic studies were conducted by the United States Geological Survey on the continental shelf and the upper continental slope in the Gulf of Alaska. Several areas of slope instability were discovered; these are characterized by submarine slides and slump blocks (12,45). One area of instability is the Copper River prodelta from which the clay samples used in this study were obtained.

The Copper River is a major source of Holocene sediment; the annual sediment discharge being 107×10^6 tons. Much of this sediment has accumulated on the prodelta, reaching a maximum thickness of 350 meters, with an average thickness of 150 meters. The rate of sedimentation is very high in this area, being on the order of 10-15 meters per 1,000 years (12).

Seismic reflection surveys of the Copper River prodelta show disrupted bedding and irregular topography, indicating submarine slides or slumps. This type of structure is evident across the entire span of the prodelta, an area of 1,700 km^2. The sea floor in this area has a slope of approximately 0.5° (12).

The most notable characteristic of submarine slope failures is that they can occur on extremely flat slopes. Since the extent of many submarine slopes is fairly large, the infinite slope method of analysis can be used to advantage (87). From this simple model (Figure 10), the equation for stability is

$$FS = \left[1 - \frac{\Delta u}{\gamma' H \cos^2 i}\right] \frac{\tan \phi'}{\tan i}$$

where

FS = Factor of safety

Δu = Excess pore water pressure

γ' = Buoyant unit weight of soil

H = Depth of failure surface measured from the surface of the sediment

i = Slope angle

ϕ' = Effective stress friction angle of soil.

The effect of the excess pore pressure is to reduce the effective normal stress on the failure plane. The shearing resistance is therefore reduced, while the applied shear stress caused by the weight of the slope material remains constant. The effective stress friction angle for the Copper River prodelta is about 24° (45). If no excess pore pressures are present

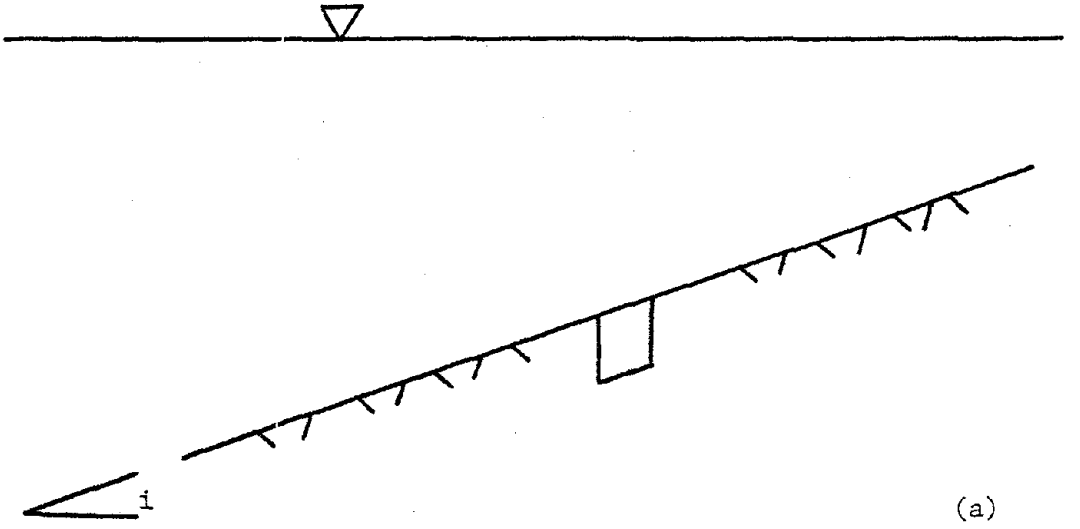

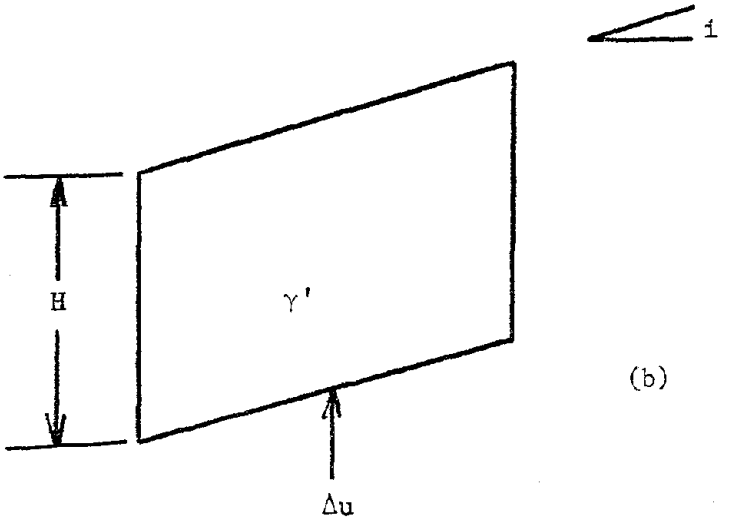

FIGURE 10. SUBMARINE SLOPES AND STABILITY ANALYSIS USING INFINITE SLOPE METHOD

(a) SUBMARINE SLOPE

(b) SOIL SLICE USED FOR STABILITY ANALYSIS

in the sediment, the theoretical maximum slope angle should also be 24°.

Excess pore pressures in marine sediments can be produced by cyclic loading, high rates of sedimentation, and the presence of gas charged sediments (111). All of these factors must be taken into consideration in the Copper River prodelta. Other factors which should also be considered for marine slope stability determinations are removal of slope support by faulting or erosion, seismic forces and accelerations, and tectonic slope steepening.

The high rate of sedimentation in the Copper River prodelta causes a lag between sediment accumulation and subsequent consolidation leading to an excess pore pressure build up. This is frequently referred to in the literature as underconsolidation. Hampton et al (45) investigated the significance of the excess pore pressure resulting from high sedimentation rates in the Copper River delta. The theoretical approach developed by Gibson (42) was used to determine the excess pore pressures. Using the infinite slope method of analysis, along with the theoretical pore pressures, it was determined that only slopes with angles less than 2.6° would be stable. This is a substantial decrease from the 24° angle determined for the condition of no excess pore pressures.

Excess pore pressures are also developed by earthquake loadings. The forces and accelerations generated by the earthquake increase the applied shear stresses acting on potential slope failure surfaces causing further instability. Reimnitz (102) attributed slump structures seen on seismic records from the Copper River prodelta to the 1964 Alaska earthquake.

Excess pore pressures can also be generated by storm wave loading. The waves induce pressure variations on the seafloor. The magnitude of these pressure fluctuations depends upon wave height, wave length, and water depth. Hampton et al (45) show that wave induced pressure fluctuations can be of importance in water depths of up to at least 150 meters. The wave action can also cause erosion on the seafloor.

Indications of free gas were noted by seismic data in the Copper River prodelta. The gas could be methane generated within the holocene sediment or it could be gas that has been liberated from underlying rock and has migrated up fault planes (67).

In summary, all of the factors noted above can lead to the instability of submarine slopes. For the Copper River prodelta, the rapid rate of sedimentation is important. The Gulf of Alaska is also in an area of intense seismic activity. Storms with large waves are common, especially in the winter months (18). Therefore, it is imperative to determine the behavior of these submarine soils under cyclic loading.

A four inch inside diameter undisturbed core sample was obtained from the United States Geological Survey (USGS) for laboratory testing. The sample was taken in the Copper River prodelta and it contains sediment from one to two meters depth below the seafloor. Pertinent geotechnical data is given in Table 1.

B. Concord Blue Clay

The Concord Blue Clay used in this study was obtained from a site Southeast of Buffalo, New York. The clay is a glacial lake deposit, and it is readily attainable. Samples were taken in 1 ft^3 undisturbed blocks from a depth of approximately 10 ft below the ground surface. Pertinent geotechnical data is given in Table 2.

GULF OF ALASKA SAMPLES

SITE: COPPER RIVER DELTA

TYPE: 4" DIAMETER UNDISTURBED CORES

GEOTECHNICAL DATA

WATER CONTENT	57 - 65%
LIQUID LIMIT	48%
PLASTIC LIMIT	25%
SPECIFIC GRAVITY	2.84
ϕ	24°
SENSITIVITY (FALL CONE)	4.0
CONSOLIDATION HISTORY	UNDERCONSOLIDATED
% SAND	1
% SILT	34
% CLAY	65
SEDIMENTATION RATE	10-15 m/1000 years

TABLE 1. GEOTECHNICAL DATA FOR THE GULF OF ALASKA CLAY

CONCORD BLUE CLAY

SITE: SE CF BUFFALO, N.Y.

TYPE: UNDISTURBED 1 ft^3 BLOCKS

GEOTECHNICAL DATA

WATER CONTENT	27 - 28%
LIQUID LIMIT	34%
PLASTIC LIMIT	21%
SPECIFIC GRAVITY	2.76
ϕ	25°
SENSITIVITY (FALL CONE)	1.4
CONSOLIDATION HISTORY	NORMALLY CONSOLIDATED

TABLE 2. GEOTECHNICAL DATA FOR CONCORD BLUE CLAY

PART 7

TEST RESULTS

This section summarizes the data obtained from the laboratory direct simple shear tests that were performed for this investigation. The data include horizontal stress measurements for the tests on the Gulf of Alaska clay, but not for the tests on the Concord Blue clay.

A. Gulf of Alaska Clay

Introduction

The tests performed on the Gulf of Alaska clay are summarized in Table 3. A test number followed by an S indicates a static test and a C indicates a cyclic test. An explanation for each column of data is presented in Table 4.

A total of 9 tests were performed on Copper River prodelta clay samples which were normally consolidated in the laboratory. Data for all of these tests include the measurement of lateral, horizontal stresses using calibrated reinforced rubber membranes.

The static tests were performed under controlled strain conditions with a strain rate of 75 minutes per millimeter of horizontal movement of the sample top. The cyclic tests were performed using a controlled stress mode with various magnitudes of cyclic stresses. Square wave load shapes were used with a cyclic frequency of 0.1 Hz. This frequency was chosen to simulate both earthquake and storm wave loadings while allowing ample time for data acquisition. The standard 50 cm^2 sample size was used for all tests.

1	2	3	4	5	6	7	8	9	10	11	12	13	14	15
		BUILDING IN							CONSOLIDATION					
Test No.	D	w %	e	H_i cm	S_{u_2} kg/cm^2	S_{u_2} kg/cm^2	S_{u_2} kg/cm^2	S_t	σ_{vo_2} kg/cm^2	τ_{ho_2} kg/cm^2	σ_{vm_2} kg/cm^2	OCR	H_f cm	ε_v %
01S	L	63.0	1.79	1.72	-	-	-	-	.510	0.0	.510	1.0	1.53	10.0
02S	L	58.0	1.65	1.64	-	-	.039	-	.510	0.0	.510	1.0	1.48	9.7
03S	L	60.4	1.72	1.72	-	-	.039	-	.240	0.0	.240	1.0	1.59	7.5
04C	L	59.3	1.68	1.74	-	-	.036	-	.510	0.0	.510	1.0	1.60	8.3
05C	L	67.2	1.91	1.66	-	-	.025	-	.510	0.0	.510	1.0	1.39	16.2
06C	L	64.8	1.84	1.65	-	-	.024	-	.510	0.0	.510	1.0	1.40	13.0
07C	L	61.6	1.75	1.40	-	-	.033	4.2	.510	0.0	.510	1.0	1.22	13.0
08C	L	57.5	1.63	1.80	-	-	.036	3.9	.510	0.0	.510	1.0	1.62	10.0
09C	L	64.0	1.82	1.84	-	-	.032	3.4	.510	0.0	.510	1.0	1.61	12.4

TABLE 3. SUMMARY OF TESTS - GULF OF ALASKA CLAY

	16	17	18	19	20	21	22	23	24	25	26	27	28
	CYCLIC LOADING						STATIC LOADING				AFTER TEST		
Test No.	τ_c kg/cm^2	τ_c/S_u %	N	γ_n %	u_n kg/cm^2	f Hz	S_u kg/cm^2	γ_f %	u_f kg/cm^2	RATE min/mm	w %	e	Remarks
01S	-	-	-	-	-	-	-	-	-	-	-	-	Bottom of core, cancelled
02S	-	-	-	-	-	-	.134	16.9	.270	75	51.5	1.46	Top of core
03S	-	-	-	-	-	-	.087	22.2	.101	75	57.5	1.63	
04C	.047	33	1030	14.9	.436	.1	-	-	-	-	52.3	1.49	
05C	.056	40	925	19.1	.436	.1	-	-	-	-	52.9	1.50	Membrane stretched
06C	.070	50	105	17.9	.414	.1	-	-	-	-	54.4	1.55	
07C	.084	60	60	27.5	.425	.1	-	-	-	-	45.7	1.30	
08C	.098	70	26	17.5	.384	.1	-	-	-	-	49.4	1.41	
09C	.035	25	3000	.04	.076	.1	.160	17.6	.252	75	49.2	1.40	No failure in cyclic loading

TABLE 3. (CONTINUED)

COLUMN	EXPLANATION
1.	Test No.
2.	Sample Size : L = Large, S = Small
3.	Water Content of Trimmings
4.	Void Ratio of Trimmings
5.	Sample Height
6.	Undrained Shear Strength (Pocket Penetrometer)
7.	Undrained Shear Strength (Torvane)
8.	Undrained Shear Strength (Swedish Fall Cone)
9.	Sensitivity (Swedish Fall Cone)
10.	Vertical Consolidation Stress
11.	Static Shear Stress
12.	Maximum Consolidation Stress
13.	Overconsolidation Ratio
14.	Sample Height Following Consolidation
15.	Vertical Strain
16.	Cyclic Shear Stress
17.	Cyclic Shear Stress as a Percent of Static Strength
18.	Number of Cycles Tested
19.	Shear Strain at N Cycles
20.	Pore Pressure at N Cycles
21.	Frequency of Loading
22.	Static Undrained Shear Strength (Peak of Stress-Strain Curve)
23.	Shear Strain at Peak of Stress-Strain Curve
24.	Pore Pressure at Peak of Stress-Strain Curve
25.	Strain Rate
26.	Water Content of Sample (After Test)
27.	Void Ratio of Sample (After Test)

TABLE 4. EXPLANATION FOR TABLES 3 and 5

Static Test Results

Stress-strain curves for the static tests are shown in Figure 11. The shear stress was normalized by dividing by the consolidation stress σ_{vo}. Test No. 01 was performed on a highly disturbed sample taken from the bottom of the core tube. This was a pilot test, and the results will not be presented. Test No. 02 was performed on a sample taken from the top of the core tube; it appeared to be somewhat disturbed. This may explain the low stress-strain curve obtained for this test. The normalized stress strain curve for Test No. 03 was taken to be typical for undisturbed samples tested at the strain rates used in this investigation. Test No. 09 was performed following cyclic loading which did not cause failure. The stress-strain curve obtained for this test is consistent with published literature (80,90,140).

Pore pressure-strain curves for the static tests are shown in Figure 12. The pore pressure was normalized by dividing by the consolidation stress. The pore pressures increase continuously throughout the tests, although the largest increase occurs during the first few percent of strain. These curves are directly opposite of the stress-strain curves in Figure 11, i.e., excess pore pressures are greatest for the lowest stress-strain curve. Therefore, there is a good correlation between excess pore pressures and the shear stress that a sample can develop. Test No. 03 was again taken to be typical for undisturbed samples. Note that Test No. 09 had significant pore pressures at the beginning of the test that were caused by the previous cyclic loading.

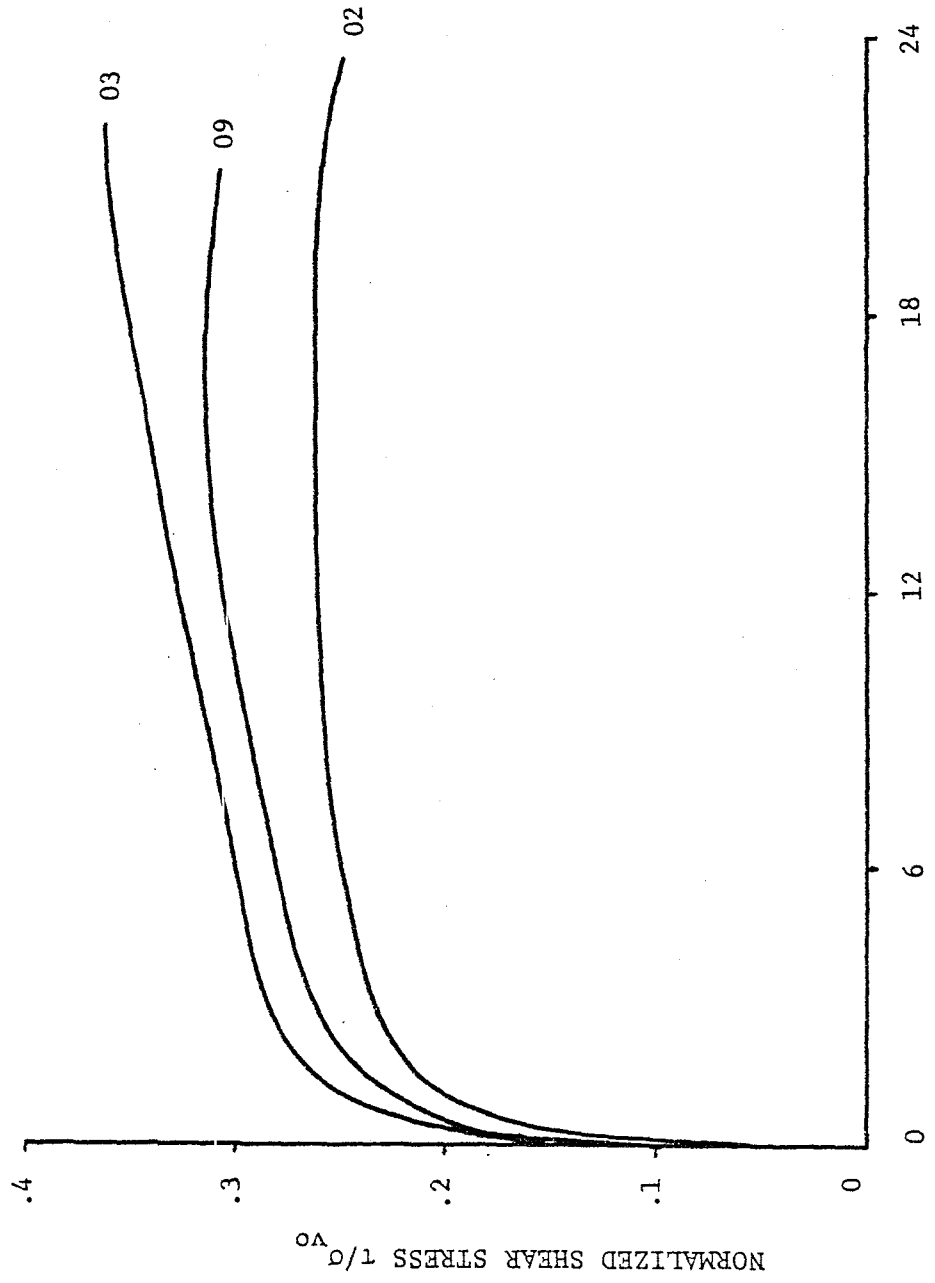

FIGURE 11. STRESS-STRAIN CURVES FOR STATIC TESTS PERFORMED ON GULF OF ALASKA CLAY

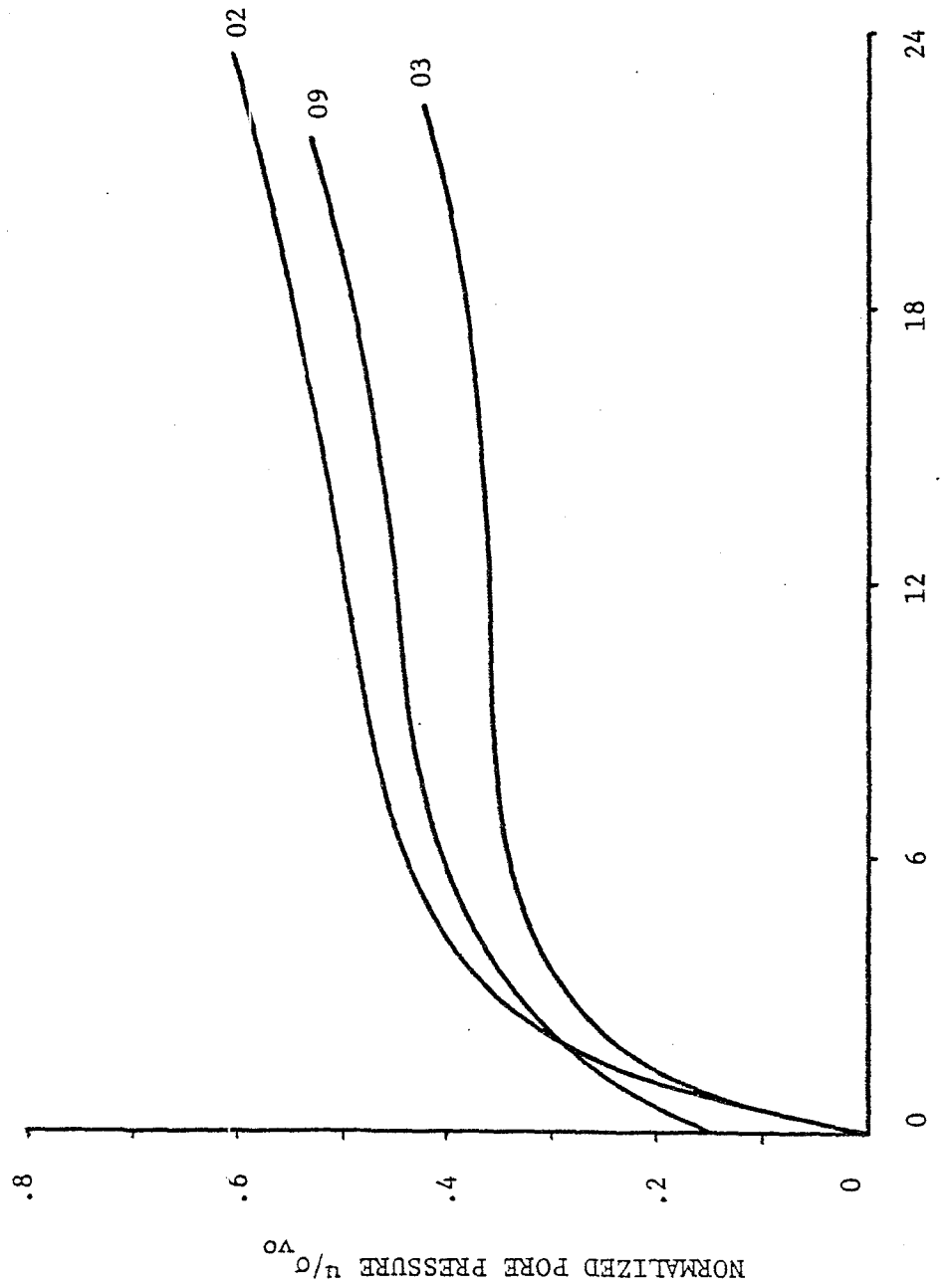

FIGURE 12. PORE PRESSURE - STRAIN CURVES FOR STATIC TESTS PERFORMED ON GULF OF ALASKA CLAY

"Stress path" data for the static tests showing horizontal shear stress vs. vertical normal stress is presented in Figure 13. The data for Test 02 does not seem consistent with the other test results; this is probably caused by sample disturbance. A failure line was drawn through the tips of these curves. This line corresponds to approximately 22% shear strain at which the static tests were terminated. Using the assumption that

$$\phi = \tan^{-1} [\text{slope of the failure line}],$$

the angle of internal friction ϕ for the clay was computed to be 30°. Another failure line based on the more realistic assumption of failure at 3% shear strain is also shown in Figure 13. For this failure line, ϕ was computed to be 21°.

Shear modulus vs. shear strain data for the static tests are shown in Figure 14. The shear modulus was normalized by dividing by the consolidation stress.

Vertical and horizontal normal stress vs. shear strain for the static tests are shown in Figures 15 and 16. The data was normalized by dividing by the consolidation stress. The vertical normal stress decreases throughout the tests corresponding to the continuous increase in pore pressures shown in Figure 12. The horizontal normal stress that was measured using calibrated wire reinforced rubber membranes first decreases, reaching a minimum value at approximately 6.0 to 9.0 percent shear strain. Thereafter, the horizontal normal stress increases, reaching values equal to or greater than the initial horizontal normal stress. Since pore pressures do not

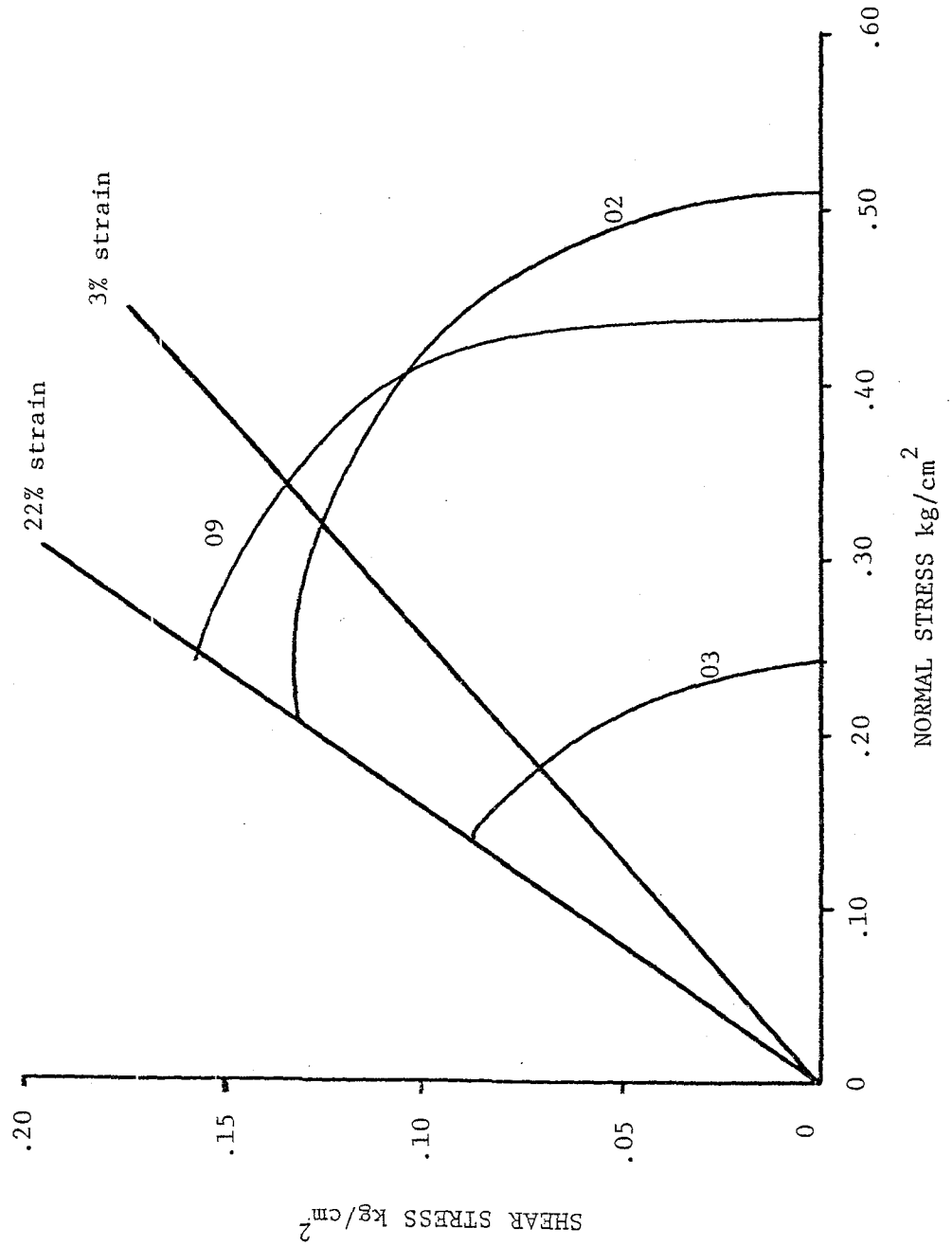

FIGURE 13. "STRESS PATHS" FOR STATIC TESTS PERFORMED ON GULF OF ALASKA CLAY

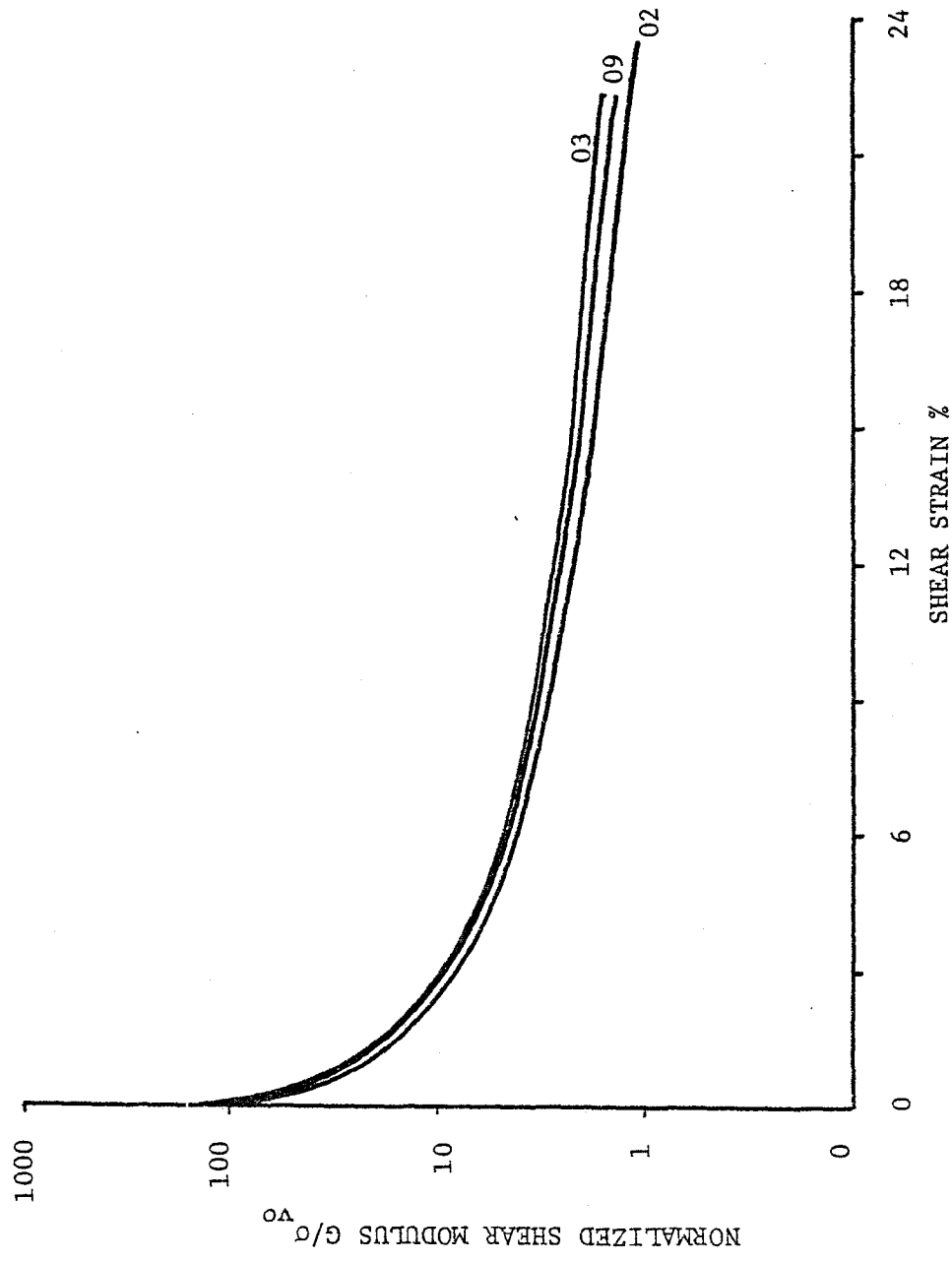

FIGURE 14. NORMALIZED SHEAR MODULUS DATA FOR STATIC TESTS PERFORMED ON GULF OF ALASKA CLAY

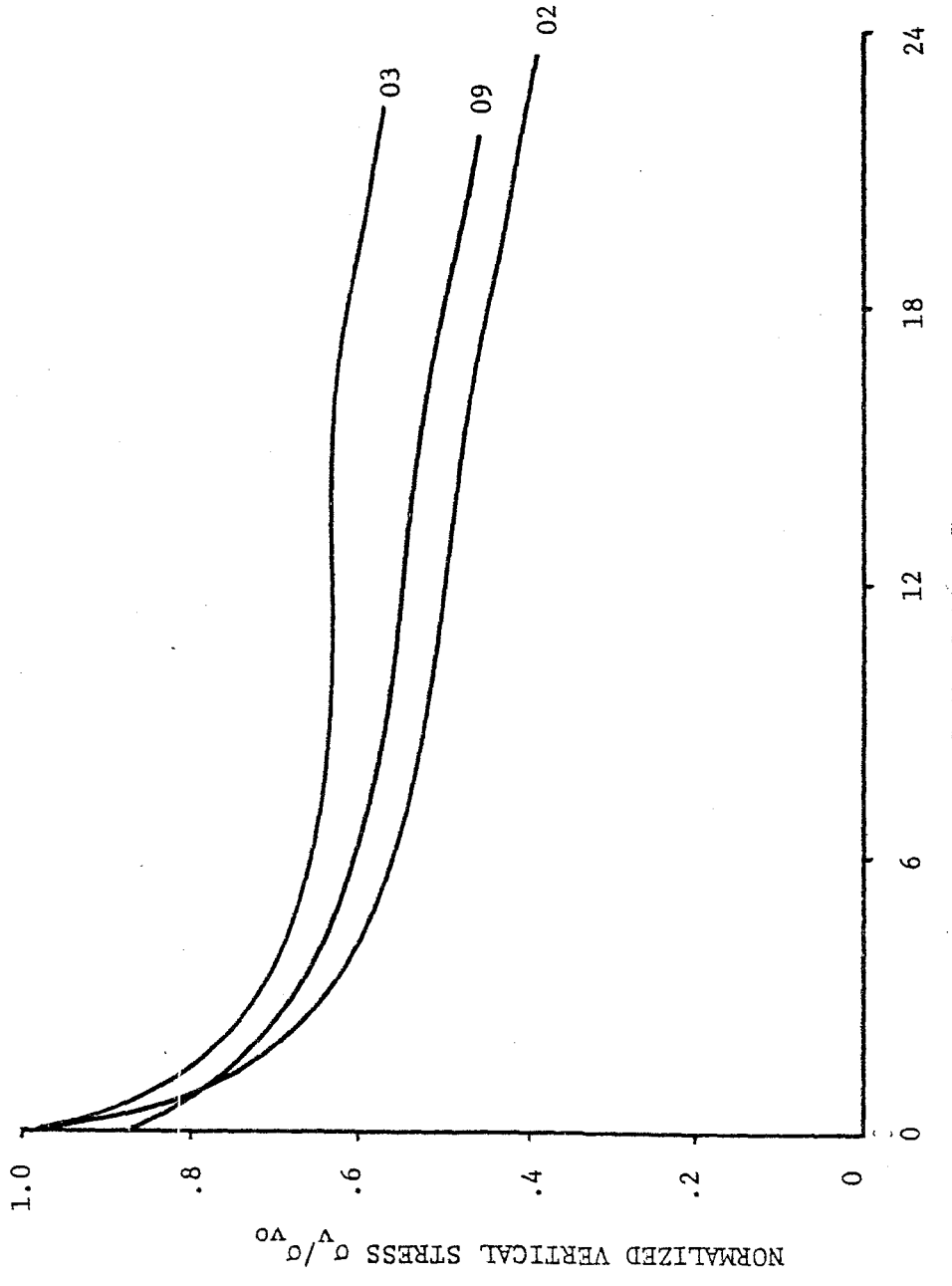

FIGURE 15. NORMALIZED VERTICAL STRESS VS. SHEAR STRAIN FOR STATIC TESTS PERFORMED ON GULF OF ALASKA CLAY

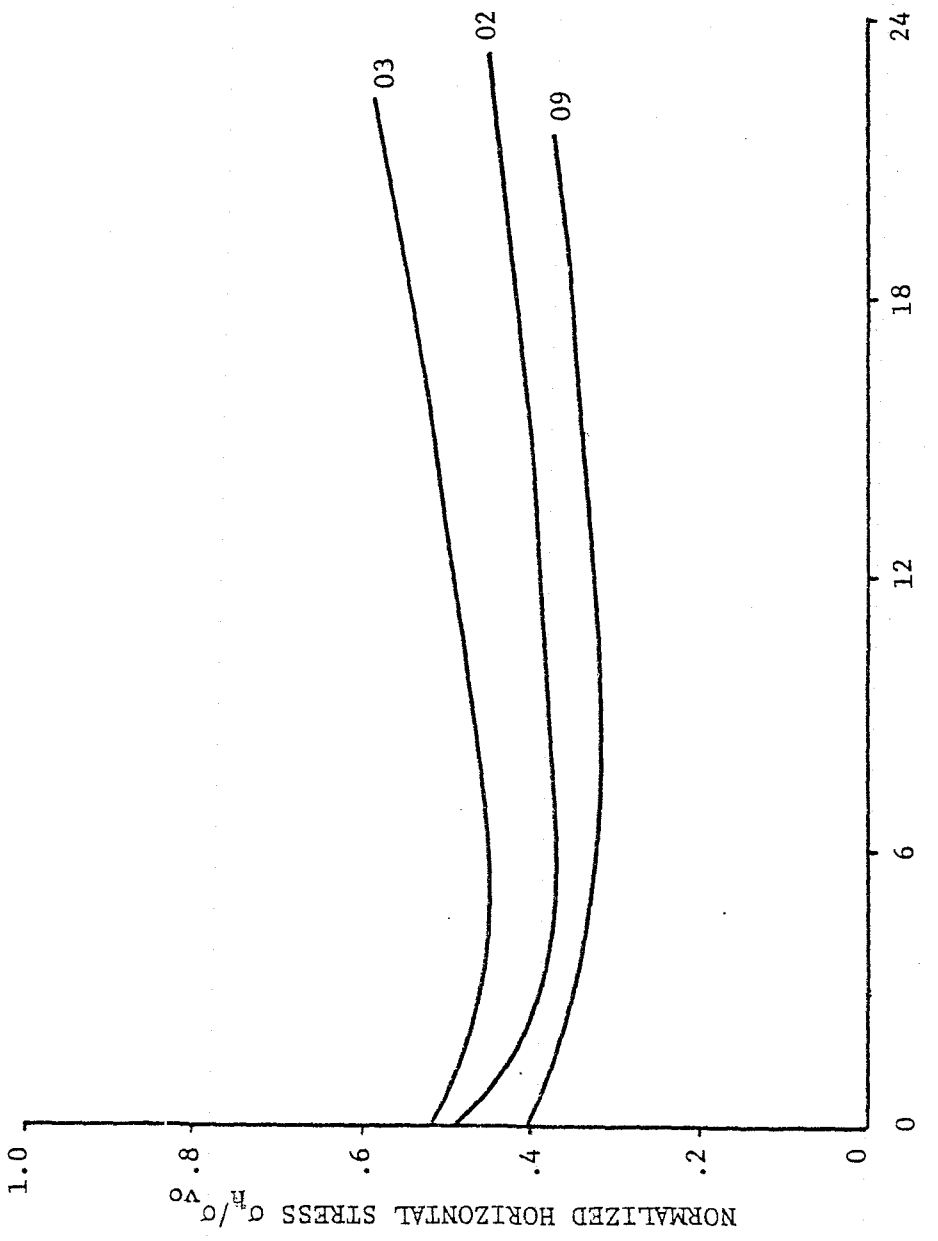

FIGURE 16. NORMALIZED HORIZONTAL (LATERAL) STRESS VS. SHEAR STRAIN FOR STATIC TESTS PERFORMED ON GULF OF ALASKA CLAY

develop in the sample during constant volume tests, the measured horizontal and vertical stresses are effective stresses.

The ratio of the horizontal normal stress to the vertical normal stress vs. shear strain for the static tests is shown in Figure 17. The ratio increases continuously during the tests from an initial value corresponding to the coefficient of lateral stress at rest, K_o. At very large strains, the ratio approaches a value of unity. The ratio $\bar{\sigma}_3/\bar{\sigma}_1$ vs. shear strain is shown in Figure 18. This ratio was computed based on the assumptions and equations presented in Part 5. The value of this ratio decreases throughout the tests. Initially, its value also corresponds to K_o conditions. The results for Test No. 09 fall below the curves for the static tests without previous cyclic loading.

The angle θ_q between horizontal plane and the plane on which the maximum shear stress acts vs. shear strain is shown in Figure 19 for the static tests. The angle θ_q decreases rapidly up to 3 percent shear strain, and thereafter decreases gradually throughout the test. At large values of shear strain, θ_q approaches zero indicating that the horizontal plane is the plane on which the maximum shear stress acts. Roscoe et al (107) found similar results for sands and isotropic plastic materials using the Cambridge direct simple shear device. Although the assumption that the horizontal plane is the plane of maximum shear stress may not be valid for all soils, it seems to be valid at large strains for the Copper River prodelta clay tested.

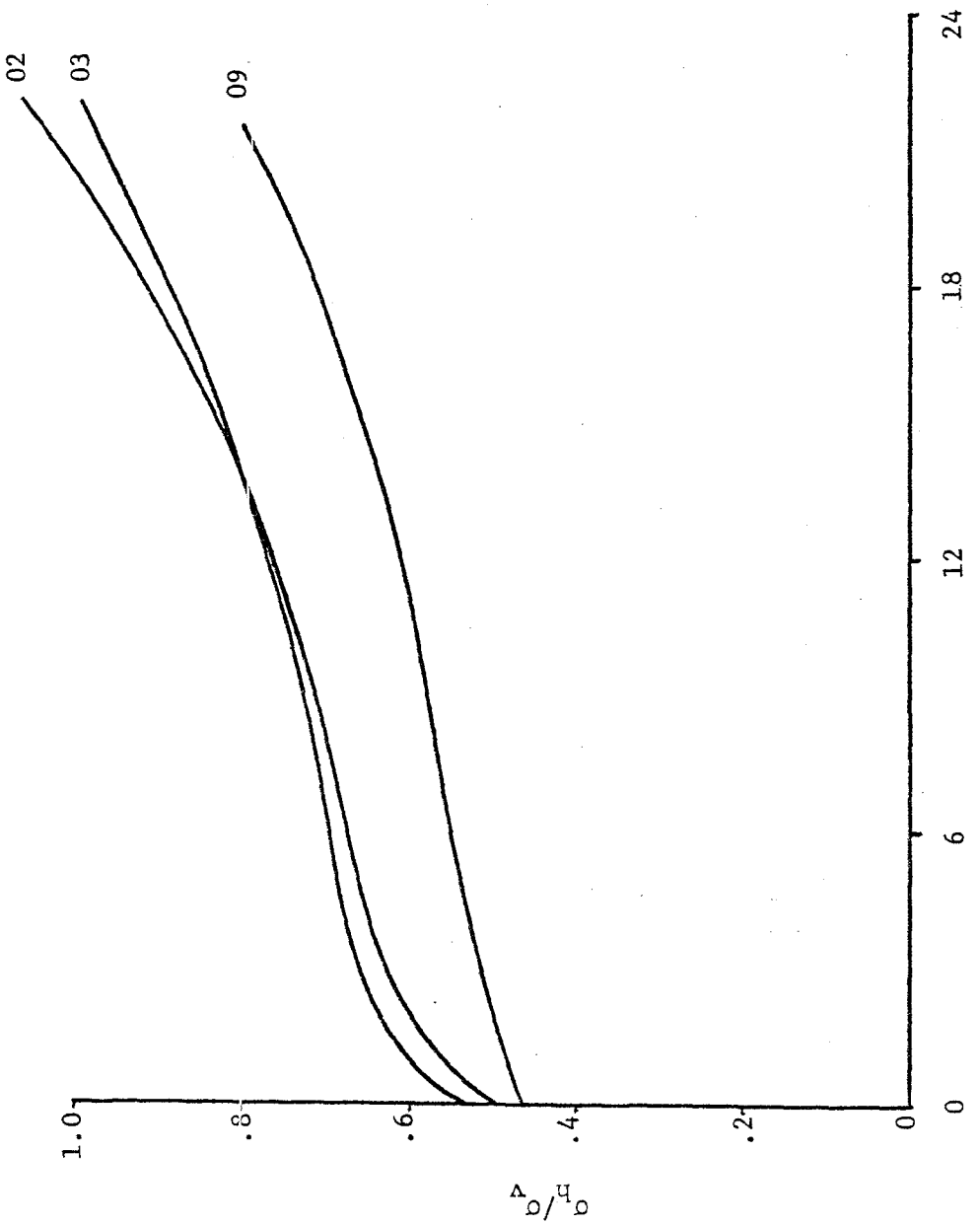

FIGURE 17. THE RATIO OF HORIZONTAL NORMAL STRESS TO VERTICAL NORMAL STRESS VS. SHEAR STRAIN FOR STATIC TESTS PERFORMED ON GULF OF ALASKA CLAY

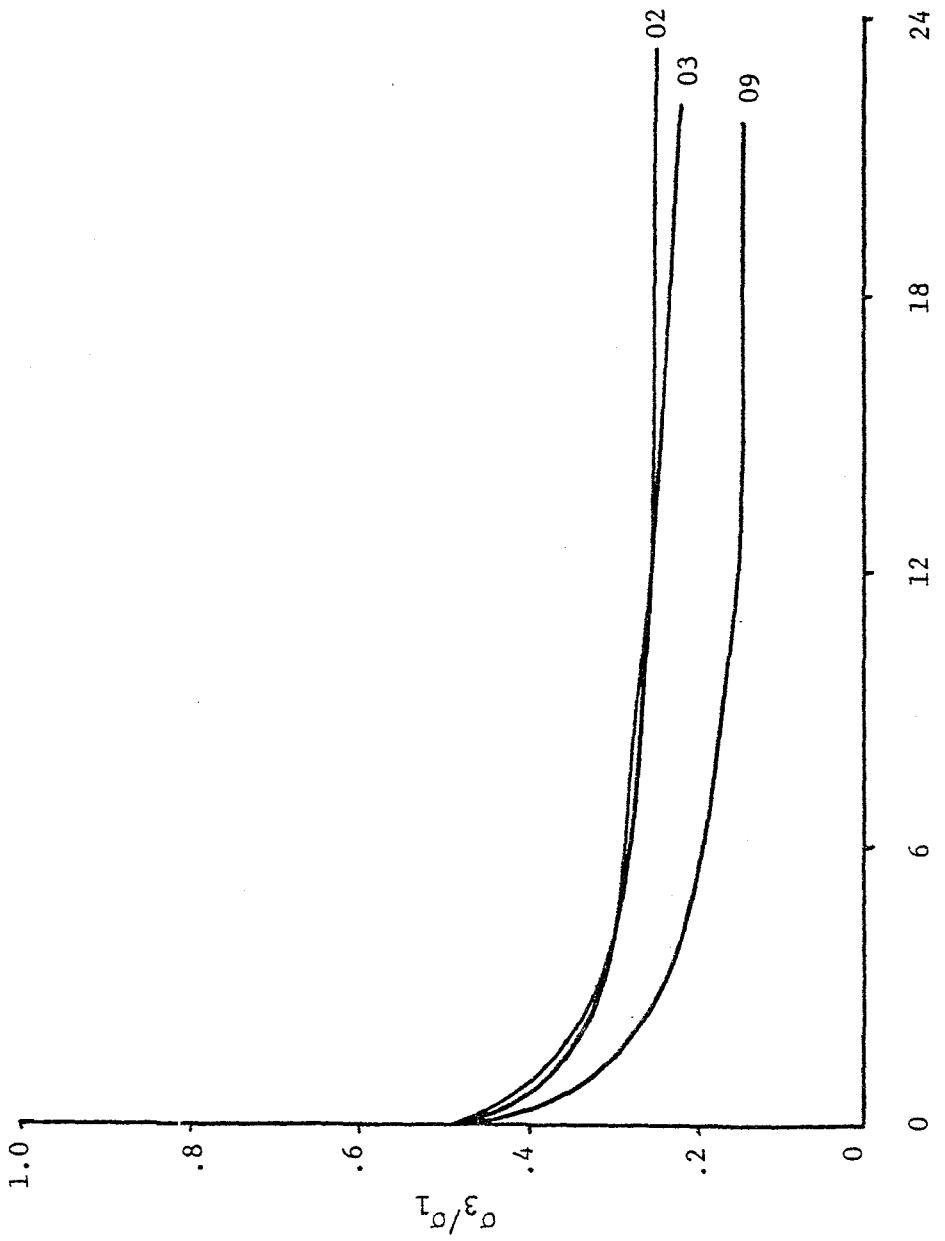

FIGURE 18. THE RATIO σ_3/σ_1 VS. SHEAR STRAIN FOR STATIC TESTS PERFORMED ON GULF OF ALASKA CLAY

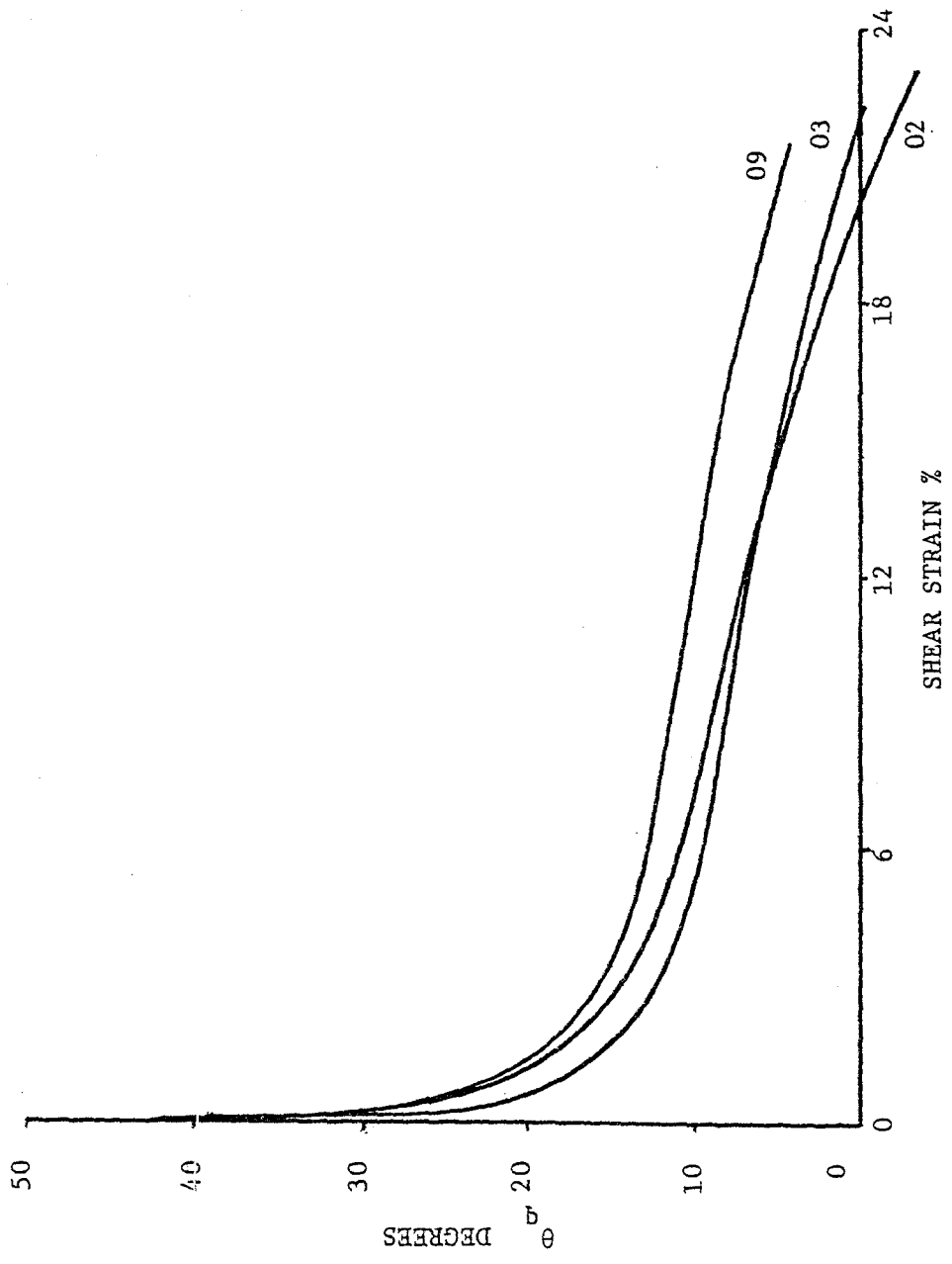

FIGURE 19. THE ANGLE BETWEEN THE HORIZONTAL PLANE AND THE PLANE ON WHICH THE MAXIMUM SHEAR STRESS ACTS VS. SHEAR STRAIN FOR STATIC TESTS PERFORMED ON GULF OF ALASKA CLAY

The angle θ_f between the horizontal plane and the plane of maximum obliquity vs. shear strain is presented in Figure 20 for the static tests. The angle θ_f decreases rapidly at small shear strains after which it remains fairly constant. At large shear strains, θ_f again decreases slightly. Because of the large values of θ_f throughout the test, the common assumption that the horizontal plane is the plane of maximum obliquity does not appear to be valid for this clay. Roscoe et al (107) found similar results using the Cambridge direct simple shear device.

Figure 21 presents static test results showing the angle θ_p between the horizontal plane and the plane on which the major principle stress acts vs. shear strain. The angle θ_p increases rapidly at small strains followed by a gradual increase throughout the remainder of the test. At large values of shear strain, θ_p approaches 45°. This is consistent with the result that the horizontal plane is the plane of maximum shear stress.

The mobilized angle of internal friction ϕ_m vs. shear strain relationships for the static tests are shown in Figure 22. The maximum value of the ϕ parameter for static test Nos. 02 and 03 is approximately 35°. This strength value was mobilized at about 10 percent shear strain. Note that this value of the strength parameter is considerably different than the one that was computed from Figure 13 using the assumption that the horizontal plane is the plane of maximum obliquity. The ϕ parameter obtained for Test No. 09 seems to be unreasonably high. However, Andersen (2,3) concluded that cyclic loading of normally consolidated clays causes an increase in effective cohesion c while the effective friction angle ϕ remains un-

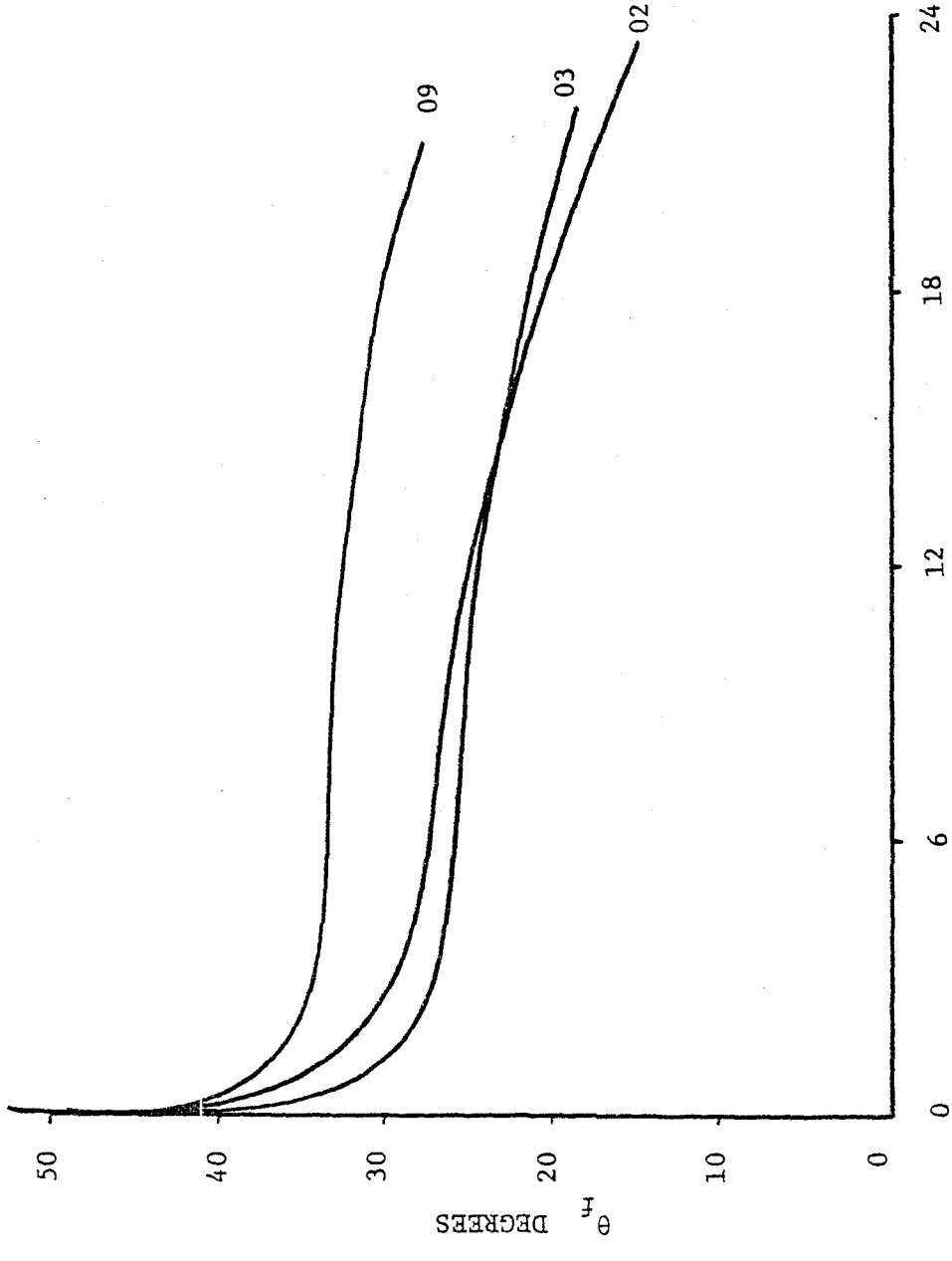

FIGURE 20. THE ANGLE BETWEEN THE HORIZONTAL PLANE AND THE PLANE OF MAXIMUM OBLIQUITY VS. SHEAR STRAIN FOR STATIC TESTS PERFORMED ON GULF OF ALASKA CLAY

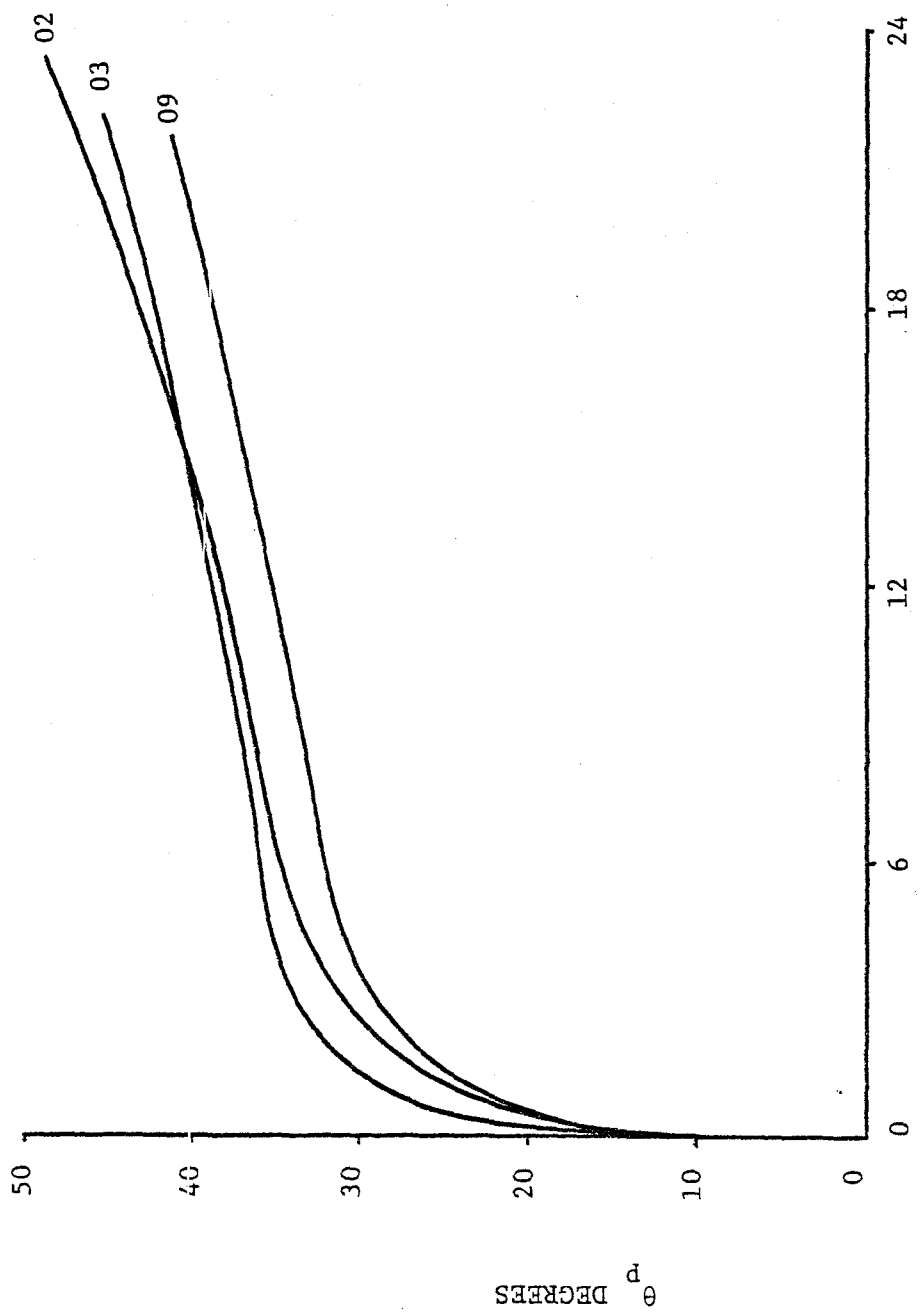

FIGURE 21. THE ANGLE BETWEEN THE HORIZONTAL PLANE AND THE PLANE ON WHICH THE MAXIMUM PRINCIPLE STRESS ACTS VS. SHEAR STRAIN FOR STATIC TESTS PERFORMED ON GULF OF ALASKA CLAY

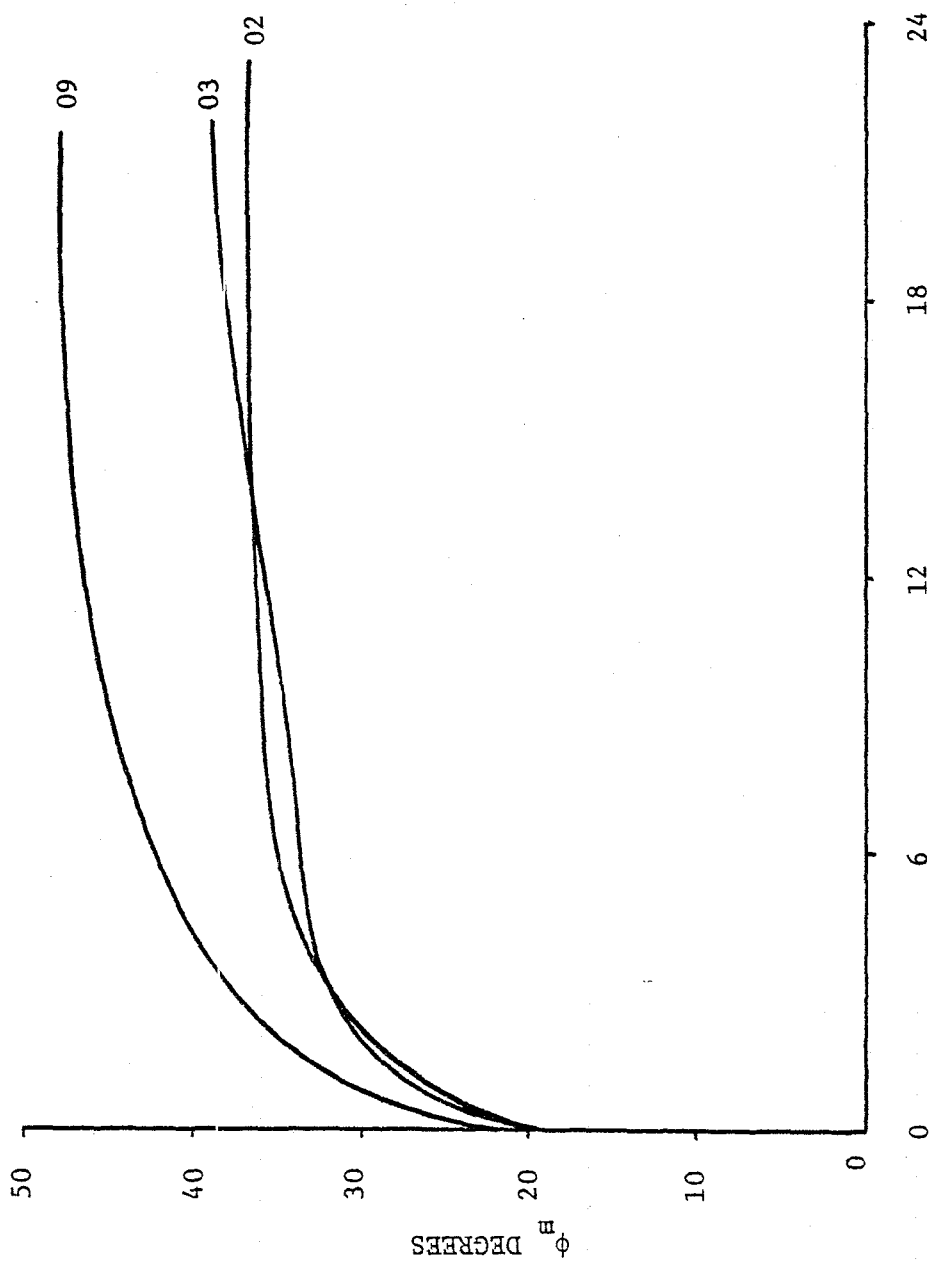

FIGURE 22. MOBILIZED ANGLE OF INTERNAL FRICTION VS. SHEAR STRAIN FOR STATIC TESTS PERFORMED ON GULF OF ALASKA CLAY

affected. The values of ϕ_m presented in Figure 22 were based on the assumption of zero cohesion, and the presence of even a small cohesion c will reduce the internal friction angle to the value indicated by Test Nos. 02 and 03. At 3 percent shear strain, ϕ_m is approximately 31° for Test Nos. 02 and 03.

A $\bar{p}$ - q stress plot is shown in Figure 23 where

$$\bar{p} = (\bar{\sigma}_1 + \bar{\sigma}_3)/2$$

$$q = (\bar{\sigma}_1 - \bar{\sigma}_3)/2$$

The K_o line was drawn based on the K_o conditions measured in the soil samples prior to shearing. A K_f failure line was drawn through the tips of the stress paths for static test Nos. 02 and 03. These points correspond to approximately 22 percent shear strain. It is believed that the inconsistent shape of the stress path for Test No. 02 was caused by sample disturbance. Another failure line is shown in Figure 23 based on the assumption that failure occurs at 3 percent shear strain.

Test No. 09 was performed following non-failure cyclic loading. The stress path for this test crosses the failure lines shown, but this can be explained by an increase in effective cohesion (2,3).

Cyclic Loading Test Results

Cyclic shear strain vs. number of cycles of loading is shown plotted in Figure 24. The shear strain for all cyclic loading tests is taken to be one-half the peak to peak shear strain. Typically, the cyclic shear strains increase gradually until failure is imminent, after which the cyclic

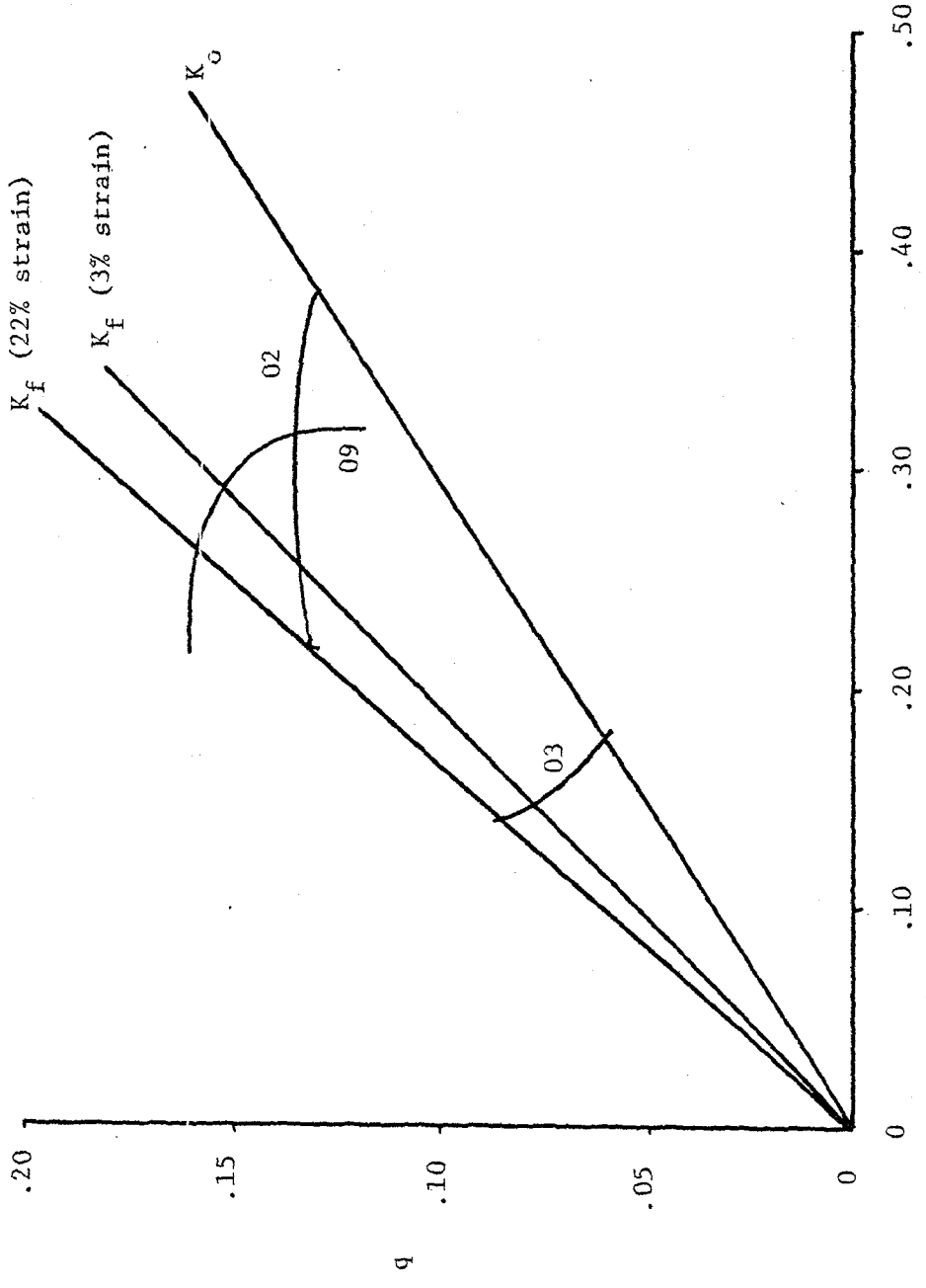

FIGURE 23. $\bar{p}$ - q STRESS PLOTS FOR STATIC TESTS PERFORMED ON GULF OF ALASKA CLAY

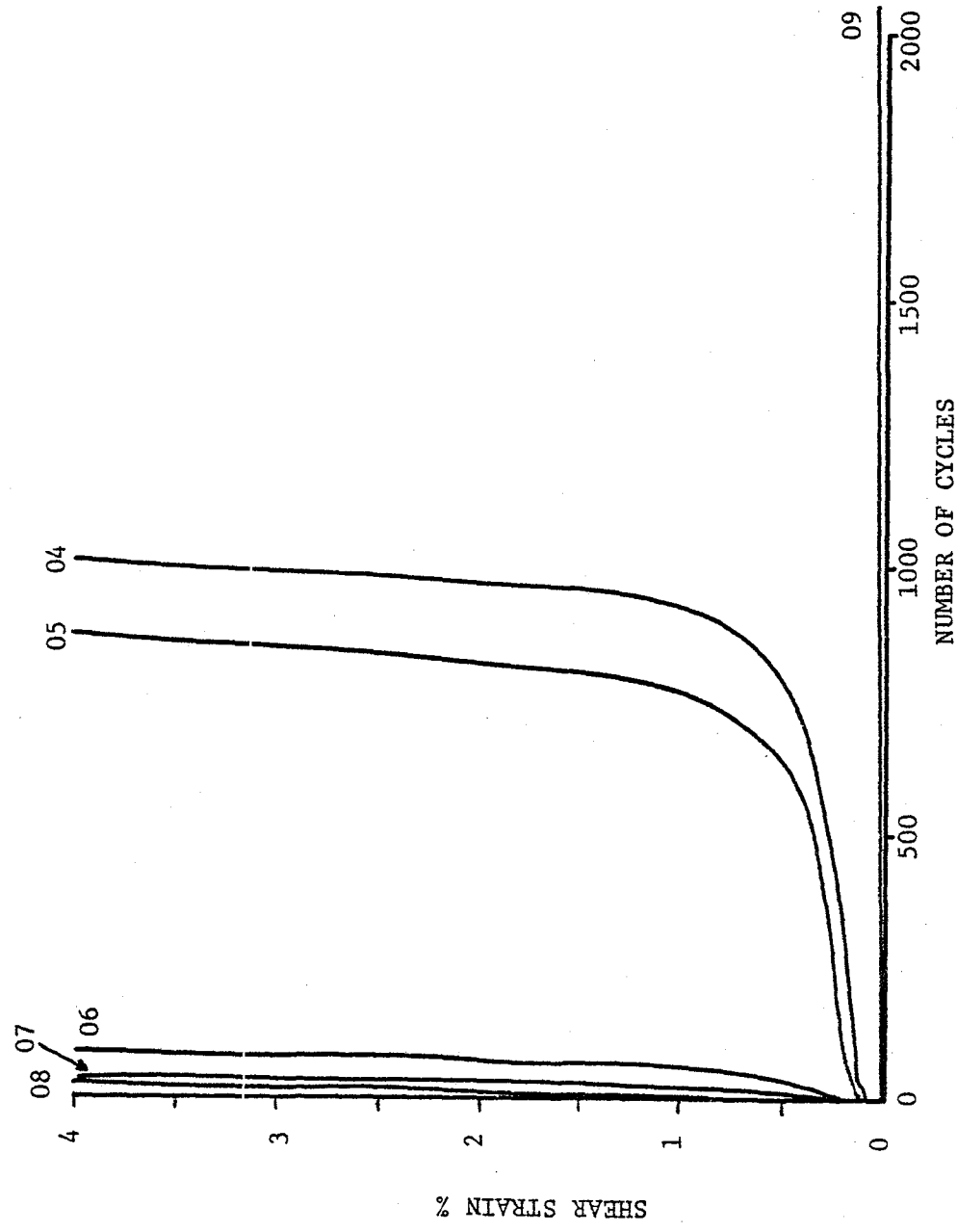

FIGURE 24. SHEAR STRAIN VS. NUMBER OF CYCLES FOR TESTS PERFORMED ON GULF OF ALASKA CLAY

shear strains increase very rapidly. Test No. 09 showed no signs of imminent failure after 3,000 cycles of loading, and the cyclic shear strains remained approximately constant throughout the test. Such conditions have been defined to be a state of nonfailure equilibrium for the soil (115).

Normalized pore pressure vs. number of cycles of loading is shown plotted in Figure 25. These curves represent the permanent or residual excess pore pressures that are generated after a given number of loading cycles. The variations in pore pressure during a given cycle of loading were not measured. These curves show the same general trend as the cyclic shear strain vs. number of cycles curves in Figure 24. It appears that there is an excellent correlation between excess pore pressures and shear strains for these stress controlled tests. Test No. 09 shows a very gradual increase in pore pressure with number of loading cycles. It is uncertain whether the pore pressures will level off or continue to increase with further cycles of loading. Therefore it is also uncertain whether the state of nonfailure equilibrium will persist with further loading cycles. However, 3000 loading cycles is an adequate practical limit for earthquake and storm wave loading situations.

"Stress path" data showing horizontal shear stress vs. vertical normal stress is presented in Figure 26. The failure lines determined by the static tests are also shown in this figure. The data for the cyclic tests is shown for the positive peak points only, i.e., when the shear stress has its maximum positive value. The actual "stress path" would cycle symmetrically

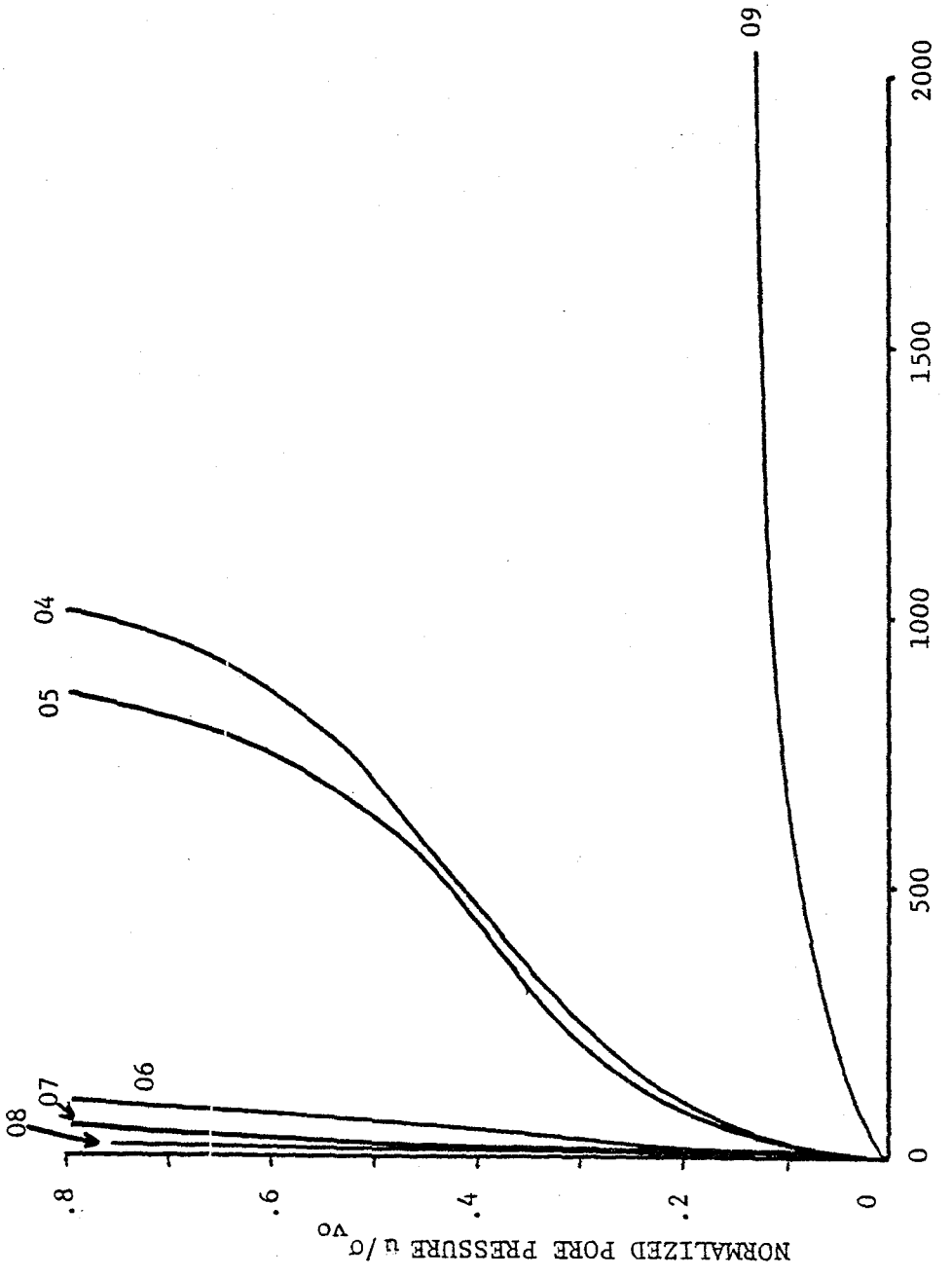

FIGURE 25. PORE PRESSURE VS. NUMBER OF CYCLES FOR TESTS PERFORMED ON GULF OF ALASKA CLAY

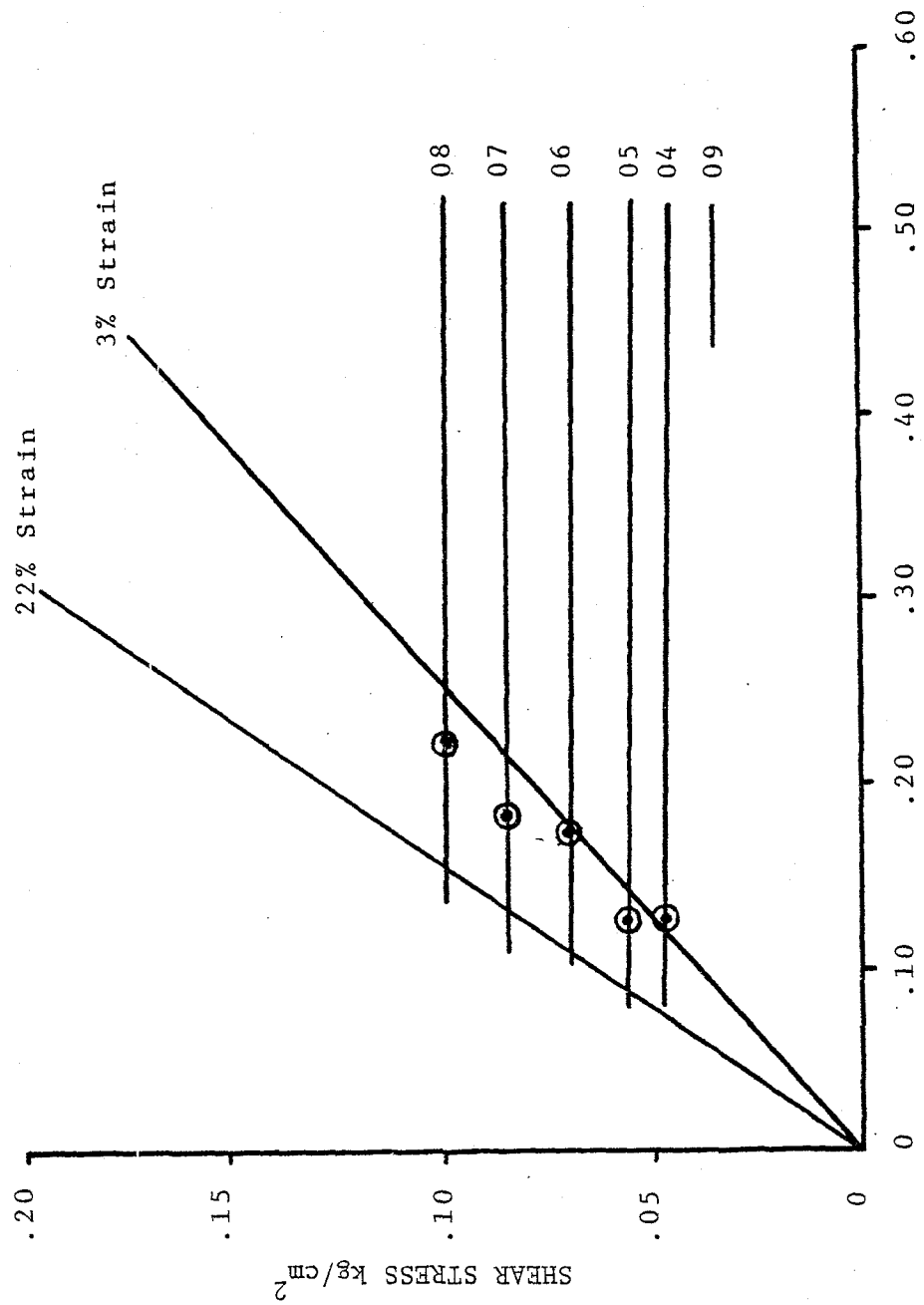

FIGURE 26. "STRESS PATHS" FOR CYCLIC TESTS ON GULF OF ALASKA CLAY. THE FAILURE LINES SHOWN WERE DETERMINED FROM STATIC TESTS. THE POINTS SHOWN CORRESPOND TO 3 PERCENT STRAIN IN THE CYCLIC TESTS

above and below the horizontal axis. The points shown on each stress path correspond to 3 percent shear strain; the stress paths terminate at 15 percent shear strain. For the tests in which failure occurred, the stress paths reach and cross the static failure lines. The reason the stress paths cross the failure lines may be attributed to an increase in effective cohesion c caused by the cyclic loading (2,3). It should be noted however that at 3 percent shear strain, the stress paths correspond closely with the failure line. The stress path for Test No. 09 which exhibited a state of nonfailure equilibrium did not reach the static failure lines.

Normalized shear modulus vs. number of loading cycles is presented in Figure 27. The shear modulus decreases gradually with number of loading cycles until failure is imminent; thereafter the shear modulus rapidly decreases. Before failure, the shear modulus vs. number of loading cycles relation can be approximated by a straight line on this log-log plot. As the cyclic shear stress increases, the initial shear modulus (for the first loading cycle) decreases and the slope of the modulus vs. number of cycles curve increases.

Normalized vertical and horizontal normal stress vs. number of loading cycles are shown in Figures 28 and 29. Both the vertical and horizontal normal stresses decrease with increasing number of loading cycles. The decrease in vertical normal stress is directly related to the increase in excess pore pressures. The measured horizontal stresses show some scatter with various curves crossing each other. This is probably caused by experimental error originating from the calibrated reinforced rubber membranes used to measure the lateral stresses. The problems associated with the use of these membranes is discussed in Part 3. However, the general trend of decreasing lateral stresses with increasing number of loading cycles was displayed by each test, and appears to be valid for the soil tested.

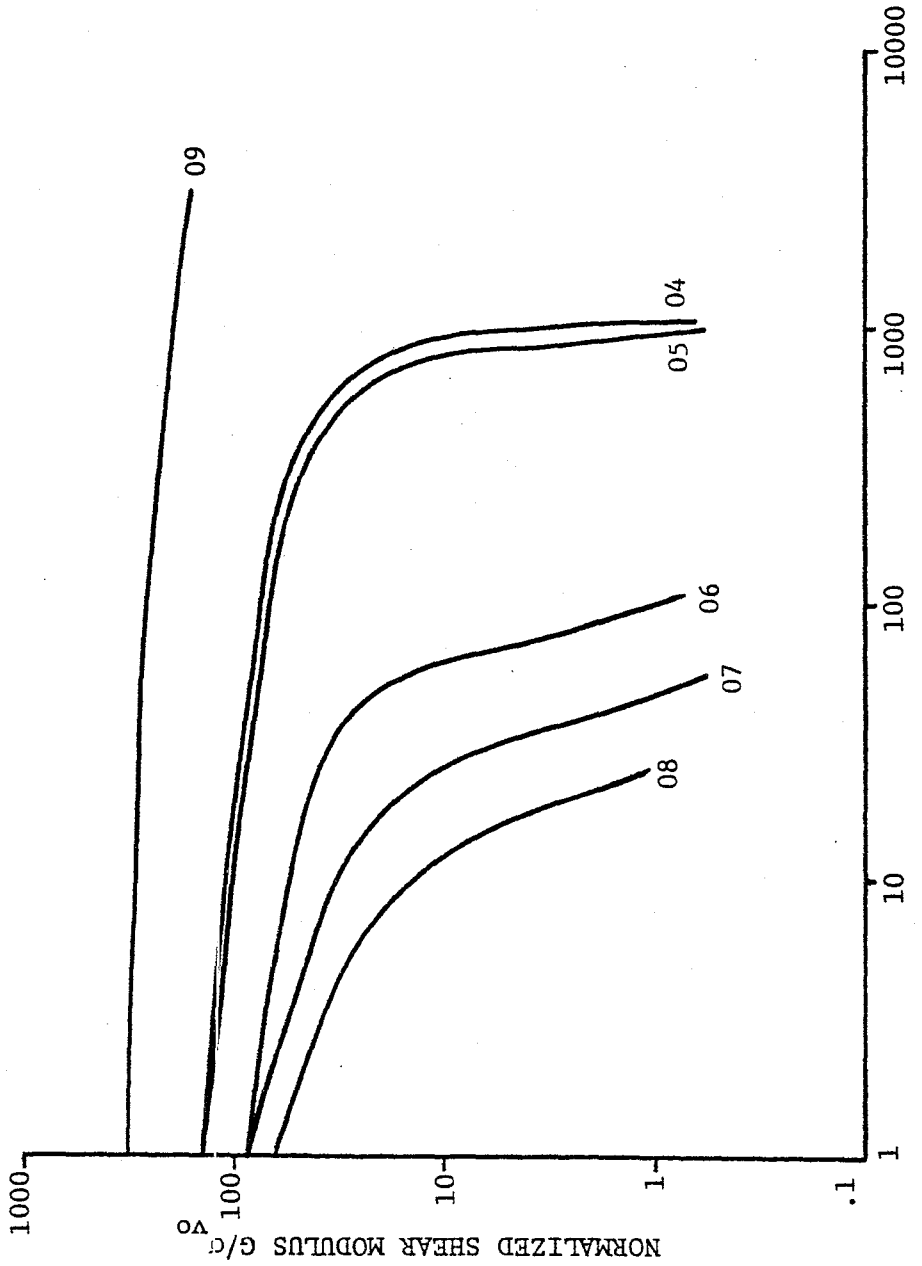

FIGURE 27. SHEAR MODULUS VS. NUMBER OF CYCLES FOR TESTS PERFORMED ON GULF OF ALASKA CLAY

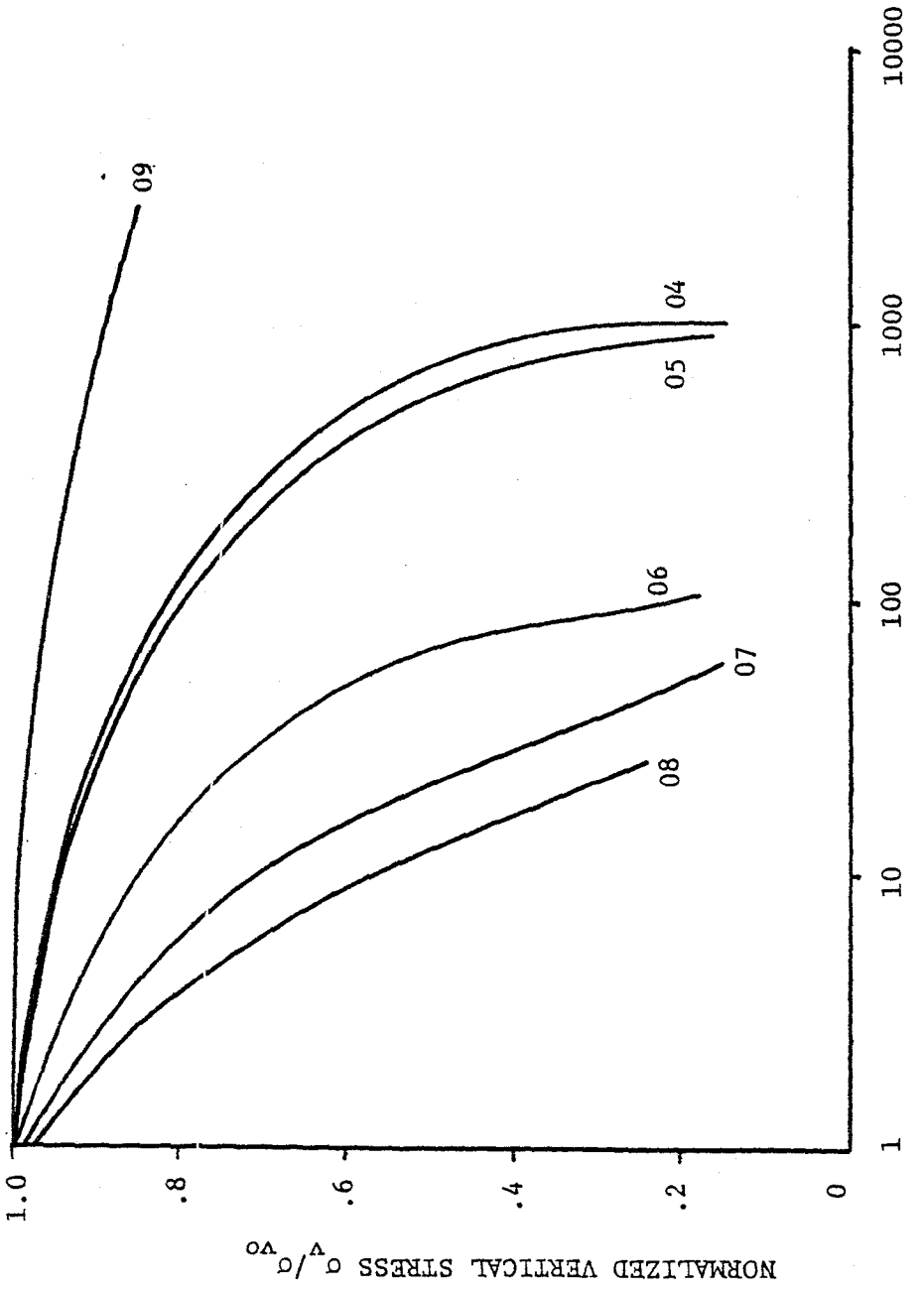

FIGURE 28. VERTICAL STRESS VS. NUMBER OF CYCLES FOR TESTS ON GULF OF ALASKA CLAY

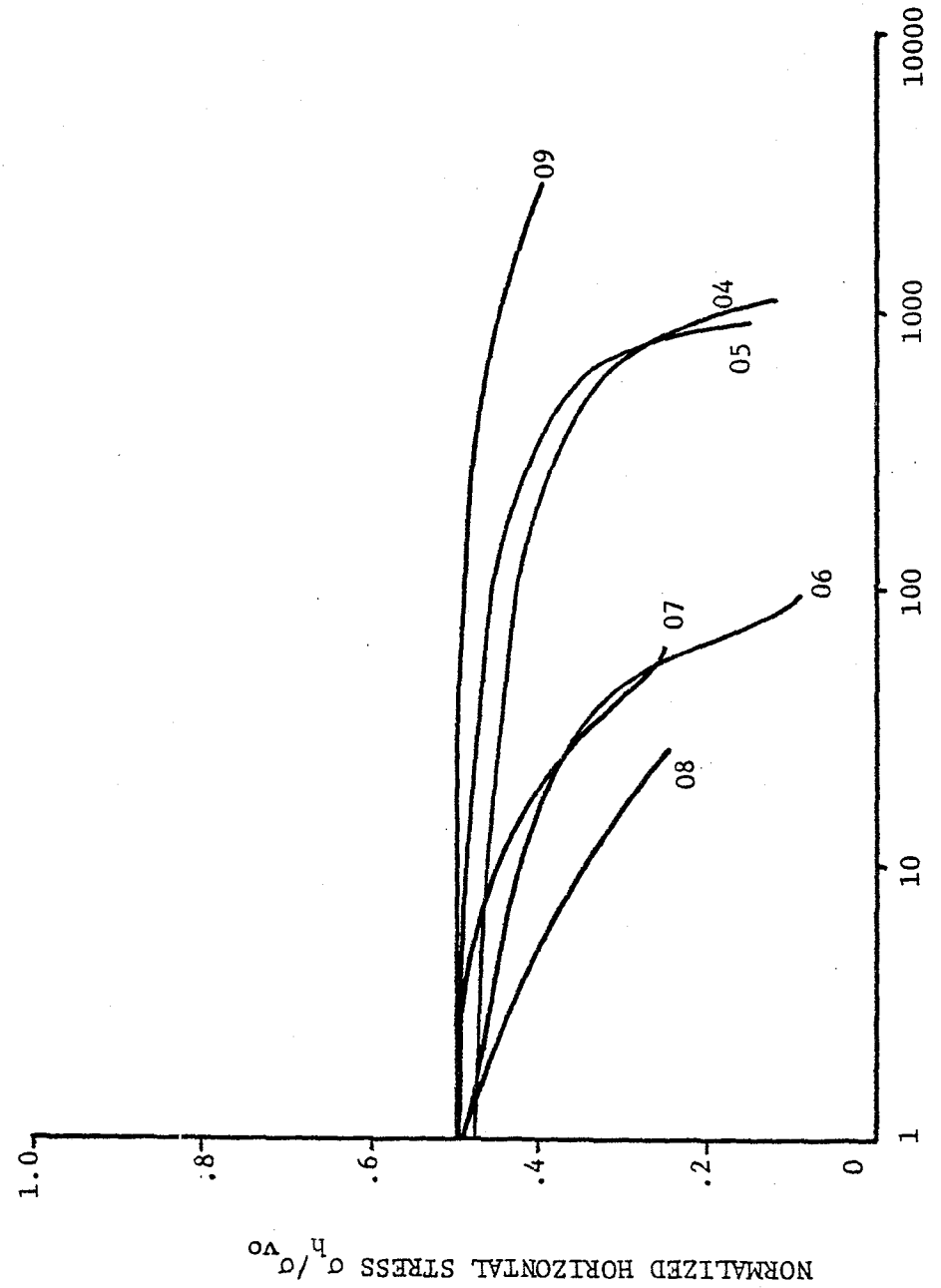

FIGURE 29. HORIZONTAL STRESS VS. NUMBER OF CYCLES FOR TESTS ON GULF OF ALASKA CLAY

The ratio of the horizontal normal stress to the vertical normal stress vs. number of loading cycles is shown in Figure 30. Similar to the static test results, this ratio tends to increase, and approaches a value of unity when failure occurs. The ratio remained approximately constant for Test No. 09 which exhibited a state of nonfailure equilibrium. Some scatter is again evident in this diagram, but this is a direct consequence of the scatter obtained in the lateral stress measurements. The general trend with the ratio of lateral stress to vertical stress approaching unity as failure occurs seems to be valid for this soil.

Figure 31 presents data showing the variation of the ratio $\bar{\sigma}_3/\bar{\sigma}_1$ vs. number of loading cycles. The value of this ratio approaches zero as failure occurs. This trend was also found for the static tests. The ratio remained approximately constant for Test No. 09 which did not fail during cyclic loading. The scatter shown in this diagram can again be attributed to the scatter present in the lateral stress measurements.

The angle θ_q between the horizontal plane and the plane on which the maximum shear stress acts is plotted vs number of cycles in Figure 32. The angle θ_q approaches zero as failure occurs. Similar results were found for the static tests. The angle θ_q remained approximately constant for Test No. 09 which did not fail during cyclic loading. The assumption that the horizontal plane is the plane of maximum shear stress seems to be valid at failure for the Copper River prodelta clay that was tested.

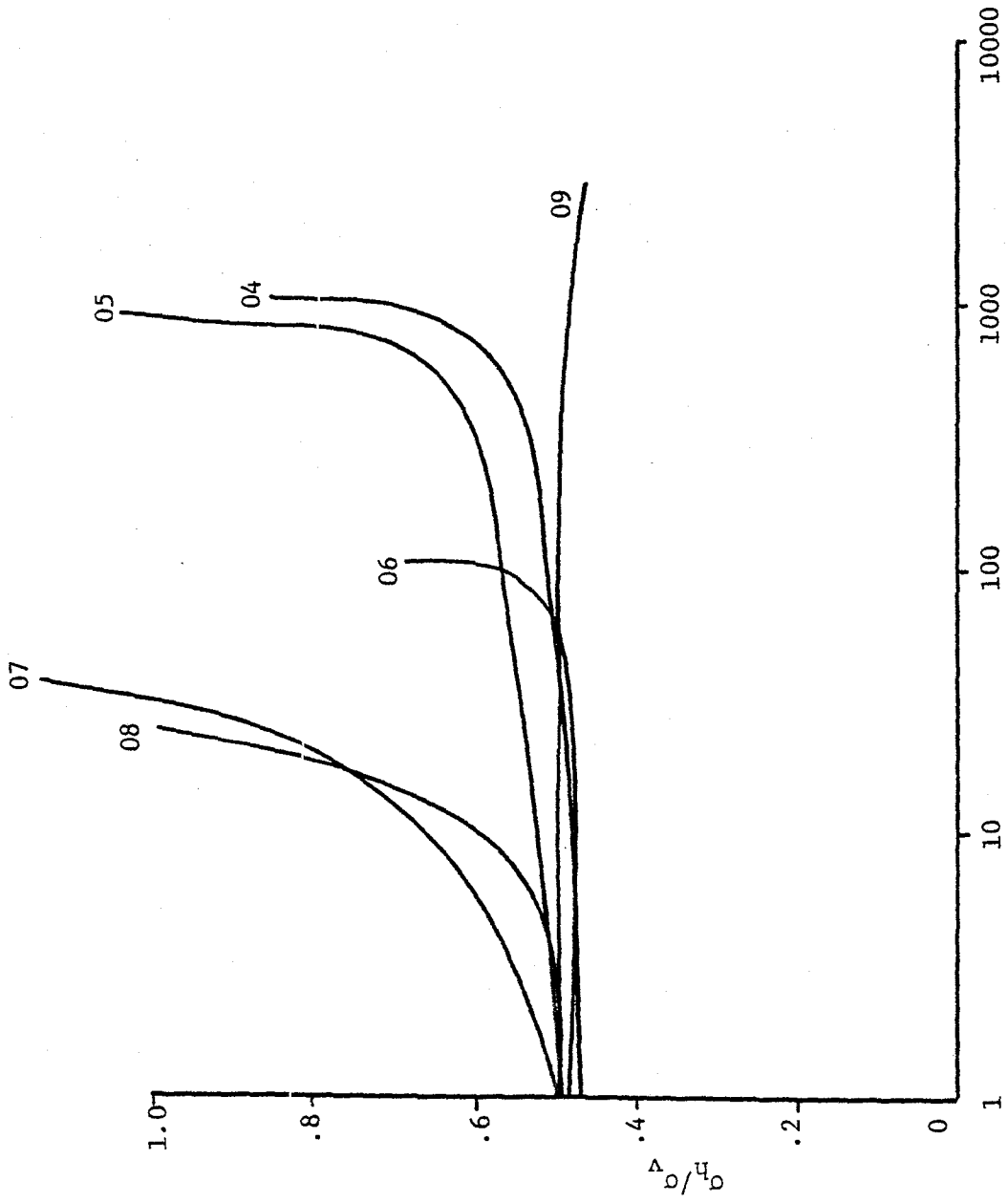

FIGURE 30. THE RATIO OF HORIZONTAL NORMAL STRESS TO VERTICAL NORMAL STRESS VS. NUMBER OF CYCLES FOR TESTS ON GULF OF ALASKA CLAY

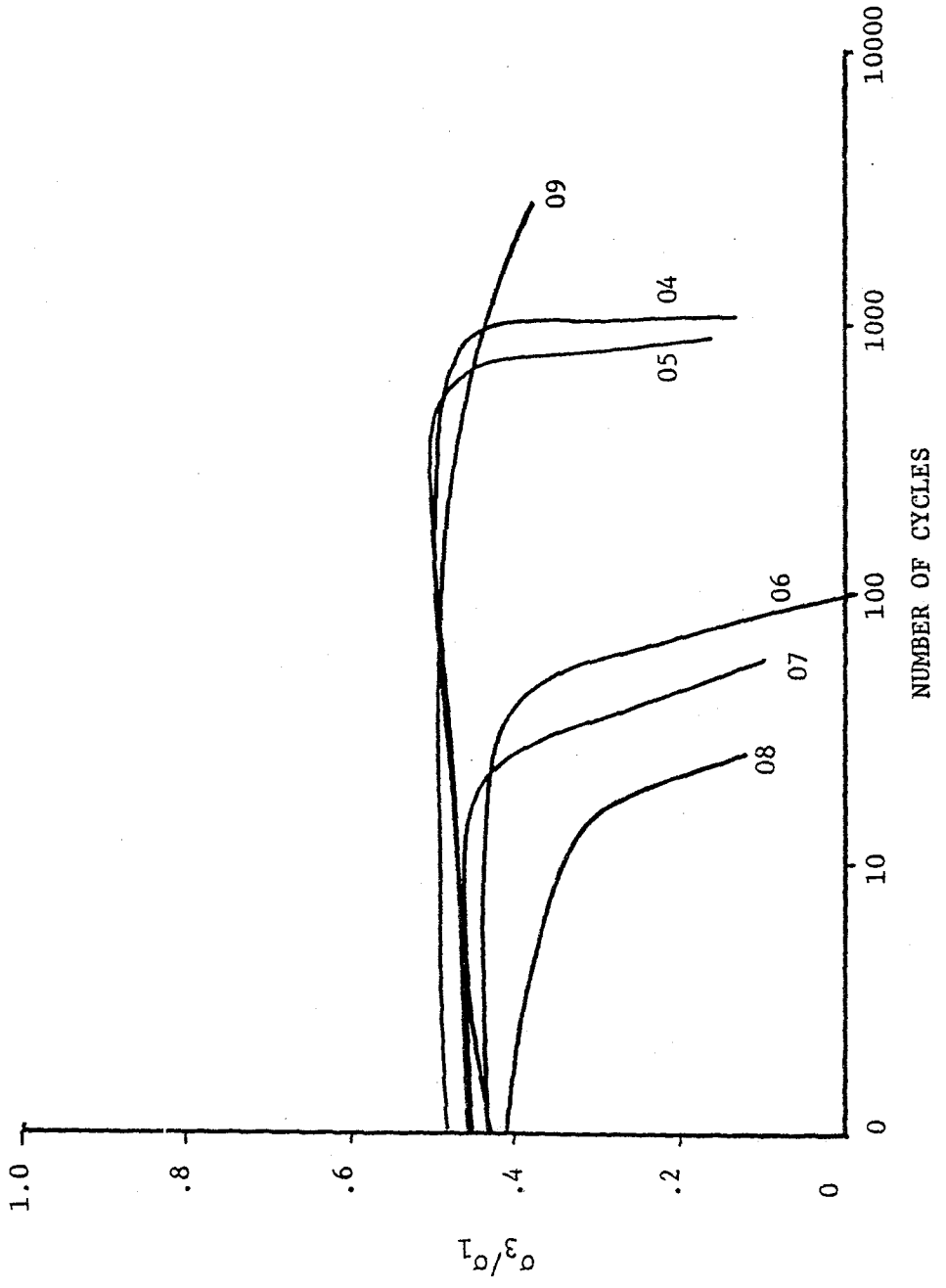

FIGURE 31. THE RATIO σ_3/σ_1 VS. NUMBER OF CYCLES FOR TESTS ON GULF OF ALASKA CLAY

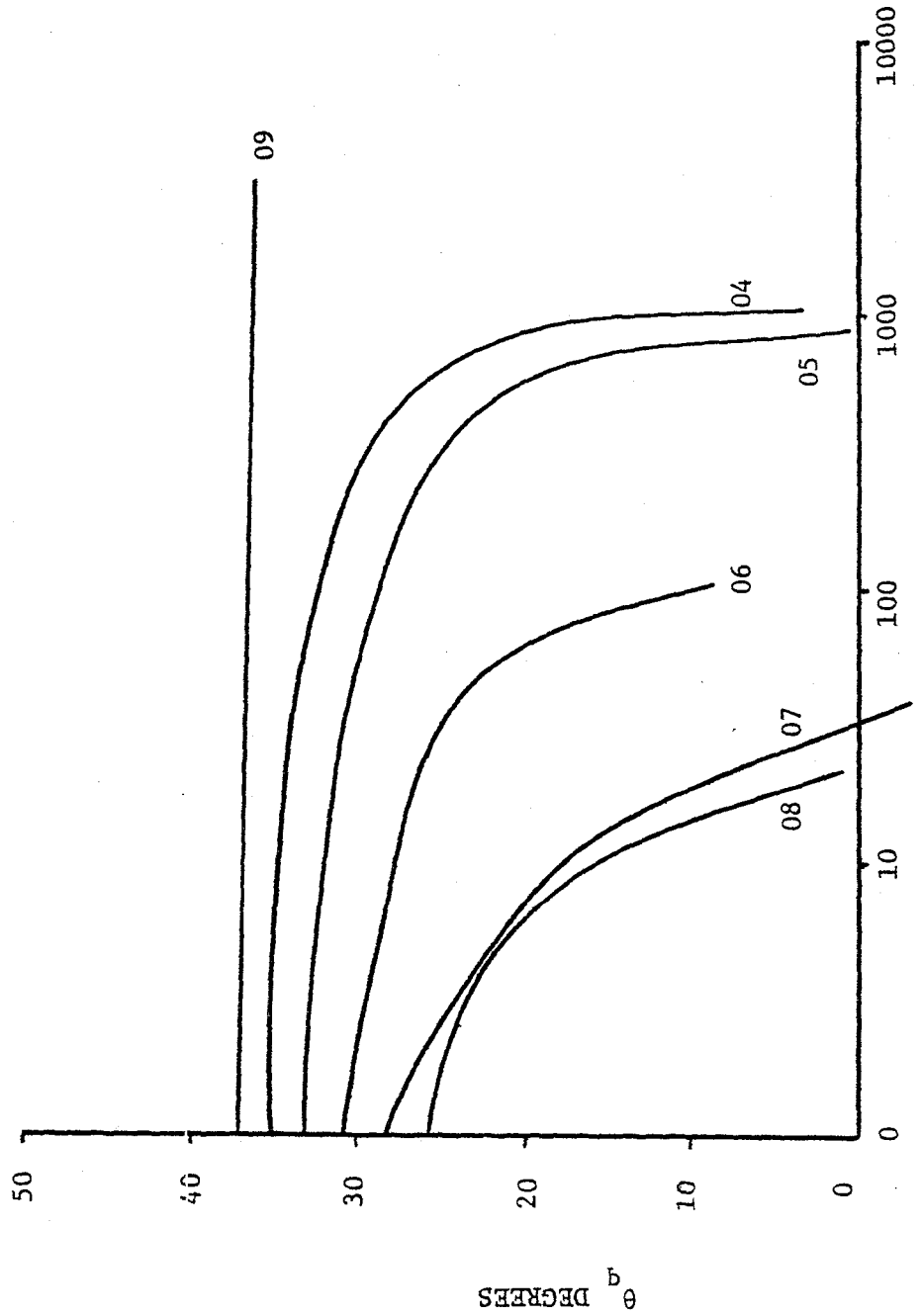

FIGURE 32. THE ANGLE BETWEEN THE HORIZONTAL PLANE AND THE PLANE ON WHICH THE MAXIMUM SHEAR STRESS ACTS VS. NUMBER OF CYCLES FOR TESTS ON GULF OF ALASKA CLAY

Figure 33 shows the relationship for the angle θ_p between the horizontal plane and the major principle plane vs. number of loading cycles. Similar to the static test results, this angle approaches 45° as failure occurs. Since at failure the horizontal plane is approximately the plane on which the maximum shear stress acts, the angle θ_p should approach 45° at failure as shown in the figure.

The angle θ_f between the horizontal plane and the plane of maximum obliquity is plotted vs. number of loading cycles in Figure 34. It can be observed that this angle generally decreases with increasing number of loading cycles. An exception is Test No. 06 that was cycled at 50% of the static shear strength. This is assumed to be caused by experimental error in the measurement of lateral stresses. It is evident however, that the horizontal plane is not the plane of maximum obliquity for the clay tested. This fact was also noted in the discussion of the static test results.

A p-q stress plot is shown in Figure 35. The K_o and K_f lines as determined by static test results are also shown. The stress paths for all tests in which failure occurred reach and cross the failure lines. As noted previously, cyclic loading causes an increase in effective cohesion c for the soil (2,3). This may explain the reason why the stress paths cross the failure lines. The stress path for Test No. 09 which exhibited a state of nonfailure equilibrium did not reach the failure line.

For practical purposes, the failure line determined by the static tests can be used for the interpretation of the cyclic loading tests.

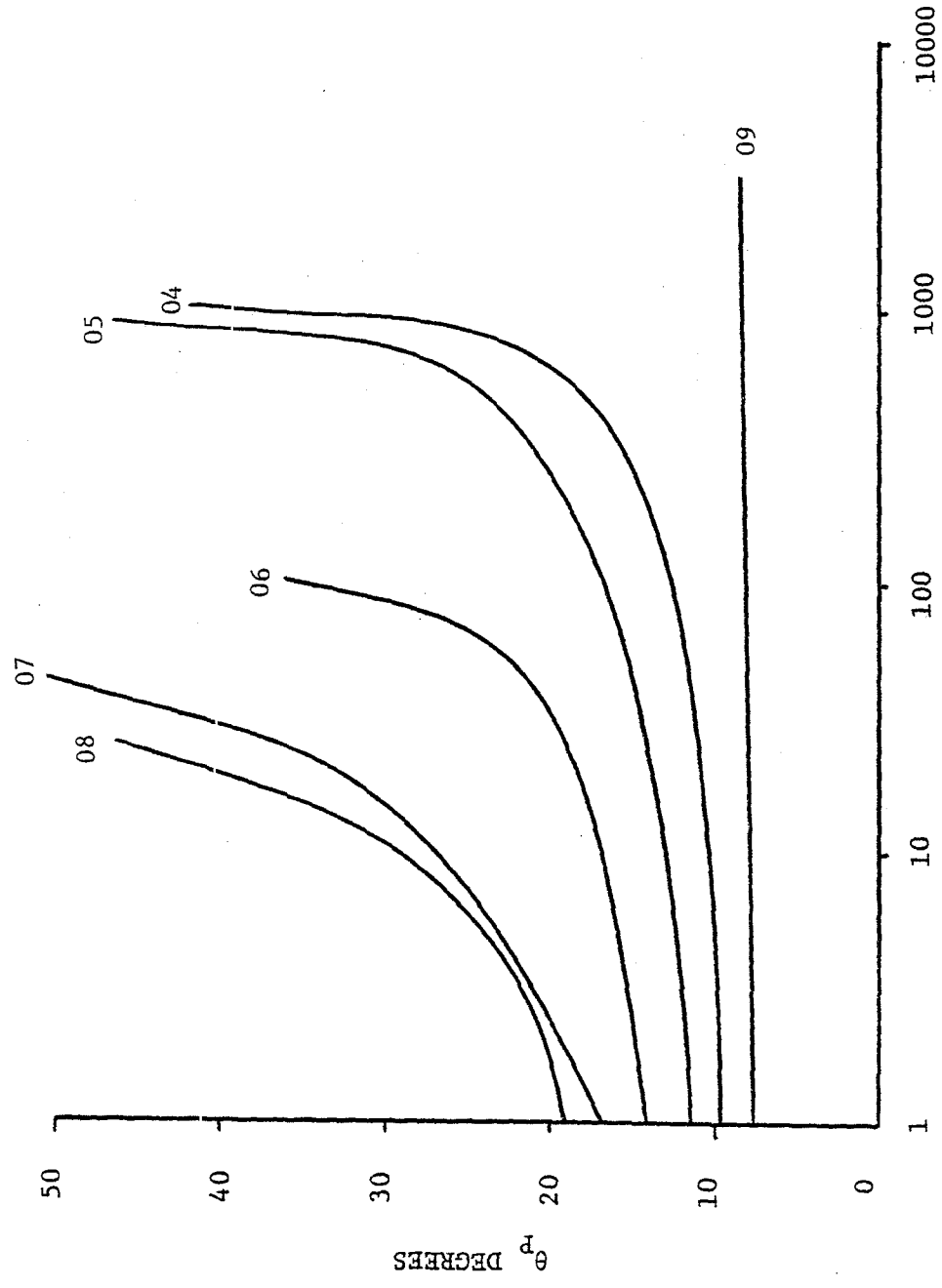

FIGURE 33. THE ANGLE BETWEEN THE HORIZONTAL PLANE AND THE MAJOR PRINCIPLE PLANE VS. NUMBER OF CYCLES FOR TESTS ON GULF OF ALASKA CLAY

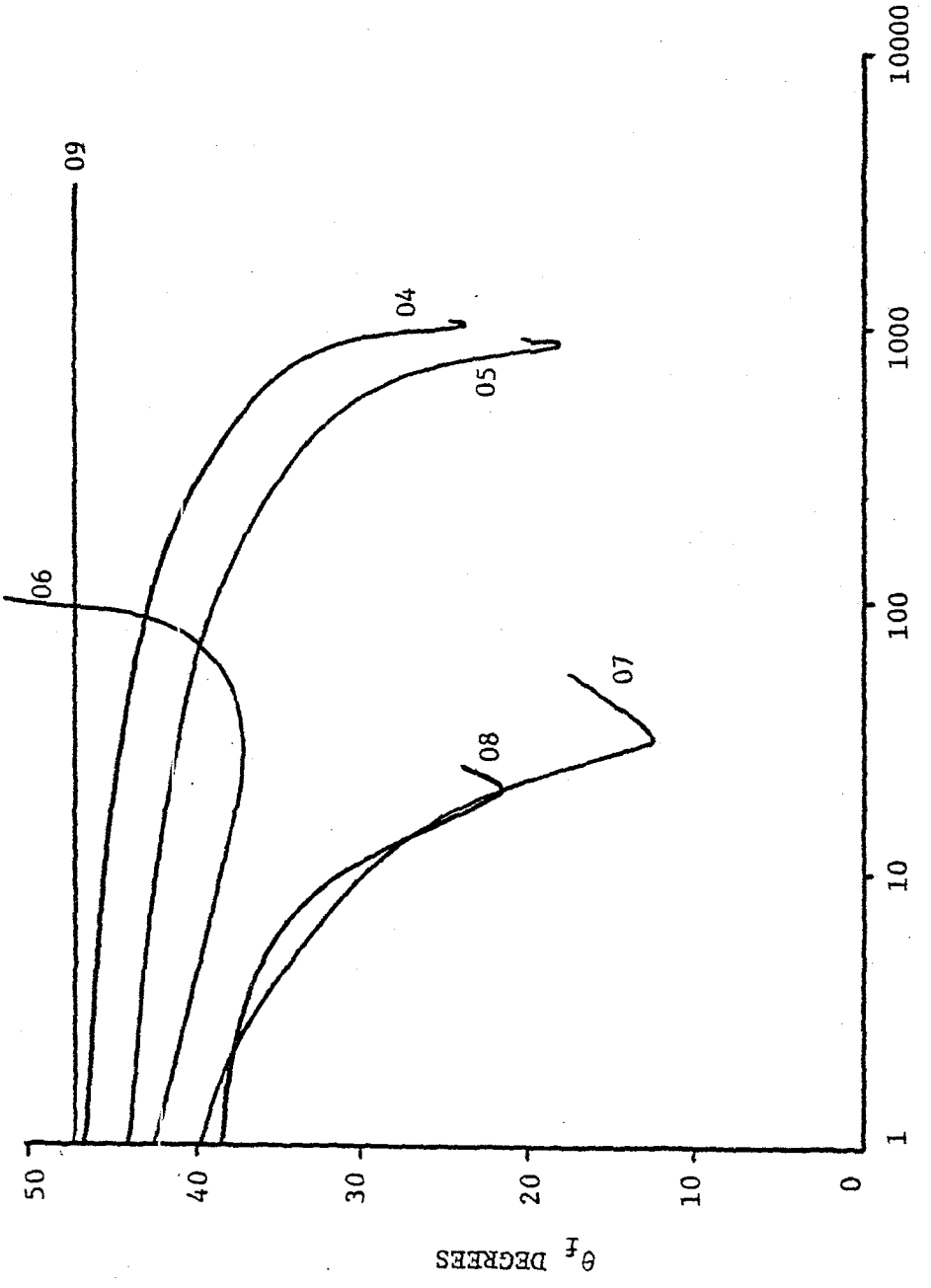

FIGURE 34. THE ANGLE BETWEEN THE HORIZONTAL PLANE AND THE PLANE OF MAXIMUM OBLIQUITY VS. NUMBER OF CYCLES FOR TESTS ON GULF OF ALASKA CLAY

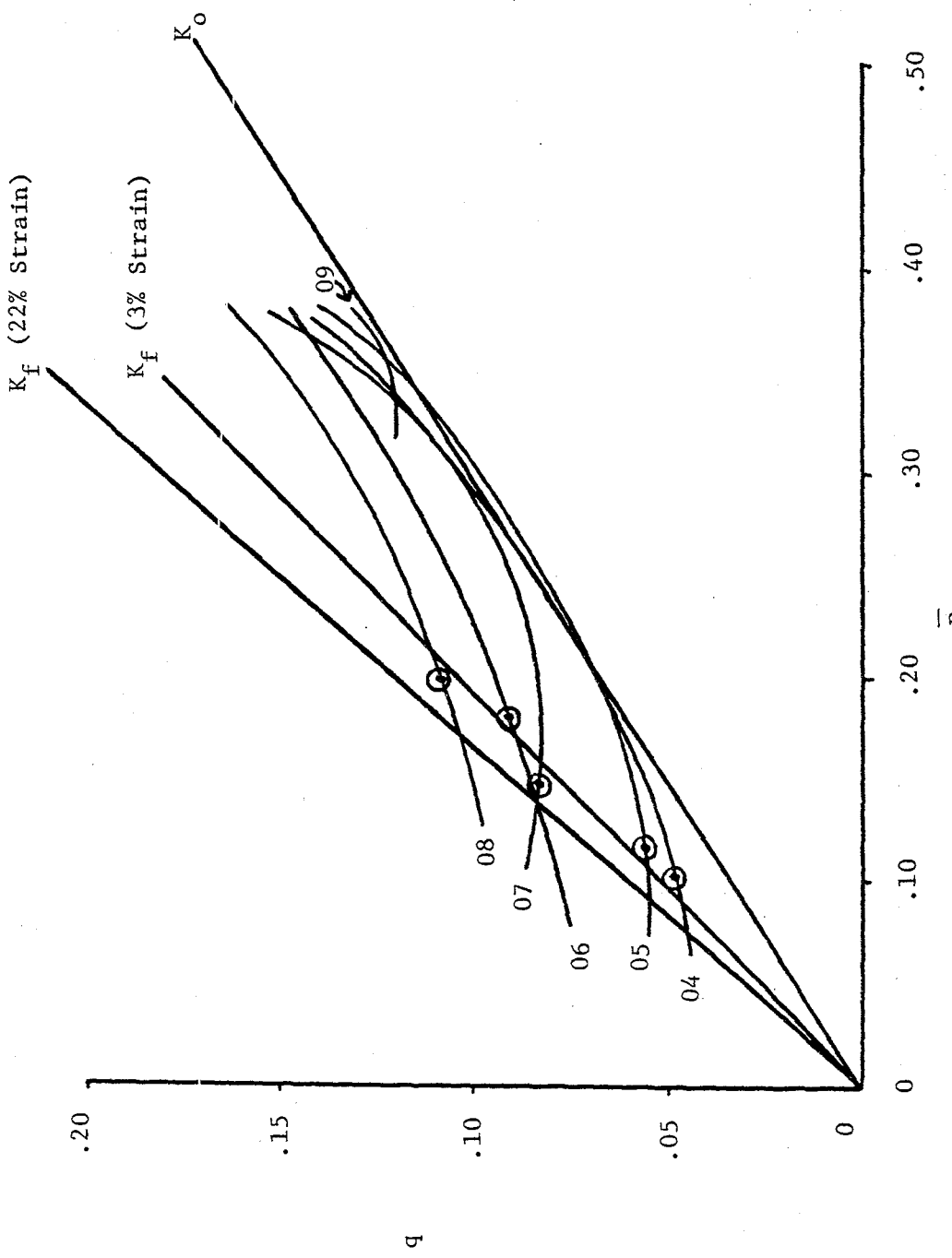

FIGURE 35. STRESS PLOT FOR CYCLIC TESTS ON GULF OF ALASKA CLAY. THE K_f and K_o LINES WERE DETERMINED FROM STATIC TESTS. THE POINTS SHOWN CORRESPOND TO 3 PERCENT SHEAR STRAIN.

The points shown in Figure 35 on each stress path correspond to 3 percent shear strain. These points correspond closely with the static failure line for 3 percent shear strain. For practical problems a shear strain of 3 percent (or even less) constitutes failure. The shear strain rapidly increased after this failure line was reached, and only a few more cycles of loading were applied before very large shear strains were generated and the test terminated. Note that the stress paths shown correspond to the positive peak points only, i.e., when the shear stress has its maximum positive value.

B. Concord Blue Clay

Introduction

The tests performed on the Concord Blue clay are summarized in Table 5. A test number followed by an S indicates a static test, whereas a C indicates a cyclic loading test. The columns of data are explained in Table 4.

A series of 10 tests were performed on normally consolidated Concord Blue clay. Two of these were not completed. Another series of 11 tests were performed on samples overconsolidated in the laboratory to an overconsolidation ratio of 2. The maximum preconsolidation stress applied to these samples was identical to the consolidation stress applied to the normally consolidated samples.

The static tests were performed under controlled strain conditions with a strain rate of 75 minutes per millimeter. The stress controlled cyclic tests were performed with various magnitudes of cyclic stresses. Square wave load shapes were used with a cyclic frequency of 0.5 Hz. This frequency was chosen to simulate earthquake loading conditions. Since lateral stress measurements were not taken, there was ample time for data acquisition at this frequency. The smaller 1.875 in diameter sample size was used. Any exceptions to these conditions are noted in Table 5.

Normally Consolidated Samples

Static stress-strain curves for the normally consolidated samples are shown in Figure 36. The shear stress was normalized by dividing by the consolidation stress σ_{vo}. Test Nos. 09 and 10 were performed following cyclic load-

1	2	3	4	5	6	7	8	9	10	11	12	13	14	15
		BUILDING IN							CONSOLIDATION					
Test No.	D	w %	e	H_i cm	S_u kg/cm^2	S_u kg/cm^2	S_u kg/cm^2	S_t	σ_{vo} kg/cm^2	τ_{ho} kg/cm^2	σ_{vm} kg/cm^2	OCR	H_f cm	ε_v %
01S	S	28.4	.785	1.75	-	-	-	-	1.12	0.0	1.12	1.0	1.69	3.4
02S	S	27.8	.767	1.54	1.00	.60	.58	-	3.37	0.0	3.37	1.0	1.44	6.6
03														
04														
05C	S	28.2	.781	1.49	.80	.40	.46	-	3.37	0.0	3.37	1.0	1.44	3.0
06C	S	28.1	.776	1.97	.75	-	-	-	3.37	0.0	3.37	1.0	1.84	6.6
07C	S	27.4	.759	2.05	-	-	-	-	3.37	0.0	3.37	1.0	1.90	6.9
08C	S	27.6	.762	1.58	-	-	-	-	3.37	0.0	3.37	1.0	1.47	6.9
09C	S	27.0	.759	1.42	.80	-	-	-	3.37	0.0	3.37	1.0	1.33	6.8
10C	S	27.9	.770	1.49	-	-	-	-	3.37	0.0	3.37	1.0	1.39	6.4
11S	S	28.5	.787	2.03	-	-	.31	-	3.37	0.0	6.74	2.0	1.91	5.5

TABLE 5. SUMMARY OF TESTS - CONCORD BLUE CLAY

1	2	3	4	5	6	7	8	9	10	11	12	13	14	15
		BUILDING IN							CONSOLIDATION					
Test No.	D	w %	e	H_i cm	S_u kg/cm^2	S_u kg/cm^2	S_u kg/cm^2	S_t	σ_{vo} kg/cm^2	τ_{ho} kg/cm^2	σ_{vm} kg/cm^2	OCR	H_f cm	ε_v %
12S	S	29.2	.806	1.74	.60	-	.31	-	1.68	0.0	3.37	2.0	1.61	7.7
13C	S	29.1	.803	1.52	.75	.35	.31	-	1.68	0.0	3.37	2.0	1.41	7.4
14C	S	28.6	.789	1.77	.70	-	.31	-	1.68	0.0	3.37	2.0	1.63	7.7
15C	S	28.5	.787	1.78	.75	.40	.37	-	1.68	0.0	3.37	2.0	1.65	7.3
16C	S	29.2	.806	1.98	.80	.40	.37	-	1.68	0.0	3.37	2.0	1.84	7.2
17C	S	29.8	.822	1.89	.75	.40	.37	-	1.68	0.0	3.37	2.0	1.74	8.3
18C	S	29.5	.817	1.54	.75	.45	.37	-	1.68	0.0	3.37	2.0	1.39	9.4
19C	S	29.8	.820	1.82	.70	.40	.37	-	1.68	0.0	3.37	2.0	1.68	7.3
20C	S	29.0	.800	1.70	.80	.45	-	-	1.68	0.0	3.37	2.0	1.55	9.1
21C	S	29.2	.806	1.78	.75	.35	-	-	1.68	0.0	3.37	2.0	1.63	8.2

TABLE 5. (CONTINUED)

	16	17	18	19	20	21	22	23	24	25	26	27	28
	CYCLIC LOADING						STATIC LOADING				AFTER TEST		
Test No.	τ_c kg/cm^2	τ_c/S_u %	N	γ_n %	u_n kg/cm^2	f Hz	S_u kg/cm^2	γ_f %	u_f kg/cm^2	RATE min/mm	w %	e	Remarks
01S	-	-	-	-	-	-	.347	12.2	.302	30	28.7	.792	No corrections
02S	-	-	-	-	-	-	.744	10.3	1.260	200	-	-	
03													Large Stone in Sample
04													Large Stone in Sample
05C	.352	48	570	28.1	3.044	.5	-	-	-	-	26.0	.718	
06C	.437	59	27	9.2	2.621	.5	-	-	-	-	25.1	.693	
07C	.296	40	1360	10.7	2.923	.5	-	-	-	-	25.5	.704	
08C	.212	29	5960	14.4	3.024	.5	-	-	-	-	26.5	.731	
09C	.156	21	3000	.04	.292	.5	.772	8.63	1.310	100	25.8	.712	
10C	.184	25	5000	.13	.726	.5	.675	14.1	1.613	100	-	-	
11S	-	-	-	-	-	-	1.106	10.8	.171	75	25.1	.693	

TABLE 5. (CONTINUED)

	16	17	18	19	20	21	22	23	24	25	26	27	28
	CYCLIC LOADING						STATIC LOADING				AFTER TEST		
Test No.	τ_c kg/cm^2	τ_c/S_u %	N	γ_n %	u_n kg/cm^2	f Hz	S_u kg/cm^2	γ_f %	u_f kg/cm^2	RATE min/mm	w %	e	Remarks
12S	-	-	-	-	-	-	.692	12.5	-.020	75	27.4	.756	
13C	.219	32	625	12.0	1.411	.5	-	-	-	-	26.5	.731	
14C	.191	28	789	11.7	1.512	.5	-	-	-	-	26.5	.731	
15C	.163	24	3630	11.3	1.512	.5	-	-	-	-	26.6	.734	
16C	.185	27	1286	9.2	1.411	.5	-	-	-	-	26.4	.729	
17C	.350	51	30	15.6	1.210	.5	-	-	-	-	26.8	.740	
18C	.124	18	4280	8.5	1.462	.5	-	-	-	-	26.9	.742	
19C	.180	26	510	10.6	1.411	.1	-	-	-	-	25.2	.690	
20C	.320	46	28	15.8	1.310	.1	-	-	-	-	25.9	.715	
21C	.067	10	6000	.05	-.010	.5	.568	11.0	.161	75	26.0	.718	

TABLE 5. (CONTINUED)

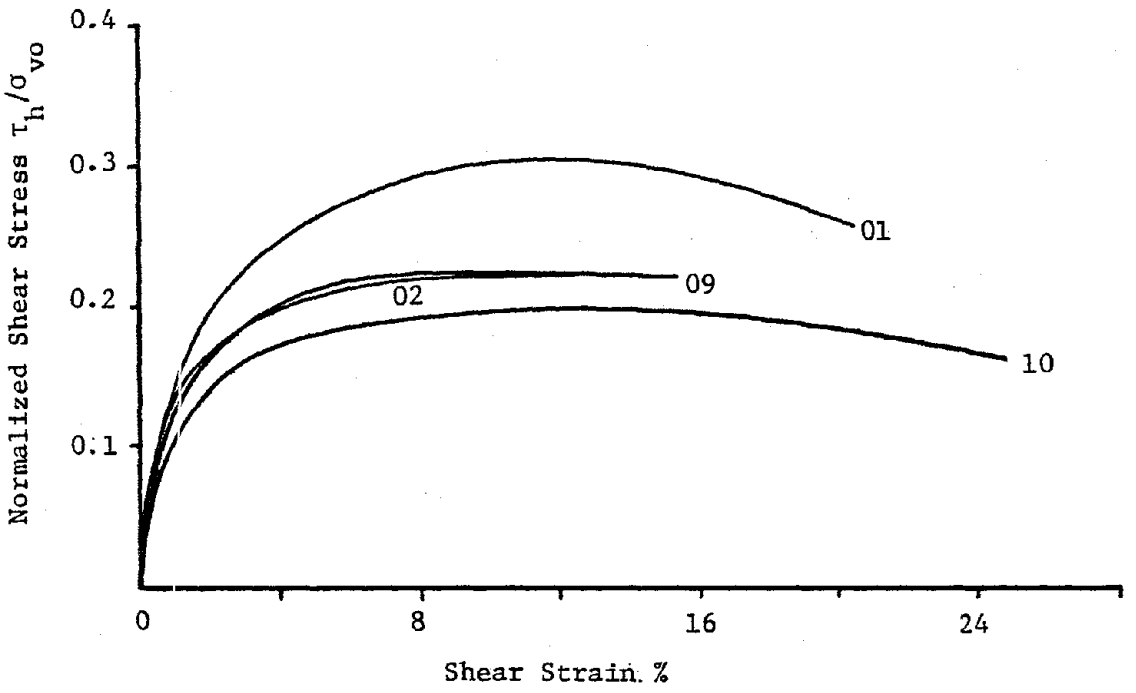

FIGURE 36. STATIC STRESS-STRAIN CURVES - NORMALLY CONSOLIDATED CONCORD BLUE CLAY

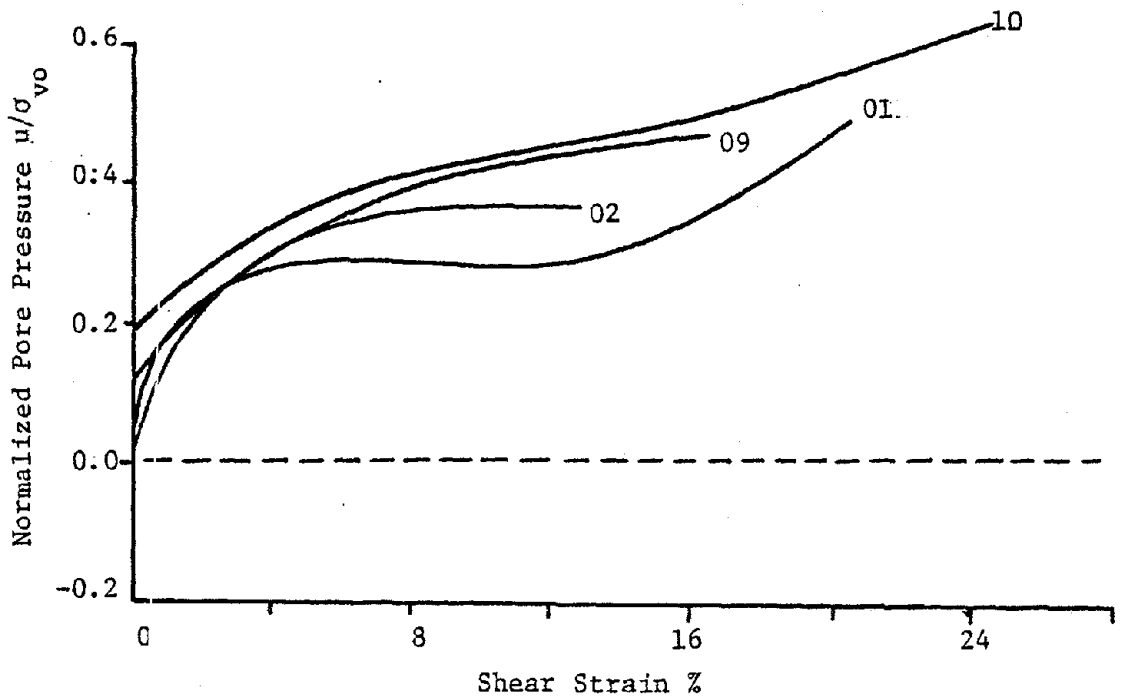

FIGURE 37. NORMALIZED PORE PRESSURE VS. SHEAR STRAIN - NORMALLY CONSOLIDATED CONCORD BLUE CLAY

ing which did not cause failure. The stress-strain curves for these tests were considerably lower than the curve obtained for Test No. 01. This can be expected since cyclic loading reduces the stiffness and undrained shear strength in a subsequent static test (80,90,140). Test No. 10 was tested at a larger cyclic shear stress than Test No. 09; as a result the stress-strain curve for Test No. 10 is lower than the one obtained from Test No. 09. The stress-strain curve for Test No. 02 appears to be rather low. The reason for this is not readily apparent, but it may be caused by the different strain rates used or sample disturbance.

Pore pressure vs. shear strain data are shown in Figure 37 for the static tests. The consolidation stress was used to normalize the pore pressures. The pore pressure increases continuously throughout the tests, although the largest increase occurs during the first few percent of shear strain. Comparing these curves with the stress-strain data shown in Figure 36, it is evident that there is a correlation between the pore pressures generated and the shear stress that the sample can sustain. The samples with the lowest stress-strain curves have the highest pore pressures. Higher pore pressures are generated in the samples that were previously subjected to cyclic loading than those that were not. The pore pressures are highest for Test No. 10 that was tested at a higher cyclic stress level than Test No. 09. Note that there is also an initial pore pressure for these tests that was caused by the previous cyclic loading.

Cyclic shear strain vs. number of loading cycles is shown in Figure 38. The shear strain for all cyclic loading tests is one-half the peak to peak shear strain. Typically, the cyclic shear strains increase gradually until

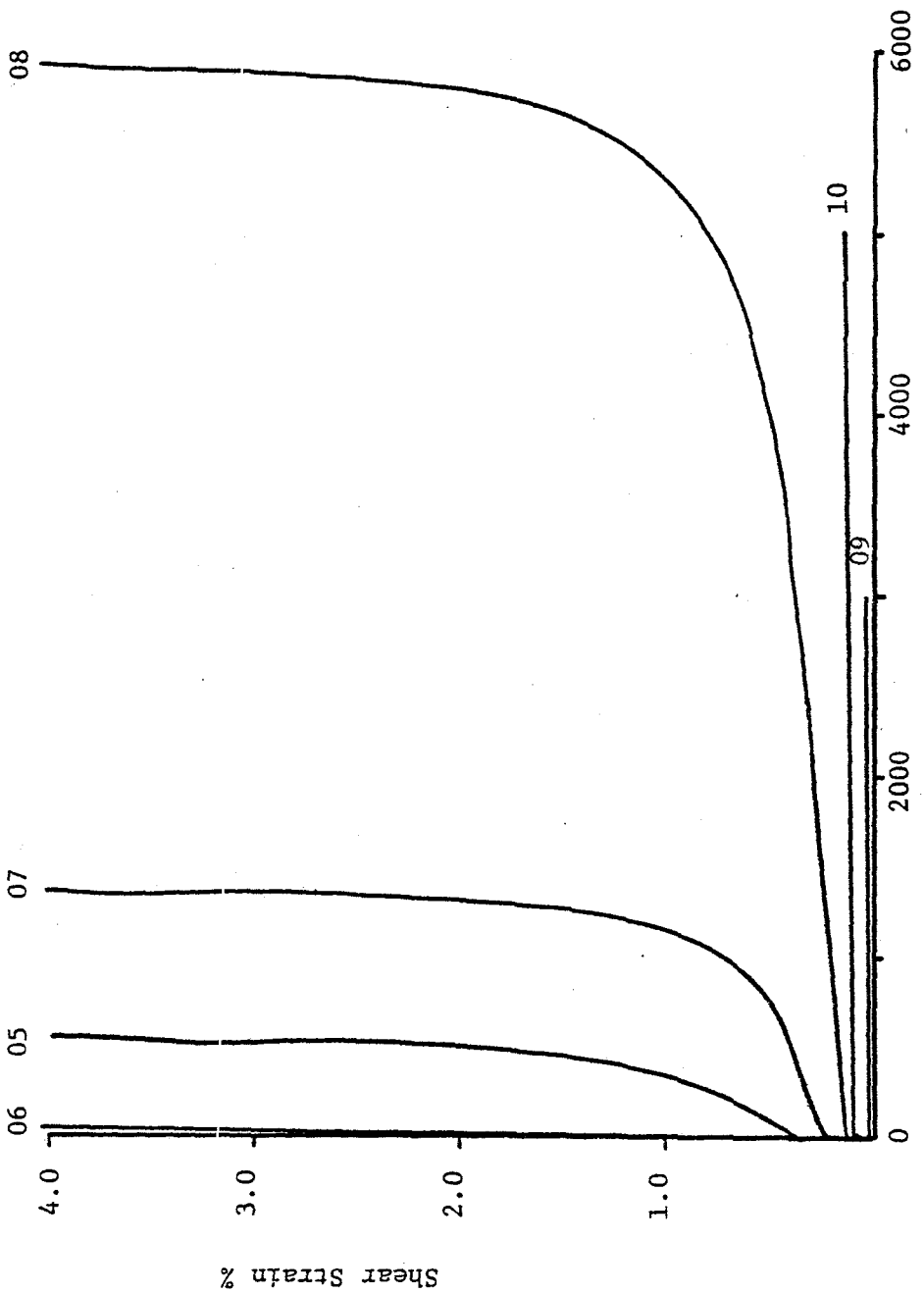

FIGURE 38. SHEAR STRAIN VS. NUMBER OF CYCLES - NORMALLY CONSOLIDATED CONCORD BLUE CLAY

failure is imminent, after which the cyclic shear strains increase very rapidly. Test Nos. 09 and 10 showed no indication of failure even after 5,000 loading cycles.

Normalized pore pressure vs number of loading cycles is shown in Figure 39. As mentioned previously, these curves show the permanent or residual increase in excess pore pressure resulting from cyclic loading. The pore pressure variation within a given loading cycle was not measured. The pore pressures increase gradually until failure is imminent after which they rapidly increase. A comparison with Figure 38 shows that there is an excellent correlation between the excess pore pressures and the shear strains that are developed in these stress controlled tests. The pore pressures remain constant during the latter parts of tests 09 and 10. It appears that the pore pressures will remain constant with further loading cycles. Therefore, these samples exhibit a state of nonfailure equilibrium.

"Stress path" data for the static and cyclic tests are shown in Figure 40. In this diagram the horizontal shear stress is plotted vs. the vertical effective normal stress. A failure line was drawn through the tip of the stress path for static test No. 01. Test No. 02 was not used to determine this failure line because it was terminated at a lower strain than the other tests. The angle of internal friction as determined from this failure line is 24°. The data for the cyclic tests are shown for the positive peak points only, i.e., when the shear stress has its maximum positive value. The actual stress path would cycle symmetrically above and below the horizontal axis. For the tests in which failure occurred, the

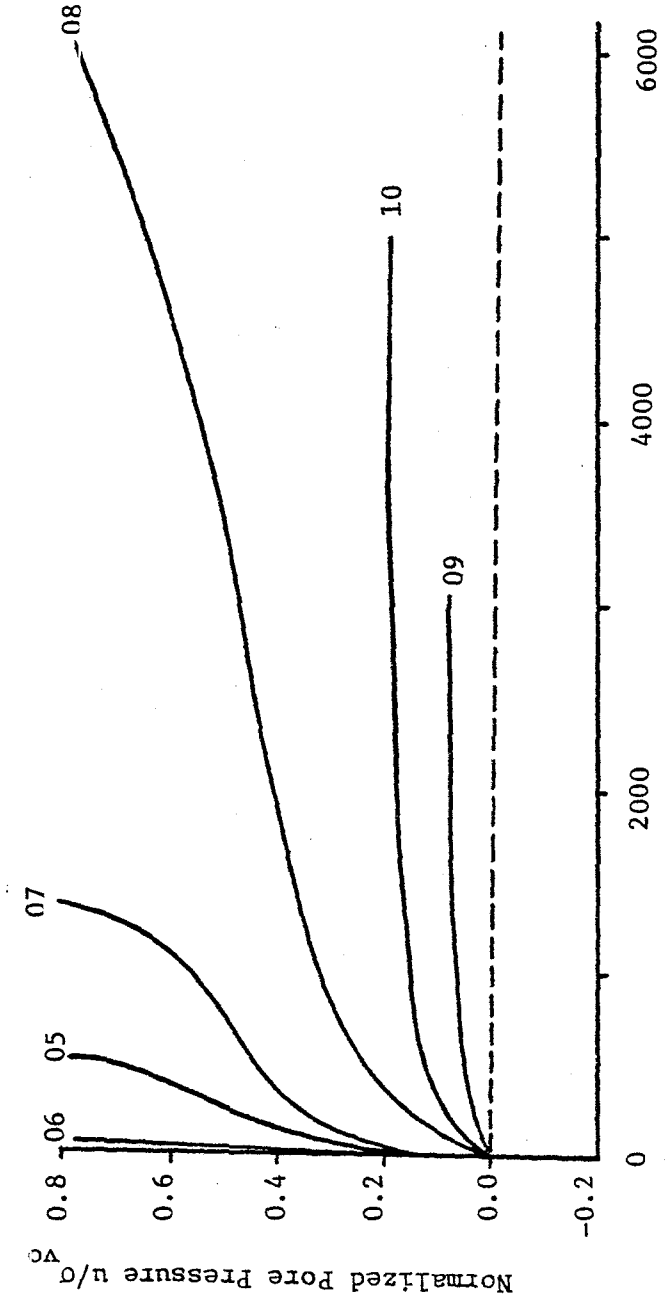

FIGURE 39. NORMALIZED PORE PRESSURE VS. NUMBER OF CYCLES - NORMALLY CONSOLIDATED CONCORD BLUE CLAY

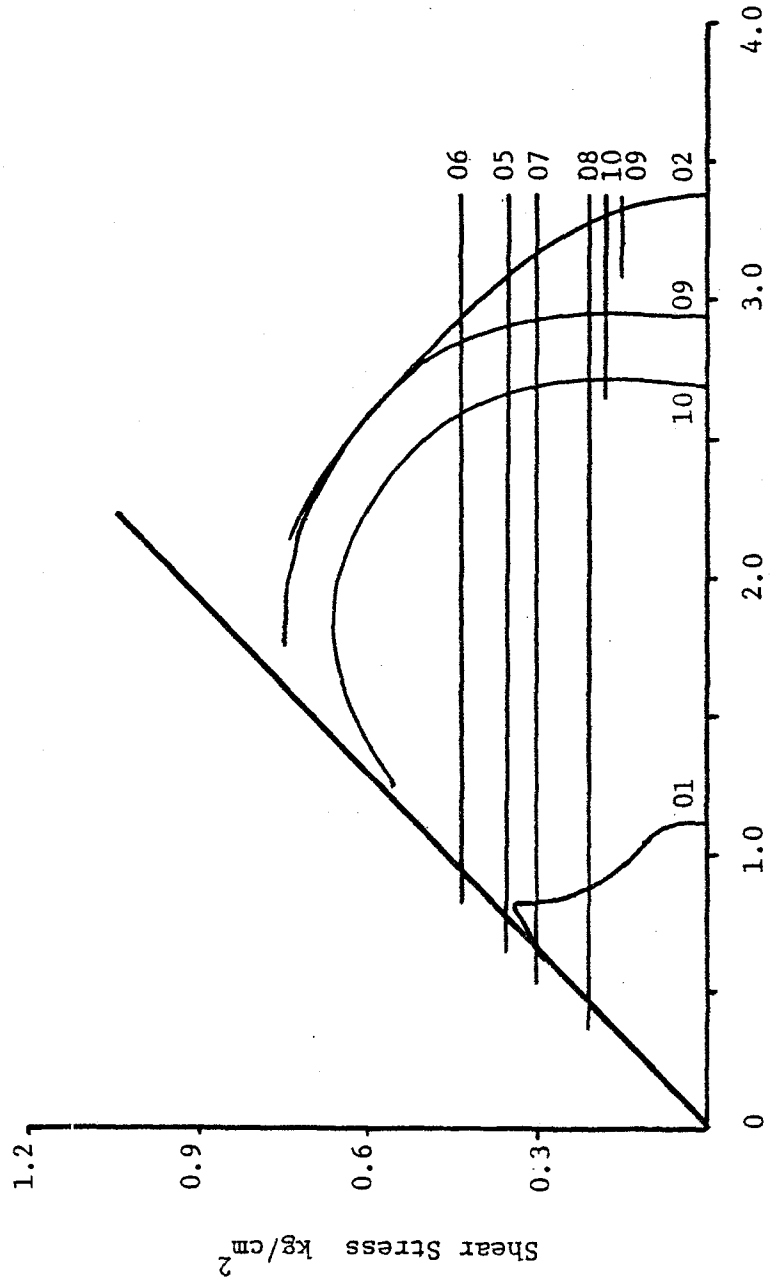

FIGURE 40. STRESS PATHS FOR STATIC AND CYCLIC TESTS - NORMALLY CONSOLIDATED CONCORD BLUE CLAY

stress paths reach the static failure line. The stress paths for test Nos. 09 and 10, which exhibited a state of non failure equilibrium, did not reach the static failure line.

Slightly Overconsolidated Samples

Static stress-strain curves for the overconsolidated samples are shown in Figure 41. The data was normalized by the final consolidation stress σ_{vo}. Test No. 21 was performed following cyclic loading which did not cause failure.

Normalized pore pressure vs. shear strain data are shown in Figure 42 for the static tests. Initially, negative pore pressures develop. This is followed by a steady increase in pore pressures, and at large strains the resulting pore pressures are positive. Higher pore pressures were generated in the sample that was previously subjected to cyclic loading than in those that were not.

Cyclic shear strain vs. number of loading cycles is shown in Figure 43. The behavior is similar to the normally consolidated samples. The cyclic shear strains increase gradually until failure is imminent, after which they increase very rapidly. Test No. 21 showed no indication of failure even after 6,000 loading cycles.

Normalized pore pressure vs. number of loading cycles is shown in Figure 44. Negative pore pressures develop during the initial loading cycles. The pore pressures rapidly increase however, and they are positive throughout the latter part of the test. The pore pressure for Test No. 21 that did not fail during cyclic loading remained approximately zero.

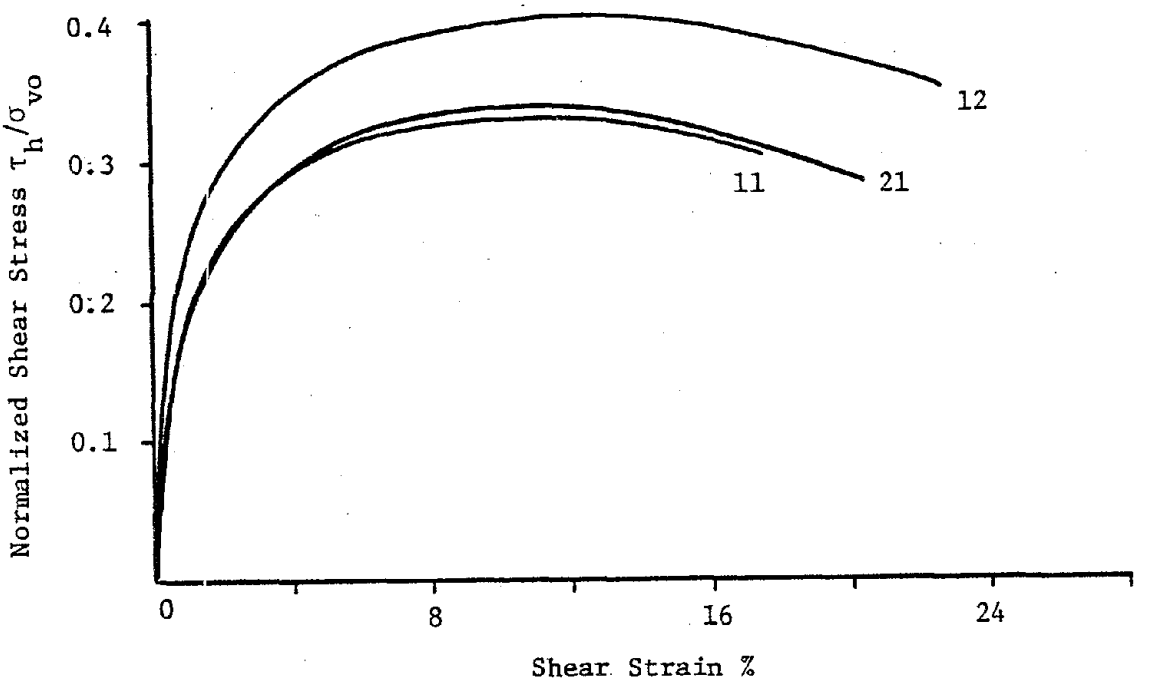

FIGURE 41. STATIC STRESS-STRAIN CURVES - SLIGHTLY OVERCONSOLIDATED CONCORD BLUE CLAY

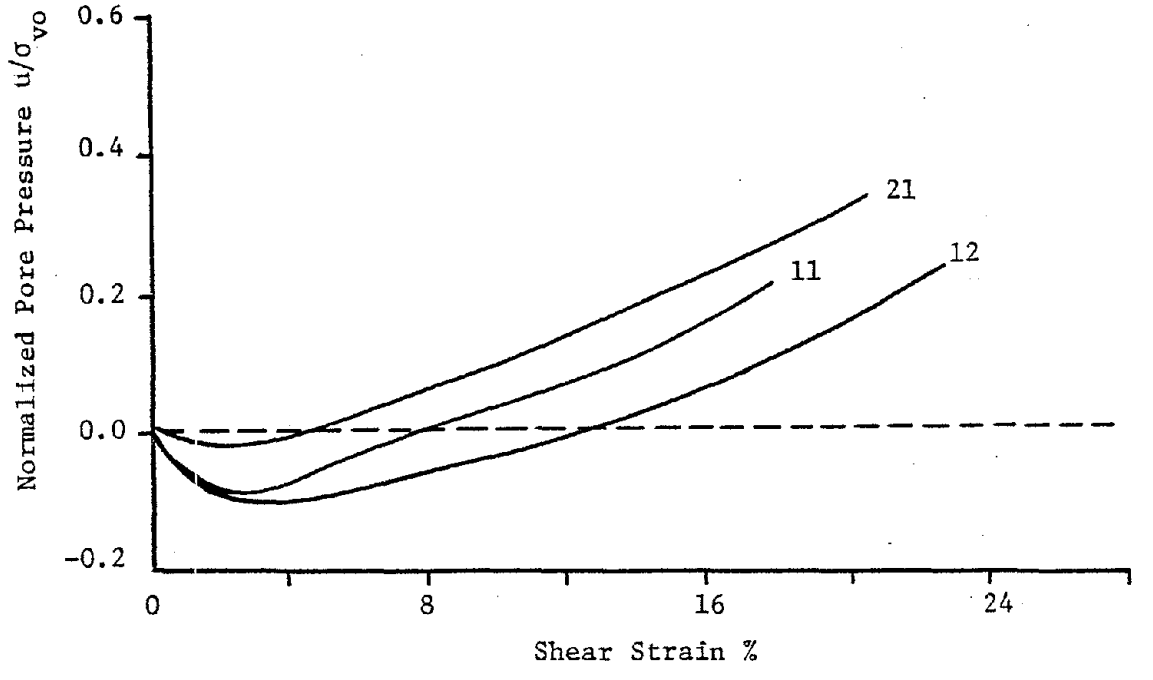

FIGURE 42. NORMALIZED PORE PRESSURE VS. SHEAR STRAIN - SLIGHTLY OVERCONSOLIDATED CONCORD BLUE CLAY

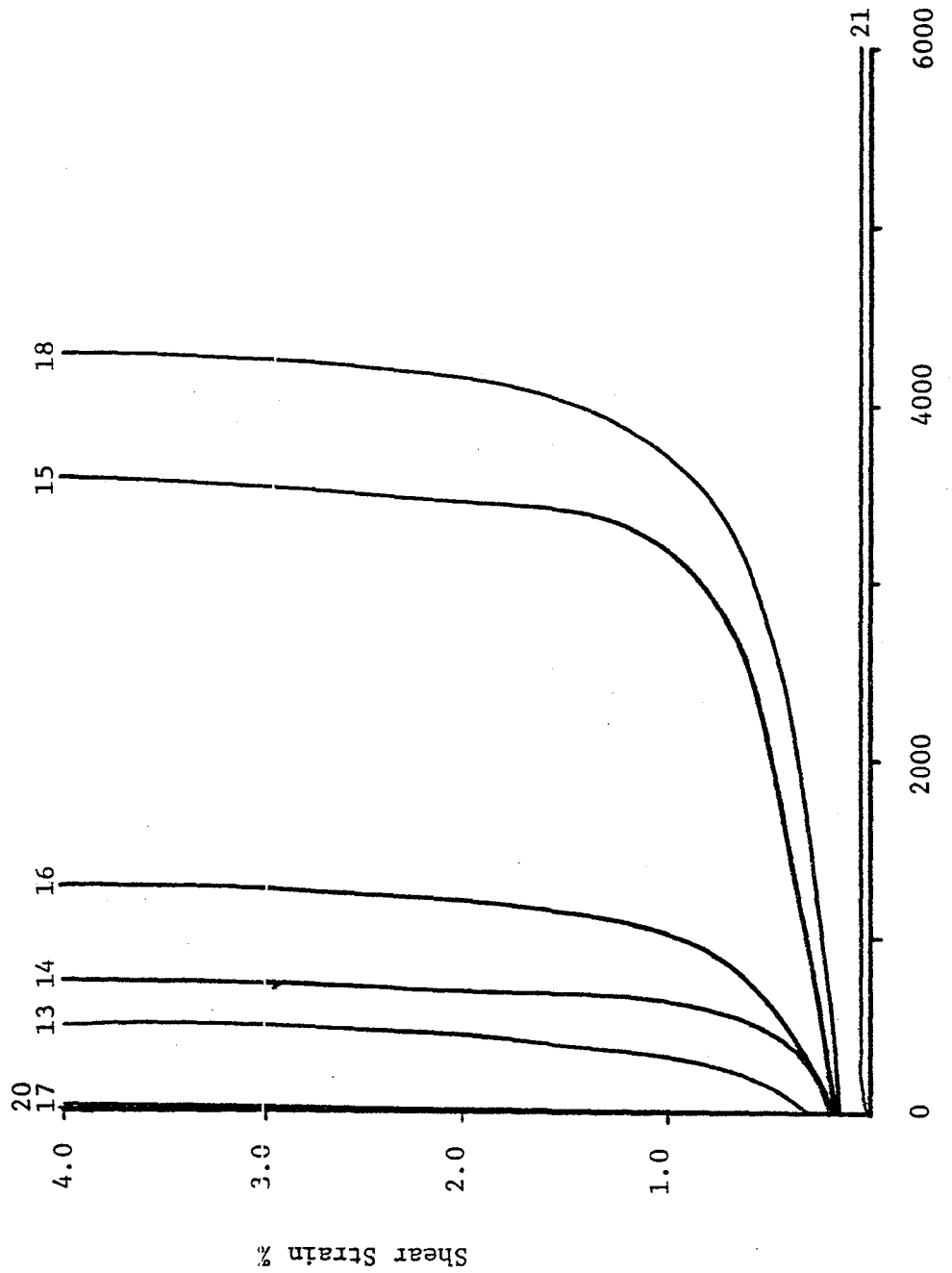

FIGURE 43. SHEAR STRAIN VS. NUMBER OF CYCLES - SLIGHTLY OVERCONSOLIDATED CONCORD BLUE CLAY

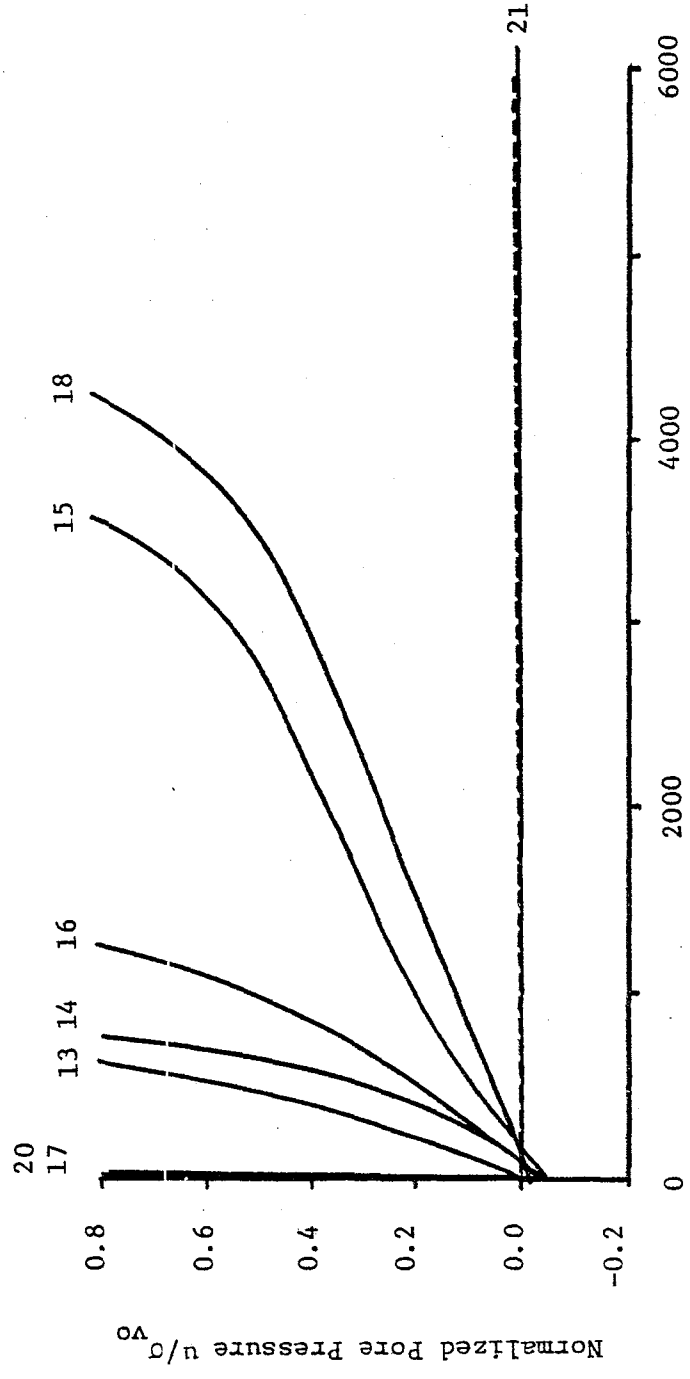

FIGURE 44. NORMALIZED PORE PRESSURE VS. NUMBER OF CYCLES - SLIGHTLY OVERCONSOLIDATED CONCORD BLUE CLAY

"Stress path" data for the static and cyclic tests are shown in Figure 45. A failure line was drawn based on the static test results. The angle of internal friction as determined from this failure line is 24°. For the cyclic tests in which failure occurred, the stress paths reach the static failure line. The stress path for Test No. 21 which exhibited a state of nonfailure equilibrium did not reach the static failure line.

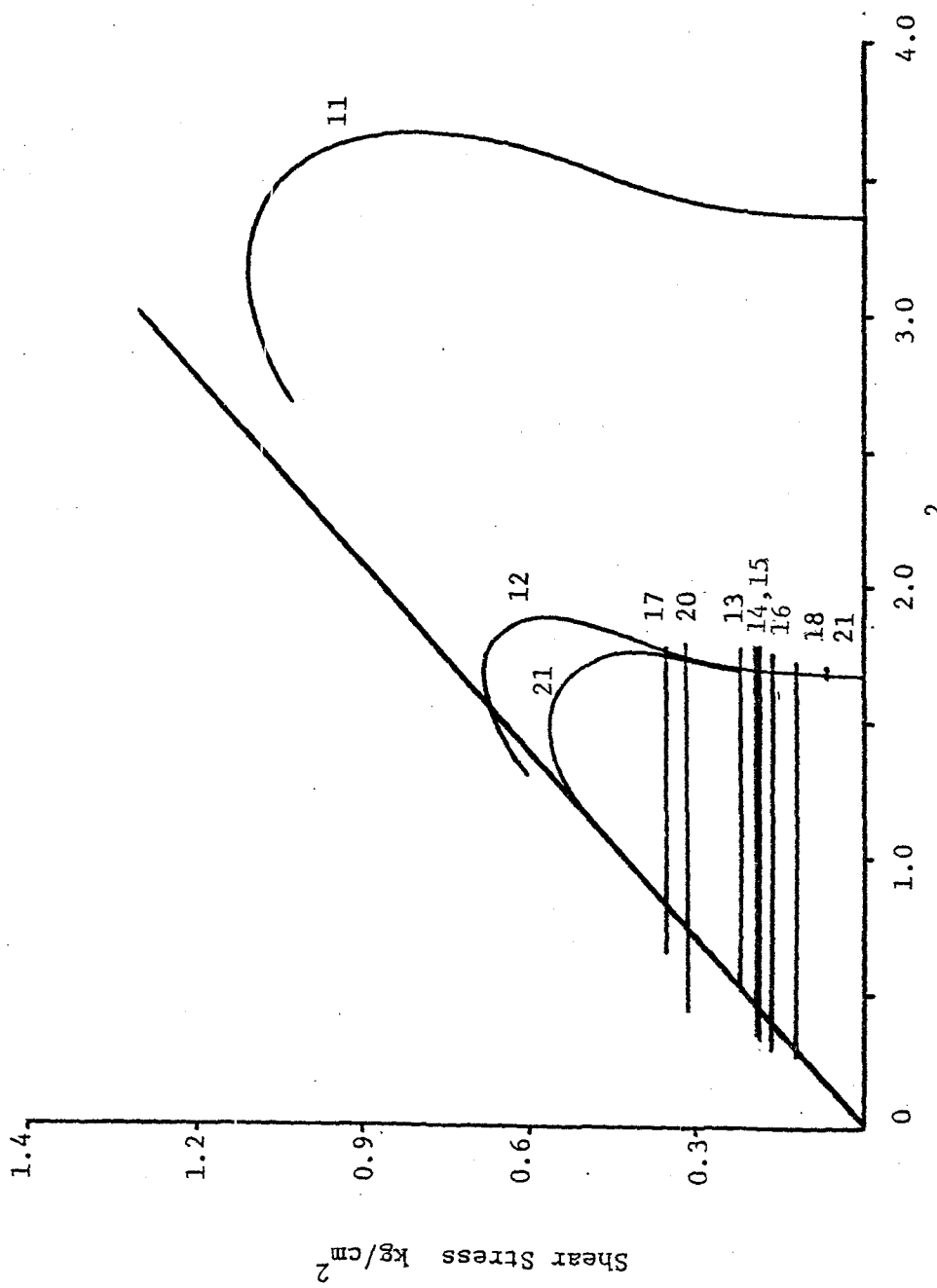

FIGURE 45. STRESS PATHS FOR STATIC AND CYCLIC TESTS - SLIGHTLY OVERCONSOLIDATED CONCORD BLUE CLAY

PART 8

DISCUSSION AND CONCLUSIONS

An understanding of the behavior of fine grained soils subjected to cyclic loading has become increasingly important for the modern geotechnical engineer. The importance of laboratory testing and research on the cyclic loading behavior of soils was stressed at a recent workshop on "Research Needs and Priorities for Geotechnical Earthquake Engineering Applications" held at Austin, Texas (103).

This report deals primarily with the results of a series of consolidated constant volume (CCV) direct simple shear tests performed on undisturbed clay samples using the Norwegian Geotechnical Institute (NGI) device. Static and cyclic tests were performed. Emphasis was placed on high strain level repetitive loading such as that which is caused by earthquakes and storm wave loads.

The stress conditions existing in direct simple shear devices were examined based on published literature. It was concluded that:

- The stress conditions existing in the direct simple shear device are not ideal. However, no geotechnical testing apparatus is perfect, and it may be impossible to construct a completely satisfactory laboratory apparatus.
- The stress conditions existing in the central part of the sample are reasonably uniform, and they are representative of the stresses imposed on the boundaries of the sample.

- Direct simple shear test results have been found to be consistent with the results of triaxial tests and shake table tests.
- Despite the internal complexities and uncertainties associated with the direct simple shear device, the test has been a useful tool in studying static and cyclic shear phenomena.

A series of tests were performed on undisturbed clay samples from the Copper River prodelta in the Gulf of Alaska. The Gulf of Alaska is in an area of intense seismic activity; storms with large waves are also common. Since petroleum related activities in the Gulf of Alaska region may stimulate major marine construction, it is important to identify and evaluate the cyclic loading behavior of these soils. The importance of testing marine sediments and improving the existing data base for these soils has also been noted in the literature (8,103,131).

All test results on the Gulf of Alaska clay include the measurement of lateral stresses using calibrated reinforced rubber membranes. The additional data provided by the lateral stress measurements considerably adds to the knowledge of the stress conditions existing in the sample. This information aids in the interpretation of test results and in the comparison of the direct simple shear apparatus with other testing devices. The assumptions used for the interpretation of the test results are discussed in Part 5. It was concluded from the static test results that for

the Gulf of Alaska clay:

- The pore pressures increase throughout the test. Therefore the vertical effective normal stress ($\bar{\sigma}_v$) decreases during the test.
- The horizontal effective normal stress ($\bar{\sigma}_h$) first decreases and then increases as the shear strains increase.
- At large shear strains, the ratio $\bar{\sigma}_h/\bar{\sigma}_v$ approaches unity.
- At large shear strains, the horizontal plane is approximately the plane on which the maximum shear stress acts. This result is important for the interpretation of tests in which lateral stress measurements are not made.
  Roscoe et al (107) found similar results for sands using the Cambridge simple shear device.
- The horizontal plane is never the plane of maximum obliquity at any stage during the test. Therefore, this common assumption that the horizontal plane is the theoretical failure plane is unwarranted for the Gulf of Alaska clay. Roscoe et al (107) found similar results for sands using the Cambridge simple shear device.
- Based on the assumption of failure at 3 percent shear strain, the angle of internal friction was found to be 31° based on $\bar{p}$ - q stress paths. Using the assumption that the horizontal plane is the theoretical failure plane (i.e., $\tan\phi = \tau/\bar{\sigma}_v$) the angle of internal friction was found to be 21°.

It was concluded from cyclic test results on the Gulf of Alaska clay that:

- Cyclic shear strains and pore pressures increased gradually until failure was imminent, after which they increased very rapidly.
- Cyclic loading failure did not occur if the cyclic shear stress was small. The critical level of repeated stress (112) was found to be approximately 25 percent of the static shear strength.
- The concept of a critical level of repeated stress was found to be valid for a large number (3000) of loading cycles.
- The shear modulus was found to decrease gradually until failure was imminent; thereafter the shear modulus rapidly decreases. Prior to failure, the shear modulus vs. number of cycles relation is linear on a log-log plot. As the cyclic shear stress increases, the slope of this relationship increases.
- The ratio $\overline{\sigma}_h/\overline{\sigma}_v$ approaches unity as failure occurs. Similar results are also cited in the literature. Youd (155) found that repeated shear straining increased the coefficient of lateral stress for sands. Ishihara et. al. (59) found that the lateral stress will change to produce an isotropic state of stress upon liquefaction in sand samples.
- At failure, the horizontal plane is approximately the plane of maximum shear stress. The plane of maximum obliquity does not correspond with the horizontal plane.

- Stress paths for the cyclic tests in which failure occurred reach and cross the failure lines that were established on the basis of static test results. This occurs for both stress paths used in this investigation ($\bar{p}$ - q and τ - $\bar{\sigma}_v$). However at 3 percent shear strain, the cyclic stress paths and the failure lines correspond quite well.

The static and cyclic loading behavior of Concord Blue clay was also investigated. Lateral stress measurements were not made for these tests. It was concluded:

- The development of cyclic shear strains and pore pressures were similar to that reported for the Gulf of Alaska clay. For the slightly overconsolidated (OCR = 2) samples, negative pore pressures were generated during the early loading cycles. However, these pore pressures became positive with further cycling.
- The critical level of repeated stress was found to be 25% of the static shear strength for the normally consolidated samples and 20% of the static shear strength for the slightly overconsolidated (OCR = 2) samples.
- The concept of a critical level of repeated stress was found to be valid up to 6000 loading cycles.
- Stress paths (τ vs. $\bar{\sigma}_v$) for the cyclic tests in which failure occurred reach and cross the failure line that was established on the basis of static test results. Stress paths for samples which exhibited a state of nonfailure equilibrium do not reach the static failure line.

- The angle of internal friction was computed to be 25° based on the assumption that $\tan\phi = \tau/\overline{\sigma}_v$.

Further research based on the results of these and other subsequent tests is currently being conducted.

PART 9

REFERENCES

1. A-Grivas, D., Editor (1977), "Research Needs in the Area of Probabilistic Soil Dynamics", Proc., Probability Theory and Reliability Analysis in Geotechnical Engineering, Rensselaer Polytechnic Institute, Troy, New York, pp. 278-285.

2. Andersen, K.H. (1976), "Behavior of Clay Subjected to Undrained Cyclic Loading", Proc. International Conf. on the Behavior of Offshore Structures, Norwegian Institute of Technology, Trondheim, Vol. 1, pp. 392-403.

3. Andersen, K.H. et. al. (1976), "Effect of Cyclic Loading on Clay Behavior", Norwegian Geotechnical Institute, Oslo, Publication 113, pp. 1-6.

4. Anderson, D.G. and Richart, F.E., Jr. (1976), "Effects of Straining on Shear Modulus of Clays", J. Geotechnical Eng. Div., ASCE, Vol. 102, No. GT9, pp. 795-987.

5. Anderson, D.G. and Woods, R.D. (1976), "Time-Dependent Increase in Shear Modulus of Clay", J. Geotechnical Eng. Div., ASCE, Vol. 102, No. GT5, pp. 525-537.

6. Arango, I. and Seed, H.B. (1974), "Seismic Stability and Deformation of Clay Slopes", J. Geotechnical Eng. Div., ASCE, Vol. 100, No. GT2, pp. 139-156.

7. Bishop, A.W. and Henkel, D.J. (1962), The Measurement of Soil Properties in the Triaxial Test, Edward Arnold Ltd., London.

8. Bjerrum, L. (1973), "Geotechnical Problems Involved in Foundations of Structures in the North Sea", Geotechnique, Vol. 23, No. 3, pp. 319-358.

9. Bjerrum, L. and Landva, A. (1966), "Direct Simple Shear Tests on a Norwegian Quick Clay", Geotechnique, Vol. 16, No. 1, pp. 1-20.

10. Brown, S.F., Andersen, K.H. and McElvaney, J. (1977), "The Effect of Drainage on Cyclic Loading of Clay", Proc., 9th ICSMFE, Tokyo, Vol. 2, pp. 195-200.

11. Brown, S.F., Lashine, A.K.F. and Hyde, A.F.L. (1975), "Repeated Load Triaxial Testing of a Silty Clay", Geotechnique, Vol. 25, No. 1, pp. 95-114.

12. Carlson, P.R. (1976), "Submarine Faults and Slides that Disrupt Surficial Sedimentary Units, Northern Gulf of Alaska", U.S. Geological Survey, Open File Report 76-294, Menlo Park, California.

13. Casagrande, A. (1936), "Characteristics of Cohesionless Soils Affecting the Stability of Slopes and Earth Fills", J. of the Boston Society of Civil Engineers, Jan.

14. Casagrande, A. and Shannon, W.L. (1948), "Strength of Soil Under Dynamic Load", Transactions, ASCE, Vol. 74, No. 4, pp. 591-608.

15. Castro, G. (1975), "Liquefaction and Cyclic Mobility of Saturated Sands", J. Geotechnical Eng. Div., ASCE, Vol. 101, No. GT6, pp. 551-569.

16. Castro, G. and Poulos, S.J. (1976), "Factors Affecting Liquefaction and Cyclic Mobility", Liquefaction Problems in Geotechnical Engineering, ASCE National Convention, Philadelphia, pp. 105-137.

17. Christian, J.T. and Swiger, W.F. (1975), "Statistics of Liquefaction and SPT Results", J. Geotechnical Eng. Div., ASCE, Vol. 101, No. GT11, pp. 1135-1150.

18. Danielson, E.F., Burt, W.V. and Rattray, M.,Jr. (1957), "Intensity and Frequency of Severe Storms in the Gulf of Alaska", Transactions, American Geophysical Union, Vol. 38, No. 1, pp. 44-49.

19. De Alba, P., Seed, H.B. and Chan, C.K. (1976), "Sand Liquefaction in Large-Scale Simple Shear Tests", J. Geotechnical Eng. Div., ASCE, Vol. 102, No. GT9, pp. 909-927.

20. Dobry, R. (1970), "Damping in Soils: Its Hysteretic Nature and the Linear Approximation", Soils Publication No. 253, Dept. of Civil Engineering, Massachusetts Institute of Technology, Cambridge, Ma.

21. Donovan, N.C. (1971), "A Stochastic Approach to the Seismic Liquefacation Problem", Proc., 1st Int. Conf. on Applications of Statistics and Probability to Soil and Structural Engineering, Hong Kong.

22. Donovan, N.C. and Singh., S. (1976), "Liquefaction Criteria for the Trans-Alaska Pipeline", Liquefaction Problems in Geotechnical Engineering, ASCE National Convention, Philadelphia, pp. 139-167.

23. Duncan, J.M. and Dunlop, P. (1969), "Behavior of Soils in Simple Shear Tests", Proc., 7th ICSMFE, Mexico City, Vol. 1, pp. 101-109.

24. Egan, J.A. and Sangrey, D.A. (1978), "Critical State Model for Cyclic Load Pore Pressure", Proc., Earthquake Engineering and Soil Dynamics, ASCE Specialty Conf., Pasadena, Vol. 1, pp. 410-424.

25. Eide, O. (1974), "Marine Soil Mechanics", Norwegian Geotechnical Institute, Oslo, Publication 103, pp. 1-20.

26. Esrig, M.I., Kirby, R.G., Bea, R.G. and Murphy, B.S. (1977), "Initial Development of a General Effective Stress Method for the Prediction of Axial Capacity for Driven Piles in Clay", Proc., 9th Offshore Technology Conf., Houston, pp. 495-506.

27. Esrig, M.I., Ladd, R.S. and Bea, R.G. (1975), "Material Properties of Submarine Mississippi Delta Sediments Under Simulated Wave Loadings", Proc., 7th Offshore Technology Conf., Houston, pp. 399-411.

28. Ferritto, J.M. and Forrest, J.B. (1977), "Siting Structures in Seismic Liquefaction Areas", Proc., 9th ICSMFE, Tokyo, Vol. 2, pp. 225-229.

29. Finn, W.D.L. (1972), "Liquefaction of Sands", Proc., International Conf. on Microzonation, Seattle, Vol. 1, pp. 87-111.

30. Finn, W.D.L., Byrne, P.M. and Martin, G.R. (1976), "Seismic Response and Liquefaction of Sands:, J. Geotechnical Eng. Div., ASCE, Vol. 102, No. GT8, pp. 841-856.

31. Finn, W.D.L., Emery, J.J. and Gupta, Y.P. (1971), "Liquefaction of Large Samples of Saturated Sand on a Shaking Table", Proc., 1st Canadian Conference on Earthquake Engineering, Vancouver, pp. 97-110.

32. Finn, W.D.L., Lee, K.W. and Martin, G.R. (1977), "Dynamic Effective Stress Analysis of Sands", Proc., 9th ICSMFE, Tokyo, Vol. 2, pp. 231-235.

33. Finn, W.D.L., Lee, K.W. and Martin, G.R. (1976), "An Effective Stress Model for Liquefaction", Liquefaction Problems in Geotechnical Engineering, ASCE National Convention, Philadelphia, pp. 169-198.

34. Finn, W.D.L., Lee, K.W., and Martin, G.R. (1976), "Constitutive Laws for Sand in Dynamic Shear", Proc., 2nd International Conf. on Numerical Methods in Geomechanics, Blacksburg, Virginia, Vol. 1, pp. 270-281.

35. Finn, W.D.L., Martin, G.R., and Lee, K.W. (1978), "Application of Effective Stress Methods for Offshore Seismic Design in Cohesionless Seafloor Soils", Proc., 10th Offshore Technology Conf., Houston, Vol. 1, pp. 521-528.

36. Finn, W.D.L., Pickering, D.J. and Bransby, P.L. (1971), "Sand Liquefaction in Triaxial and Simple Shear Tests", J. Soil Mech. and Found. Div., ASCE, Vol. 97, No. SM4, pp. 639-659.

37. Fischer, J.A., Koutsoftas, D.C. and Lu, T.D. (1976), "The Behavior of Marine Soils Under Cyclic Loading", Proc., International Conf. on the Behavior of Offshore Structures, Norwegian Institute of Technology, Trondheim, Vol. 2, pp. 407-417.

38. Flaate, K. (1972), "Effects of Pile Driving in Clays", Canadian Geotechnical Jour., Vol. 9, p. 81.

39. Foss, I., Dahlberg, R. and Kvalstad, T. (1978), "Foundation Design for Gravity Structures with Respect to Failure in Cyclic Loading", Proc., 10th Offshore Technology Conf., Houston, Vol. 1, pp. 535-545.

40. France, J.W. (1976), "An Investigation of the Effects of Drainage on the Repeated Load Behavior of Soils", Geotechnical Engineering Report 76-2, Cornell University, Ithaca, New York

41. Geonor (1968), "Description and Instruction for Use of Direct Simple-Shear Apparatus Model h-12", Geonor A/S, Oslo.

42. Gibson, R.E. (1958), "The Progress of Consolidation in a Clay Layer Increasing in Thickness with Time", Geotechnique, Vol. 8, pp. 171-182.

43. Green, P.A. and Ferguson, P.A.S. (1971), "On Liquefaction Phenomena, by Professor A. Casagrande: Report of Lecture", Geotechnique, Vol. 21, No. 3, pp. 197-202.

44. Hamilton E.L. (1971), "Elastic Properties of Marine Sediments", Journal of Geophysical Research, American Geophysical Union, Vol. 76, No. 2, pp. 579-604.

45. Hampton, M.A., Bouma, A.H., Carlson, P.R., Molina, B.F. and Clukey, E.C. (1978), "Quantitative Study of Slope Instability in the Gulf of Alaska", Proc., 10 Offshore Technology Conf., Houston, pp. 2307-2318.

46. Hara, A. and Kiyota, Y. (1977), "Dynamic Shear Tests of Soils for Seismic Analyses", Proc., 9th ICSMFE, Tokyo, Vol. 2, pp. 247-250.

47. Hardin, B.O. (1978), "The Nature of Stress-Strain Behavior for Soils", Proc., Earthquake Engineering and Soil Dynamics, ASCE Specialty Conf., Pasadena, pp. 3-90.

48. Hardin, B.O. and Black, W.L. (1968), "Vibration Modulus for Normally Consolidated Clay", J. Soil Mech. and Found. Div., ASCE, Vol. 94, No. SM2, pp. 353-369.

49. Hardin, B.O. and Drnevich, V.P. (1972), "Shear Modulus and Damping in Soils: Measurement and Parameter Effects", J. Soil Mech. and Found. Div., ASCE, Vol. 98, No. SM6, pp. 603-624.

50. Hardin, B.O. and Drnevich, V.P. (1972), "Shear Modulus and Damping in Soils, Design Equations and Curves", J. Soil Mech. and Found. Div., ASCE, Vol. 98, No. SM7, pp. 667-692.

51. Harr, M.E. (1977), Mechanics of Particulate Media, McGraw-Hill, Inc.

52. Harmann, H.G. and Houston, W.N. (1976), "Response of Seafloor Soils to Combined Static and Cyclic Loading", Proc., 8th Offshore Technology Conf., Houston, pp. 53-60.

53. Höeg, K. (1976), "Foundation Engineering for Fixed Offshore Structures", Proc., International Conf. on the Behavior of Offshore Structures, Norwegian Institute of Technology, Trondheim, Vol. 1, pp. 39-69.

54. Humphries, W.K. and Wahls, H.E. (1968), "Stress History Effects on Dynamic Modulus of Clay", J. Soil Mech. and Found. Div., ASCE, Vol. 94, No. SM2, pp. 371-389.

55. Hvorslev, M.J. and Kaufman, R.I. (1952), "Torsion Shear Apparatus and Testing Procedures", USAE Waterways Experiment Station, Bulletin No. 38, May.

56. Idriss, I.M., Dobry, R., Doyle, E.H. and Singh, R.D. (1976), "Behavior of Soft Clays Under Earthquake Loading Conditions", Proc., 8th Offshore Technology Conf., Houston, pp. 605-616.

57. Idriss, I.M., Dobry, R. and Power, M.S. (1976), "Soil-Response Considerations in Seismic Design of Offshore Platforms", Jour. of Petroleum Technology, March, pp. 244-252.

58. Ishibashi, I. and Sherif, M.A. (1974), "Soil Liquefaction by Torsional Simple Shear Device", J. Geotechnical Eng. Div., ASCE, Vol. 100, No. GT8, pp. 871-888.

59. Ishihara, K., Iwamoto, S., Yasuda, S. and Takatsu, H. (1977), "Liquefaction of Anisotropically Consolidated Sand", Proc. 9th ICSMFE, Tokyo, Vol. 2, pp. 261-264.

60. Kirby, R.C. and Wroth, C.P. (1977), "Application of Critical State Soil Mechanics to the Prediction of Axial Capacity for Driven Piles in Clay", Proc. 9th Offshore Technology Conf., Houston, pp. 483-494.

61. Kirkpatrick, W.M., Seals, R.K. and Newman, F.B. (1974), "Stress Distributions in Triaxial Compression Samples", J. Geotechnical Eng. Div., ASCE, Vol. 100, No. GT2, pp. 190-196.

62. Kjellman, W. (1951), "Testing the Shear Strength of Clay in Sweden", Geotechnique, Vol. 2, No. 3, pp. 225-235.

63. Kovacs, W.D., Seed, H.B. and Idriss, I.M. (1971), "Studies of Seismic Response of Clay Banks", J. Soil Mech. and Found. Div., ASCE, Vol. 97, No. SM2, pp. 441-455.

64. Krizek, R.J. (1971), "Rheologic Behavior of Clay Soils Subjected to Dynamic Loads", Transactions, Society of Rheology, 15:3, pp. 433-489.

65. Krizek, R.J., Ansal, A.M. and Bazant, Z.P. (1978), "Constitutive Equation for Cyclic Behavior of Cohesive Soils", Proc., Earthquake Engineering and Soil Dynamics, ASCE Specialty Conf., Pasadena, pp. 557-568.

66. Kuribayashi, E. and Tatsuoka, F. (1975), "Brief Review of Liquefaction During Earthquakes in Japan", Soils and Foundations, Vol. 15, No. 4, pp. 81-92.

67. Kvenvolden, K.A., Redden, G.D. and Carlson, P.R. (1977), "Hydrocarbon Gases in Sediments of Eastern Gulf of Alaska", American Association of Petroleum Geol. Bull., Vol. 61, p. 806.

68. Ladd, C.C. and Edgers, L. (1972), "Consolidated Undrained Direct-Simple Shear Tests on Saturated Clays", Soils Publication No. 284, Dept. of Civil Engineering, Massachusetts Institute of Technology, Cambridge, Ma.

69. Ladd, C.C. and Foott, R. (1974), "New Design Procedure for Stability of Soft Clays", J. Geotechnical Eng. Div., ASCE, Vol. 100, No. GT7, pp. 763-786.

70. Ladd, C.C., Foott, R., Ishihara, K., Schlosser, F. and Poulos, H.G. (1977), "Stress-Deformation and Strength Characteristics", Proc., 9th ICSMFE, Tokyo, Vol. 2, pp. 421-494.

71. Ladd, R.S. (1976), "Specimen Preparation and Cyclic Stability of Sands", Liquefaction Problems in Geotechnical Engineering, ASCE National Convention, Philadelphia, pp. 199-226.

72. Lambe, T.W. and Whitman, R.V. (1969), Soil Mechanics, John Wiley and Sons, Inc.

73. Landva, A. (1964), "Equipment for Cutting and Mounting Undisturbed Specimens of Clay in Testing Devices", Norwegian Geotechnical Institute, Oslo, Publication 56, pp. 1-5.

74. Larew, H.B. and Leonards, G.A. (1962), "A Strength Criterion for Repeated Loads", Proc., Highway Research Board, Vol. 41, pp. 529-556.

75. Lashine, A.K.F. (1973), "Deformation Characteristics of a Silty Clay Under Repeated Loading", Proc. 8th ICSMFE, Moscow, Vol. 1, pp. 237-244.

76. Lee, K.L. (1976), "Fundamental Considerations for Cyclic Triaxial Tests on Saturated Sand", Proc., International Conf. on the Behavior of Offshore Structures, Norwegian Institute of Technology, Trondheim, Vol. 1, pp. 355-373.

77. Lee, K.L. and Albaisa, A. (1974), "Earthquake Induced Settlements in Saturated Sands", J. Geotechnical Eng. Div., ASCE, Vol. 100, No. GT4, pp. 387-406.

78. Lee, K.L. and Fitton, J.A. (1969), "Factors Affecting the Cyclic Loading Strength of Soil", Vibration Effects of Earthquakes on Soils and Foundations, ASTM STP 450, pp. 71-95.

79. Lee, K.L. and Focht, J.A. (1975), "Liquefaction Potential at Ekofisk Tank in North Sea", J. Geotechnical Eng. Div., ASCE, Vol. 100, No. GT1, pp. 1-18.

80. Lee, K.L. and Focht, J.A. (1976), "Strength of Clay Subjected to Cyclic Loading", Marine Geotechnology, Vol. 1, No. 3, pp. 165-185.

81. Liou, C.P., Streeter, V.L. and Richart, F.E. (1976), "A Numerical Model for Liquefaction", Liquefaction Problems in Geotechnical Engineering, ASCE National Convention, Philadelphia, pp. 313-341.

82. Lucks, A.S., Christian, J.T., Brandow, G.E. and Hoeg, K. (1972), "Stress Conditions in NGI Simple Shear Test", J. Soil Mech. and Found. Div., ASCE, Vol. 98, No. SM1, pp.155-160.

83. Martin, G.R., Finn, W.D.L. and Seed, H.B. (1975), "Fundamentals of Liquefaction Under Cyclic Loading", J. Geotechnical Eng. Div., ASCE, Vol. 101, No. GT5, pp. 423-438.

84. McClelland, B. (1974), "Design of Deep Penetration Piles for Ocean Structures", J. Geotechnical Eng. Div., ASCE, Vol. 100, No. GT7, pp. 705-747.

85. Mitchell, R.J. and King, R.D. (1977), "Cyclic Loading of an Ottawa Area Champlain Sea Clay", Canadian Geotechnical Journal, Vol. 14, No. 1, pp. 52-63.

86. Mitchell, R.J., Tsui, K.K. and Sangrey, D.A. (1973), "Failure of Submarine Slopes Under Wave Action", Proc., 13th International Conf. on Coastal Eng., Vol. 1.

87. Morgenstern, N.R. and Sangrey, D.A. (1978), "Methods of Stability Analysis", Landslides: Analysis and Control, Transportation Research Board, Washington, D.C., Chpt. 7.

88. Motherwell, J.T. and Wright, S.T. (1978), "Ocean Wave Load Effects on Soft Clay Behavior", Proc., Earthquake Engineering and Soil Dynamics, ASCE Specialty Conf., Pasadena, pp. 620-635.

89. Mulilis, J.P., et.al. (1977), "Effects of Sample Preparation on Sand Liquefaction", J. Geotechnical Eng. Div., ASCE, Vol. 103, No. GT2, pp. 91-108.

90. Norwegian Geotechnical Institute (1975), "Research Project, Repeated Loading on Clay: Summary and Interpretation of Test Results", Oslo.

91. Ogawa, S., Shibayama, T. and Yamaguchi, H. (1977), "Dynamic Strength of Saturated Cohesive Soil", Proc., 9th ICSMFE, Tokyo, Vol. 2, pp. 317-320.

92. Park, T.K. and Silver, M.L. (1975), "Dynamic Triaxial and Simple Shear Behavior of Sand", J. Geotechnical Eng. Div., ASCE, Vol. 101, No. GT6, pp. 513-529.

93. Pender, M.J. (1977), "Modelling Soil Behavior under Cyclic Loading", Proc., 9th ICSMFE, Vol. 2, pp. 325-331.

94. Perloff, W.H. and Baron, W. (1976), Soil Mechanics Principles and Applications, Ronald Press Co., New York.

95. Prevost, J.H. (1977), "Mathematical Modelling of Monotonic and Cyclic Undrained Clay Behaviour", International Journal for Numerical and Analytical Methods in Geomechanics", Vol. 1, pp. 195-216.

96. Prevost, J.H. (1976), "Undrained Stress-Strain-Time Behavior of Clays", J. Geotechnical Eng. Div., ASCE, Vol. 102, No. GT12, pp. 1245-1259.

97. Prevost, J.H. and Hoeg, K. (1977), "Plasticity Model for Undrained Stress Strain Behavior", Proc., 9th ICSMFE, Tokyo, Vol. 1, pp. 255-261.

98. Prevost, J.H. and Hoeg, K. (1976), "Reanalysis of Simple Shear Soil Testing", Canadian Geotechnical Journal, Vol. 13, pp. 418-429.

99. Prevost, J.H. and Hughes, T.J.R. (1978), "Mathematical Modeling of Cyclic Soil Behavior", Proc. Earthquake Engineering and Soil Dynamics, ASCE Specialty Conf., Pasadena, pp. 746-761.

100. Pugsley, A.G. (1955), "Structural Safety", Jour. Royal Aeronautical Society, Vol. 58.

101. Pyke, R.M., Seed, H.B. and Chan, C.K. (1975), "Settlement of Sands Under Multidirectional Shaking", J. Geotechnical Eng. Div., ASCE, Vol. 101, No. GT4, pp. 379-398.

102. Reimnitz, E. (1972), "Effects in the Copper River Delta", The Great Alaskan Earthquake of 1964: Oceanography and Coastal Engineering, National Academy of Sciences, Washington, D.C., pp. 290-302.

103. "Research Needs and Priorities for Geotechnical Earthquake Engineering Applications" (1977), Report of Workshop, Univ. of Texas, Austin, NSF, NBS Sponsored, June.

104. Richart, F.E. (1975), "Some Effects of Dynamic Soil Properties on Soil-Structure Interaction", J. Geotechnical Eng. Div., ASCE, Vol. 101, No. GT12, pp. 1193-1240.

105. Richart, F.E., Jr., Hall, J.R., Jr. and Woods, R.D. (1970), Vibrations of Soils and Foundations, Prentice Hall, Inc.

106. Roscoe, K.H. (1953), "An Apparatus for the Application of Simple Shear to Soil Samples", Proc., 3rd ICSMFE, Zurich, Vol. 1, pp. 186-191.

107. Roscoe, K.H., Bassett, R.H. and Cole, E.R.L. (1967), "Principle Axes Observed During Simple Shear of a Sand", Proc., Geotechnical Conference, Oslo, pp. 231-237.

108. Roscoe, K.H., Schofield, A.N. and Wroth, C.P. (1968), "On the Yielding of Soils", Geotechnique, Vol. 8, No. 1, pp. 22-53.

109. Rowe, R.W. (1975), "Displacement and Failure Modes of Model Offshore Gravity Platforms Founded on Clay", Offshore Europe 1975, Aberdeen, Scotland, Conf. Paper OE-75 218.1.

110. Saada, A.S., Bianchini, G.F., and Shook, L.P. (1978), "The Dynamic Response of Anisotropic Clay", Proc., Earthquake Engineering and Soil Dynamics, ASCE Specialty Conf., Pasadena, pp. 777-801.

111. Sangrey, D.A. (1977), "Marine Geotechnology - State of the Art", Marine Geotechnology, Vol. 2, pp. 45-80.

112. Sangrey, D.A. (1971), "Changes in Strength of Soils Under Earthquake and Other Repeated Loading", Proc., 1st Canadian Conference on Earthquake Engineering, Vancouver, pp. 82-96.

113. Sangrey, D.A. (1977), "Response of Offshore Piles to Cyclic Loading", Proc., 9th Offshore Technology Conf., Houston, pp. 507-512.

114. Sangrey, D.A., Castro, G., Poulos, S.J. and France, J.W. (1978), "Cyclic Loadings of Sands, Silts and Clays", Proc., Earthquake Engineering and Soil Dynamics, ASCE Specialty Conf., Pasadena, pp. 836-851.

115. Sangrey, D.A., Henkel, D.J. and Esrig, M.I. (1969), "The Effective Stress Response of a Saturated Clay Soil to Repeated Loading", Canadian Geotechnical Journal, Vol. 6, pp. 241-252.

116. Sangrey, D.A., Pollard, W.S. and Egan, J.A., (1977), "Errors Associated with Rate of Undrained Cyclic Testing of Clay Soils", Dynamic Geotechnical Testing, ASTM STP 654, pp. 280-294.

117. Schofield, A. and Wroth, P. (1968), Critical State Soil Mechanics, McGraw-Hill Book Co.

118. Seed, H.B. (1968), "Landslides During Earthquakes Due to Soil Liquefaction", J. Soil Mech. and Found. Div., ASCE, Vol. 94, No. SM5, pp. 1053-1122.

119. Seed, H.B. (1976), "Evaluation of Soil Liquefaction Effects on Level Ground During Earthquakes", Liquefaction Problems in Geotechnical Engineering, ASCE, National Convention, Philadelphia, pp. 1-104.

120. Seed, H.B. (1976), "Some Aspects of Sand Liquefaction Under Cyclic Loading", Proc., International Conf. on the Behavior of Offshore Structures, Norwegian Institute of Technology, Trondheim, Vol. 1, pp. 374-391.

121. Seed, H.B., Chan, C.K. (1966), "Clay Strength Under Earthquake Loading Conditions", J. Soil Mech. and Found. Div., ASCE, Vol. 92, No. SM2, pp. 53-78.

122. Seed, H.B., Chan, C.K. and Monismith, C.L. (1955), "Effects of Repeated Loading on the Strength and Deformation of Compacted Clay", Proc., Highway Research Board, Vol. 34, pp. 541-558.

123. Seed, H.B. and Idriss, I.M. (1967), "Analysis of Soil Liquefaction: Niigata Earthquake", J. Soil Mech. and Found. Div., ASCE, Vol. 93, No. SM3, pp. 83-108.

124. Seed, H.B. and Idriss, I.M. (1971), "Simplified Procedure for Evaluating Soil Liquefaction Potential", J. Soil Mech. and Found. Div., ASCE, Vol. 97, No. SM9, pp. 1249-1273.

125. Seed, H.B. and Idriss, I.M. (1970), "Soil Moduli and Damping Factors for Dynamic Response Analyses", Earthquake Engineering Research Center, Report No. EERC 70-10, U. of California, Berkeley.

126. Seed, H.B., Idriss, I.M., Lee, K.L. and Makdisi, F.I. (1975), "Dynamic Analysis of the Slide in the Lower San Fernando Dam During the Earthquake of February 9, 1971", J. Geotechnical Eng. Div., ASCE, Vol. 101, No. GT9, pp. 889-911.

127. Seed, H.B., Martin, P.P. and Lysmer, J. (1976), "Pore-Water Pressure Changes During Soil Liquefaction", J. Geotechnical Eng. Div., ASCE, Vol. 102, No. GT4, pp. 323-346.

128. Seed, H.B., Mori, K. and Chan, C.K. (1977), "Influence of Seismic History on Liquefaction of Sands", J. Geotechnical Eng. Div., ASCE, Vol. 103, No. GT4, pp. 257-270.

129. Shen, C.K., Herrmann, L.R. and Sadigh, K. (1978), "Analysis of Cyclic Simple Shear Test Data", Proc., Earthquake Engineering and Soil Dynamics, ASCE Specialty Conf., Pasadena, pp. 864-874.

130. Sherif, M.A. and Ishibashi, I. (1976), "Dynamic Shear Moduli for Dry Sands", J. Geotechnical Eng. Div., ASCE, Vol. 102, No. GT11, pp. 1171-1184.

131. Sherif, M.A., Ishibashi, I. and Ling. S.C. (1977), "Dynamic Properties of a Marine Sediment", Proc., 9th ICSMFE, Tokyo, Vol. 2, pp. 387-391.

132. Silver, M.L. et al (1976), "Cyclic Triaxial Strength of Standard Test Sand", J. Geotechnical Eng. Div., ASCE, Vol. 102, No. GT5, pp. 511-523.

133. Silver, M.L. and Park, T.K. (1975), "Testing Procedure Effects on Dynamic Soil Behavior", J. Geotechnical Eng. Div., ASCE, Vol. 101, GT10, pp. 1061-1083.

134. Skoglund, G.R., Marcuson, W.F., III and Cunny, R.W. (1976), "Evaluation of Resonant Column Test Devices", J. Geotechnical Eng. Div., ASCE, Vol. 102, No. GT11, pp. 1147-1158.

135. Stevens, H.W. (1975), "The Response of Frozen Soils to Vibratory Loads", Technical Report 265, U.S. Army, CRREL, Hanover, N.H., June.

136. Stevens, H.W. (1973), "Viscoelastic Properties of Frozen Soils Under Vibratory Loads", Proc., 2nd International Conf. on Permafrost, National Academy of Sciences, Washington, D.C., pp. 400-409.

137. Taylor, D.W. (1952), "A Direct Shear Test with Drainage Control", Symposium on Direct Shear Testing of Soils, ASTM STP 131, pp. 63-74.

138. Taylor, P.W. and Bacchus, D.R. (1969), "Dynamic Cyclic Strain Tests on a Clay", Proc., 7th ICSMFE, Vol. 1, pp. 401-409.

139. Theirs, G.R. and Seed, H.B. (1968), "Cyclic Stress-Strain Characteristics of Clay", J. Soil Mech. and Found. Div., ASCE, Vol. 94, No. SM2, pp. 555-569.

140. Theirs, G.R. and Seed, H.B. (1969), "Strength and Stress-Strain Characteristics of Clays Subjected to Seismic Loading Conditions", Vibration Effects of Earthquakes on Soils and Foundations, ASTM, STP 450, pp. 3-56.

141. Timoshenko, S.P. and Goodier, J.N. (1934), Theory of Elasticity, McGraw-Hill Book Company.

142. United States Geological Survey (1977), "Submarine Landslides", U.S. Geological Survey Yearbook, Fiscal Year 1977, Dept. of the Interior, U.S.G.S., Washington, D.C.

143. Valera, J.E. and Donovan, N.C. (1976), "Comparison of Methods for Liquefaction Evaluation", Liquefaction Problems in Geotechnical Engineering., ASCE National Convention, Philadelphia, pp. 359-388.

144. Van Eekelen, H.A.M. (1977), "Single Parameter Models for Progressive Weakening of Soils by Cyclic Loading", Geotechnique, Vol. 27, No. 3, pp. 357-368.

145. Vinson, T.S., Chaichanavong, T. and Czajkowski, R.L. (1978), "Behavior of Frozen Clay under Cyclic Axial Loading", J. Geotechnical Eng. Div., ASCE, Vol. 104, No. GT7, pp. 779-800.

146. Wilson, N.E. and Greenwood, J.R. (1974), "Pore Pressure and Strains After Repeated Loading of Saturated Clay", Canadian Geotechnical Journal, Vol. 11, pp. 269-277.

147. Wolfe, W.E., Annaki, M. and Lee, K.L. (1977), "Soil Liquefaction in Cyclic Cubic Test Apparatus", Proc., 6th World Conf. on Earthquake Engineering, New Delhi, Vol. 6, pp. 1-6.

148. Wong, R.T., Seed, H.B. and Chan, C.K. (1975), "Cyclic Loading Liquefaction of Gravelly Soils", J. Geotechnical Eng. Div., ASCE, Vol. 101, No. GT6, pp. 571-583.

149. Woods, R.D. (1978), "Measurement of Dynamic Soil Properties", Proc., Earthquake Engineering and Soil Dynamics, ASCE Specialty Conf., Pasadena, pp. 91-178.

150. Wright, D.K., Gilbert, P.A. and Saada, A.S. (1978), "Shear Devices for Determining Dynamic Soil Properties", Proc., Earthquake Engineering and Soil Dynamics, ASCE Specialty Conf., Pasadena, pp. 1056-1075.

151. Yoshimi, Y. and Oh-Oka, H. (1973), "A Ring Torsion Apparatus for Simple Shear Tests", Proc., 8th ICSMFE, Moscow, Vol. 1.2, pp. 501-506.

152. Yoshimi, Y., Richart, F.E., Jr., Prakash, S., Barkan, D.D. and Ilyichev, V.A. (1977), "Soil Dynamics and Its Application to Foundation Engineering", Proc., 9th ICSMFE, Tokyo, Vol. 2, pp. 605-650.

153. Youd, T.L. (1972), "Compaction of Sands by Repeated Shear Straining", J. Soil Mech. and Found. Div., ASCE, Vol. 98, No. SM7, pp. 709-725.

154. Youd, T.L. (1975), "Liquefaction, Flow and Associated Ground Failure", Proc., National Conf. on Earthquake Eng., Ann Arbor, Mich., pp. 146-155.

155. Youd, T.L. and Craven, T.N. (1975), "Lateral Stress in Sands During Cyclic Loading", J. Geotechnical Eng. Div., ASCE, Vol. 101, No. GT2, pp. 217-221.